

ADAMA SCIENCE AND TECHNOLOGY UNIVERSITY

SCHOOL OF APPLIED NATURAL SCIENCE

DEPARTMENT OF APPLIED CHEMISTRY



PREPARATION AND CHARACTERIZATION OF CERAMIC WATER FILTER: FOR WATER TREATMENT

THE PROJECT TEAM MEMBERS ARE:

1. Dr. Enyew Amare (PI)
2. Dr. Tegene Desalegn (Co)
3. Dr. Gelana W/Michael (Co)

May 2019

Adama, Ethiopia

Table of Contents

1. LISTS OF FIGURES.....	iv
LISTS OF TABLES	vi
ABBREVIATIONS	vii
ACKNOWLEDGMENTS.....	viii
ABSTRACT	ix
1. INTRODUCTION	1
1.1. Background	1
1.2. Statement of the Problem.....	2
1.3. General Objective	3
1.3.1. Specific Objectives	3
1.4. The significance of the study	3
1.5. The scope of the study	3
2. LITERATURE REVIEW	4
2.1. Household Water Treatments.....	4
2.2. Filtration processes	4
2.2.1. Bio-sand filtration	5
2.2.2. Solar water disinfection	6
2.2.3. Household chlorination.....	6
2.2.4. Boiling.....	6
2.2.5. Nanofiltration	7
2.2.6. Reverse osmosis (RO).....	7
2.2.7. Ceramic water filters.....	7
2.3. Physical Characteristics of Ceramic Filter.....	10
2.3.2. Porosity	13
2.3.3. Flow Rate	14
2.4. Raw Materials for Ceramic Filters.....	16
2.4.1. Clay	16
2.4.2. Burnout materials.....	19
2.4.3. Grog	20

2.4.4.	Bone Char	20
2.5.	Water Quality	20
2.5.1.	Indicator Organisms	21
2.5.2.	Turbidity of Water	22
2.5.3.	Electrical conductivity	22
2.5.4.	Iron	23
2.5.5.	Flouride	23
2.5.6.	Nitrite	24
2.5.7.	Hardness.....	25
3.	METHODS AND MATERIALS	27
3.1.	Description of the Study Area.....	27
3.2.	Ceramic Water Filter preparation process.....	29
3.3.	Ceramic Filter Test	33
3.3.1.	Flow Rate	33
3.3.2.	Escherichia coli	33
3.3.3.	Fluoride Removal Efficiency	34
3.3.4.	Conductivity.....	36
3.3.5.	Turbidity Test.....	36
3.3.6.	pH.....	37
3.3.7.	Zero point charge (pH_{zpc})	37
3.3.8.	Water Hardness Agents Removal Test	37
3.3.9.	Iron Removal Test.....	39
3.3.10.	Nitrite Removal test	40
3.4.	Composition analysis	41
3.5.	FT-IR Analysis.....	41
3.6.	Powder X-Ray Diffraction (XRD).....	42
3.7.	Field Emission Scanning Electron Microscopy (FESEM).....	42
3.8.	The porosity of Ceramic Filters	42
3.8.1.	Total porosity	42
3.8.2.	Specific surface area and pore size distribution analysis	43
3.9.	Data Analysis	43

4. RESULTS AND DISCUSSION	44
4.1. Flow Rate Test	44
4.2. Porosity Test	48
4.3. Escherichia coli Removal Efficiency	50
4.4. The microstructure of Ceramic Filters	53
4.4.1. The Micro-structure of ceramic C(800-950)-60-15-25 filters.....	53
4.4.2. The Micro-structure of a ceramic filter with 5% grog	55
4.4.3. The Micro-structure of ceramic filter C900-50-15-35 design.....	56
4.4.4. The Micro-structure of other ceramic filters design	57
4.5. BET Analysis of the sintered ceramic filter	58
4.6. Chemical Analysis	61
4.7. XRD Analysis	64
4.8. FT-IR Analysis.....	66
4.9. Removal Efficiency of Hardness Agents	70
4.10. Iron Removal Efficiency	71
4.11. Nitrite Removal Efficiency	73
4.12. The Efficiency of the ceramic Filters towards Fluoride Removal	74
4.13. Turbidity Removal Efficiency of the Filters	75
4.14. Conductivity and pH Analysis of Filtrate with Ceramic Filters.....	76
4.15. Zero point Charge (pH _{zpc})C900-50-35-15 filter	77
5. CONCLUSIONS	80
6. RECOMMENDATIONS	81
REFERENCES	82
APPENDIXES	100

1. LISTS OF FIGURES

Figure 1. The principles of surface and depth filtration.	5
Figure 2. The Order of size (μm) of pathogenic microorganisms (Doris V. 2006).	9
Figure 3. Mechanism of removing microorganisms (Molly, 2009).	12
Figure 4. Schematic diagram of clay mineral particle with cations and anions (Yong, 2001).	13
Figure 5. Schematic pores classification, according to their availability to surroundings (modified from IUPAC, 1994) a - closed pores, b, f - pores open only at one end, c, d, g – open pores, e - open at two ends (through) pores.	14
Figure 6 a): A single Si–O tetrahedron and the structure of the tetrahedral sheet and a single Al–O octahedron and the structure of the octahedral sheet. b) Schematic representation of the structure of 2:1 layer clay.	18
Figure 7. Clay soil sampling area (Kechene).	28
Figure 8. Photograph of the Water sampling area (Modjo River).	28
Figure 9. Firing summary used for ceramic filter sintering.	30
Figure 10. Some of the shaped and sintered filter elements produced.	30
Figure 11. The flow chart of the Filter production process and testing.	32
Figure 12. Solutions prepared for UV-Visible spectrophotometer.	40
Figure 13. Solutions prepared for UV-Visible spectrometer of nitrite.	41
Figure 14 (a-d). The flow rate of ceramic filter designs of Batch A, B, C and mix (d).	45
Figure 15 (e-h). The average flow rate of ceramic filter designs of Batch D, E, F and G.	46
Figure 16 (a-d). The average porosity of ceramic filter designs of Batch A, B, C and D.	49
Figure 17 (e-h). The total porosity of ceramic filter designs of Batch, E, F, G and H.	50
Figure 18. SEM micrographs of the fractured surface of C60-15-25 sintered at 800, 850, 900 & 950°C.	54
Figure 19. FESEM micrographs of porous media of C900-70-5-20 fractured surface at different magnifications.	55
Figure 20. The Microstructures of ceramic filters C900-75-5-15 and C900-80-5-15 designs.	56

Figure 21(a-d). FESEM: The Microstructures of a ceramic filter with C900-50-15-35 design micrographs at different magnifications.	57
Figure 22. FESEM micrographs on fractured surface of C900-70-15-15 and C850-70-10-20.	58
Figure 23. Adsorption and desorption Isotherm of composite filter C900-50-15-35.	59
Figure 24. Pore size distributions of sintered composite filter C900-50-15-35.....	60
Figure 25. Multipoint BET plot for C900-50-15-35 filter.....	61
Figure 26. EDS spectrum of C950-50-15-35 ceramic filter.	63
Figure 27. EDS spectrum of the sintered ceramic filter after used for hardness and iron removal tests.....	64
Figure 28. EDS spectrum of sintered ceramic filter used for E.Coli removal from Mojo river.	64
Figure 29. (a) XRD patterns of raw bulk, normal and heated clay at 550°C (b) XRD patterns of raw clay and sintered filter C950-50-15-35.	66
Figure 30.The FT-IR spectrum of raw clay.	67
Figure 31. FTIR Spectrum of sintered C800-50-15-35 ceramic filter.	68
Figure 32.The FT-IR spectrum of C900-50-35-15 with 5% Bone Char.	69
Figure 33. The FT-IR spectrum of sintered filter C1000-80-5-15.....	69
Figure 34. The calibration graph for the determination of the Iron concentration.....	72
Figure 35. Calibration graph of the determination of nitrite concentration.....	74
Figure 36. pH_i vs pH_f intersects of pH_{pzc}	78
Figure 37. Graph of ΔpH versus the initial pH of the C900-50-35-15 filter to determine pH_{pzc} . 79	79

LISTS OF TABLES

Table 1. The types of raw materials used, flow rate and E.coli removal efficiency of some ceramic water filters currently in use.	8
Table 2. Chemical composition and crystallography of some clay minerals.	19
Table 3. Chemical, E.coli and Physicochemical Risk Categories of drinking water summary.	26
Table 4. Filters developed with different designs.	31
Table 5. Test results of flow rate for filters with different ratios of clay, grog and sintered at 900 and 950°C.	46
Table 6. Test results of flow rate for filters with different ratios of grog and sawdust.	47
Table 7. The flow rate of twelve ceramic filters in a 15 minutes interval in (L/h)	48
Table 8. The % microbial removal efficiency of the ceramic filters with different Design.	52
Table 9. Textural parameters obtained by low-temperature nitrogen adsorption for sintered C900-50-15-35.	59
Table 10. BET surface area and Barret-Joyner-Halenda (BJH) pore volume and diameter.	61
Table 11. (%) chemical composition of raw clay, fired ceramic filter with & without bone char.	62
Table 12. Chemical composition (%) of the filter before and after hardness removal.	63
Table 13. The removal efficiency of water hardness agents with initial concentrations of Mg ²⁺ (546 ppm) and Ca ²⁺ (393 ppm) before filtration.	70
Table 14. The Iron removal efficiency of the filters from initial concentration (27.12 ppm) at room temperature.	72
Table 15. The nitrite removal efficiency of the ceramic filters from 4mg/L original concentration at room temperature.	73
Table 16. Fluoride removal efficiency in percent from 10mg/L of aqueous solution at pH of 8.	75
Table 17. Turbidity removal efficiency of selected filters from source water with 58 NTU.	76
Table 18. Average± SD pH, and conductivity values after filtration using ceramic filters.	77
Table 19. Experimental data for determination of zero point charge.	78

ABBREVIATIONS

AAS	Atomic Absorption Spectroscopy
ANOVA	Analysis Of Variance
APHA	American People Health Association
CF	Ceramic Filters
CFU	Colony Forming Unite
CWF	Ceramic Water Filter
EBT	Eriochrome Black-T
EDTA	Ethylene Diammine Tetra Acetic Acid
EDS	Energy Dispersive Spectrometry
FESEM	Field Emission scanning electron microscopy
FDRE	Federal Democratic Republic of Ethiopia
FT-IR	Fourier Transform Infra Red
HWTS	Household Water Treatment Safe Storage
MF	Microfiltration
NTU	Nephelo Turbidity Unit
PFP	potter for peace
UNICEF	United Nations Children’s Fund
RDIC	Resource Development International Cambodia
TCMWG	The Ceramic Manufacturing Working Group
USEPA	United State Environmental Production Agency
UV-Vis	Ultra Violet Visible Spectrophotometer
WHO	World Health Organization
XRD	X-Ray Diffraction

ACKNOWLEDGMENTS

We are grateful to Adama Science and Technology University for financial support. This research work would not have been realized without the financial support of the Research Office of Adama Science and Technology University. We would like to give our gratitude to Dr. Alemu Disassa, and Dr. Legesse Lamecha for facilitating administrative issues. We are thankful to the Chemistry Department of Addis Ababa University for allowing us to use their instruments including XRD and FT-IR. Oromia Self Help Organization (OSHO) Fluoride Technology Center for allowing us to use their laboratory to determine the amount of fluoride in sample water, turbidity, conductivity and to conduct Microbial tests.

We would like to acknowledge Professor Neeraj Gupta for taking our samples for BET and FESEM characterization to Indian Institute of Technology KANPUR, materials testing laboratory. We also would like to express our gratitude to Mr. Tesfaye Betela, Mr. Nigussa Dame and Mr. Tariku Mulugeta for their valuable contributions during experimental work. We would like to express our gratitude to all the applied chemistry staff of ASTU for their moral support and fruitful suggestion and constructive comments during the proposal review, progress report, and final report presentation.

ABSTRACT

Water is basic in life. Clean water is the key to a healthy society. A billion cases of diarrhea occur worldwide each year that result in million deaths. Ethiopia is facing the challenge of safe water coverage in rural and urban. The communities in the Ethiopia rift valley are also highly affected by fluorosis because of the high concentration of fluoride in drinking water. Inorganic ceramic is receiving more attention in recent time due to their unique characteristics which include different pore structures and content, hydrophilic surfaces, high chemical, thermal and mechanical stabilities which offer avenues for application in water treatment. The aim of this work was to develop a ceramic water filter with a good flow rate, which is capable to remove chemicals as well as microbial contaminants, by investigating the effect of altering specific design variables. Ceramic water filters were developed from different ratios of local raw materials: clay, sawdust, grog, with and without bone chars and sintered in (800-1000°C) temperature at different intervals for 6hrs. The developed ceramic filters were characterized with FE-SEM, EDX, XRD, pH meter, BET and FT-IR. The flow rate, porosity, conductivity, pH of filtered water and the removal efficiencies (microbial, water hardness agent's, fluoride, nitrite, iron, and turbidity) were analyzed. The ceramic filters with 25-35% sawdust, 50-60% clay and 15% grog that sintered in the temperature range of 900-950°C showed better flow rate (1.5-2.5 L/h), E.coli removal efficiency is greater than 99%. The pH, conductivity and other water quality parameters of the filtrate are in WHO standard. The average total porosity, BET surface area and average pore diameter determined for C900-50-15-35 ceramic filter were 36%, 6.183 m²/g, and 4.83 nm respectively. The porosity of the filter; C900-50-15-35 (36.33±0.05), its flow rate (1.91±0.55). The removal efficiency of nitrite (70.00±0.22 %) and fluoride (96.8±0.41%) are in the WHO standard. The Phase and functional group identification of sintered filter investigated with x-ray diffraction and infrared spectroscopy revealed the presence of mixed phase and hydroxyl functional group on the surface of the sintered filter. Field emission scanning electron microscopy (FESEM) revealed the porous nature of sintered filter elements with an average pore size of 5 nm. The EDS analysis results of the filter used for hardness and iron removals showed more concentration of Ca²⁺, Mg²⁺, Iron and less ion concentration of Na⁺ and K⁺ due to the ion exchange reactions. Statistical ANOVA tests showed a significant difference between ceramic filters with various compositions in their removal efficiencies of E. Coli, nitrite, and porosity (p < 0.05).

Keywords: *Ceramic filter, sintering, Indicators microorganism, microstructure, flow rate*

1. INTRODUCTION

1.1. Background

Access to safe drinking water is a basic human right, but according to World Health Organization (WHO) report a large number of world's rural population has no access to clean water (WHO, 2006, and WHO/UNICEF, 2017). Diarrhoeal diseases are responsible for approximately 2.5 million deaths annually in developing countries, affecting children younger than five years, especially those in areas devoid of access to clean water supply and sanitation (Haddis et al., 2017). Improved water supply and appropriate sanitation systems could significantly contribute to the reduction of diarrhea mortalities and improved health outcomes. In the rural area, the surface waters are contaminated for the reason that the societies near to these water sources use the water not only for drinking purpose but also for washing cloth, bathing and for drinking animals (WHO, 2016). Chemical contamination of drinking water sources is also a concern for millions of people and long-term exposure to these pollutants can have serious health implications. As an example, fluorine is a chemical contaminant that contaminates water and causes serious health problems such as dental and skeletal fluorosis (WHO, 2011).

The occurrence of high fluoride concentration in drinking water and the risk of fluorosis associated with using such water for human consumption is a problem faced by many countries and high concentrations of nitrite from ammonium fertilizers is also causing a health problem in drinking water (Fantong, 2010, Gatseva, 2008b, Clemens et al., 2003). The development of an efficient, stable, low cost and easy to use water purification system is crucial for many countries suffering from health problems due to water pollution.

The necessities for water treatment vary from region to region based on impurity characterizations such as microbes, chemicals, and organic matter. Some of the basic point-of-use methods and devices for removing the above-mentioned impurities are chlorination, solar disinfection, ceramic filters and bio-sand filters (Sobsey et al., 2008).

Ethiopia as the developing country the majority of its population have no access to safe water and sanitation coverage, (FMoH, 2007; MOWIE, 2017). The main causes of water pollution in

Ethiopia are related to sewage, industry, domestic and rural wastewater and agricultural activities (FMoH and FEPA, 2010). For this reason, a large population is suffering from water-borne and water-related diseases (Mebratu Jano, 2007 and UNICEF/WHO, 2012). This burdens the country with enormous financial and social costs to take care of such a huge number of people suffering from these debilitating infections. Ceramic filters made of clay improved with state of art technologies can be used for providing cheap potable water in the developing countries. Past research and social work have helped millions of people across the globe to take advantage of clay composite ceramic filters for water purification (Sobsey et al., 2008). Fabrication of porous ceramics with controlled pore size and surface charge can be developed by fine-tuning the relative amount and types of raw materials, and processing conditions to improve the performance of the filter. This work is trying to fill this gap.

1.2. Statement of the Problem

Water is basic in life. Clean water is the key to a healthy society. A billion cases of diarrhea occur worldwide each year that result in million deaths. Ethiopia is facing the challenge of safe water coverage in rural and urban (Desalegn et al., 2013, WHO 2010). The communities in the Ethiopia rift valley are also highly affected by fluorosis because of the high concentration of fluoride in drinking water (Abebe, 2010). According to the recent study conducted on drinking water quality in Ethiopia, Nationally, 14 percent of the population gets water from low-risk sources (no detectable *E. coli* in a 100 mL sample) (MOWIE, 2017). The survey also found that *E. coli* levels are more likely to increase than decrease between collection and consumption within the home. *E. coli* levels were lower in households that reported treating water and in piped water that had medium or high levels of residual chlorine. In addition, fluoride levels exceeding the national standard (1.5 mg/L) and affected 3.8 percent of the population. Nitrite accumulates in agricultural watersheds where farmers spread fertilizers and animal manures on cropland and becoming health problem (Gatseva,2008b). The methods of purification like chlorination, large-scale filtration cannot be afforded by many Ethiopians, especially rural people who live below poverty levels. Ceramic water filtration becomes a cheap and efficient method since all the materials required are available locally, has a relatively long lifetime of 5+ years, the technology can work all year round in different climates and does not impart an objectionable taste to the treated water (Vinka et al,

2008, Sakka Y, et al 2003 and UNICEF, 2012). Although clay filters have been developed for the removal of bacteria and other microbial pathogens. currently, there are no systems that can simultaneously remove both microbes and ions like fluoride from contaminated water. This study was aimed at looking into the effect of processing parameters on locally available raw materials towards the different design of ceramic water filters with better filtration efficiency.

1.3. General Objective

The aim of this research was to develop a ceramic filter from locally available resources for water treatment and study its performances.

1.3.1. Specific Objectives

The following are the specific objectives of this research work:

1. Preparation of ceramic water filters with different designs using clay, grog, sawdust, and bone char.
2. Investigating the effect of the ratios of sawdust, clay, and grog on the performance of the ceramic filter developed.
3. Investigating the effect of sintering temperature on ceramic filter performance.
4. Investigating the fluoride, nitrite, hardness and iron removal efficiency of the filter.
5. Characterizations of the ceramic filter elements by XRD, AAS, EDX, FT-IR, FE-SEM, BET, and pH.

1.4. The significance of the study

This study, in the long run, will help to transfer knowledge/ technology to the local potters in Ethiopia on the making of water filters from locally available materials. The project also provided opportunities for graduate students of chemistry to work on local problems that are the main concern of the society.

1.5. The scope of the study

The project presents the results of an experimental study of ceramic water filters fabricated from different ratios of clay, sawdust, and grog with and without bone char, and sintered at a different temperature.

2. LITERATURE REVIEW

2.1. Household Water Treatments

In developing countries, many people are living in rural communities and have to collect their drinking water some distances away from the household and transport it back in various types of containers (Sobsey, 2002). Microbiological contamination of the water may occur between the collection point and the point-of-use in the household due to unhygienic practices causing the water to become a health risk (Sobsey, 2002; 2004; Moyo *et al.*, 2004). Household water treatment and safe storage (HWTS) is one means for improving the quality of water for consumption within the home, especially where water handling and storage is necessary and recontamination is a real risk between the point of collection and point of use (UNICEF and WHO, 2011). Over billion people lack access to clean water source and 2.4 times population lacking adequate sanitation and HWTS methods can significantly reduce diarrheal disease, if used correctly and consistently by a population at risk (WHO, 2013, Lantagne, 2009). A number of research groups have proposed point-of-use water purification systems for improving the quality of drinking water, the advantages of being easily maintained and uses (Clasen *et al.*, 2004, Sobey *et al.*, 2007, Matt, 2006). The main reasons for treating water by (HWTS) are to remove contaminants that are harmful to health and make the water taste or smell bad. There are different water treatment techniques at home level. All the methods are used to reduce microorganisms and turbidity of water with different mechanisms. The most frequently used low-cost water purification systems include sand filters, boiling, bio-filters, chlorination units, and solar-based systems, nanofiltration, reverse osmosis and clay-based filters.

2.2. Filtration processes

One great advantage of filtration, if compared to most chemical treatments, is the simultaneous and rapid removal of turbidity and microorganisms in a one-stage process. When talking about filtration, two major processes may be distinguished, namely surface filtration and depth filtration. surface filtration relies to a great extent on the sieving effect, which is the physical straining of particles that are larger than the pore dimension of the filter media. The filter media here is often referred to as a membrane and is defined as a semi-permeable film of relatively low thickness. Particles are retained on the membrane surface and form a cake that grows in

thickness as the filtration progresses. In contrast, depth filtration corresponds to a filter media of increased thickness and hence increases the path length of contaminants in the filter media. Depth filters are often composed of materials which further elongate the path length of the media and force contaminants to travel around obstacles where they can be trapped by various transport and surface forces (Molly, 2009).

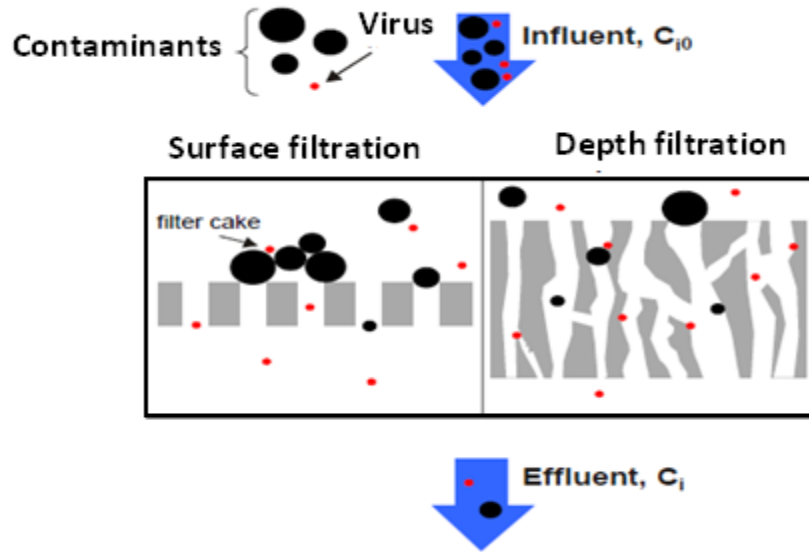


Figure 1. The principles of surface and depth filtration.

2.2.1. Bio-sand filtration

Bio-sand filtration is a method of filtering water through different sized sediment of sands. There is a biological layer on the top sand layer to remove pathogenic microorganisms. The source water will pour on the upper part, the water passes through the pores of the sand sediments and finally, it can be collected at the bottom side of the sand. It is commonly made from environmentally available materials, this technology is effective for rural poor households (Lee, 2001). The system has a good removal efficiency of microorganisms. Bio-sand filter can remove protozoa by 99.98 to 100 % (Martikainen, 2018). The limitation of this method is it takes large space and fail to remove color or dissolved substances.

2.2.2. Solar water disinfection

Solar water disinfection systems have been introduced recently as a means for treating water. It is performed by filling water in a transparent plastic bottle of one liter and putting the water on the solar radiation for one full day. Microorganisms will be deactivated due to UV radiation by this method. It is reported that the solar water disinfection method reduces fecal coliform and *Vibrio cholera* to 99.9% in a laboratory setting (Sommer et al., 2012). The limitation of this method is it needs a transparent plastic bottle and it takes a long time, especially on cloudy days. These systems, however, can affect the taste of the water. They are also not very efficient in removing the turbidity.

2.2.3. Household chlorination

It includes water treatment with a chlorine solution at the point-of-use and storage of water in a safe container. Users add one cup of solution to their storage container of 10 liters. Chlorine is effectively inactivating microorganisms in point of use water treatment, but it affects the taste and odor of the water and does not remove turbidity. The application needs some introduction or manual for the user. The serious problem of this method is halogenated organic by-products like chlorinated methane that will cause cancer. Despite the chlorine properties that can control the water-borne diseases, its side effects required regulations and standards to limit to a minimum level (Rosalam H and Duduku K 2007).

2.2.4. Boiling

Boiling is another effective household water treatment method because it can destroy the most class of microorganisms. The process is heating the water up to 60⁰C and cooling. If the source water is with high turbidity, it should be first filtered with a cloth to reduce turbidity. Boiling of untreated water for one to ten minutes can destroy disease-causing microorganisms found in water (WHO, 2002). The problem of this method is the taste of treated water due to the reduction of dissolved oxygen on heating and a significant amount of energy required, that introduces other problems associated with limited supply and depletion of natural resources.

2.2.5. Nanofiltration

Nano-filtration is a cross-flow filtration technology which ranges between ultrafiltration and reverse osmosis. The nominal pore size of the membrane is typically about ~1nm. The associated drawback is that it requires specific pre-treatment due to the fine nature of membranes (Hillie et al., 2003).

2.2.6. Reverse osmosis (RO)

It is a membrane-technology filtration method that removes many types of large molecules and ions from solutions by applying pressure to the solution when it is on one side of a selective membrane. The reverse osmosis (RO) phenomenon takes place by reversing the forward osmosis (FO) process and making the solvent filter out of high concentration into the lower concentration solution.

FO uses the osmotic pressure differential ($\Delta\pi$) across the membrane, while in reverse osmosis hydraulic pressure differential (P) is applied, as the driving force for transport of water through the membrane. For RO, water diffuses to the less saline side due to hydraulic pressure ($P > \pi$) (Cath et al., 2006).

2.2.7. Ceramic water filters

A filter is defined as a material, which removes something from whatever passes through it. Therefore, ceramic water filtration as defined by (Brown et al., 2007), is the process that makes use of a porous ceramic (fired clay) medium to filter microbes or other contaminants from water. Ceramic filtration is very important in the production of drinking water from surface water for large-scale water treatment (Doek et al., 2007). But, the WHO encourages its use as HWTS for effective treatment of drinking water (Rob et al., 2003). From the review of more than 30 technologies for water filtration at the point of use in developing countries, ceramic water filters are among the top 5 promising technologies (Sobsey, 20008, du Preez, et al., 2008). Table 1 summarized a few ceramic water filters currently in uses in different countries with the types of raw materials used for the preparation of the filter, flow rate, and E. coli removal efficiencies.

Table 1, The types of raw materials used, flow rate and *E.coli* removal efficiency of some ceramic water filters currently in use.

Clay Material	Additive	Colidial silver (CS)	(E.coli) Removal Efficiency	Flow Rate	Reference
Clay	Tealeaves/Coffee grounds/Rice husk	Nil	96.4-99.8%	0.5l/h	[Holtslag, 2010]
White Kaolin	sawdust	Nil	96 -99.4%	0.30.-84l/h	[Sagara,2000]
Red Terracota	Sawdust ,Rice husk	Nil	93-99.9%	1-1.1l/h	[Low, 2002]
White Kaolin	Charcoal powder	CS	99.9%	0.24-0.4l/h	[Dies, 2003]
Red Clay	Flour/Rice husk	Nil	99.9%	0.756l/h	[Low, 2002]
Black Clay	Flour/ Rice Husk	CS	99.3%	0.341l/h	[Hagan et al., 2009]
Clay	sawdust	CS	99-100%	1-2l/h	[Lantagne et al., 2006]
Clay	Coffee /Rice husk	CS	96-97.69%	5-9l/h	[Klarman,2009]
Diatomaceous Earth	Loose Carbon	CS	99.9%	1.3-4l/h	Franz, 2005
Terracotta clay	sawdust	CS	97.6%	1.7l/h	[Sobsey et al, 2007]
Clay	Sawdust/rice husk	Nil/CS	97-99%	1-3l/h	[Brown, 2007]

Ceramic filters are made by mixing clay with sawdust, rice husks, or other flammable organic materials. After being shaped into a filter with a press, they are fired in a kiln. The organic material burns out, leaving small pores of different sizes, which can filter out the majority of harmful microbes (Hagan et al., 2008). These kinds of clay filters can remove between 96% and 99% of *E. coli*, an important indicator of the amount of contamination present in a water sample. The filters also remove particulates and protozoan (which are larger than bacteria, Doris V. 2006).

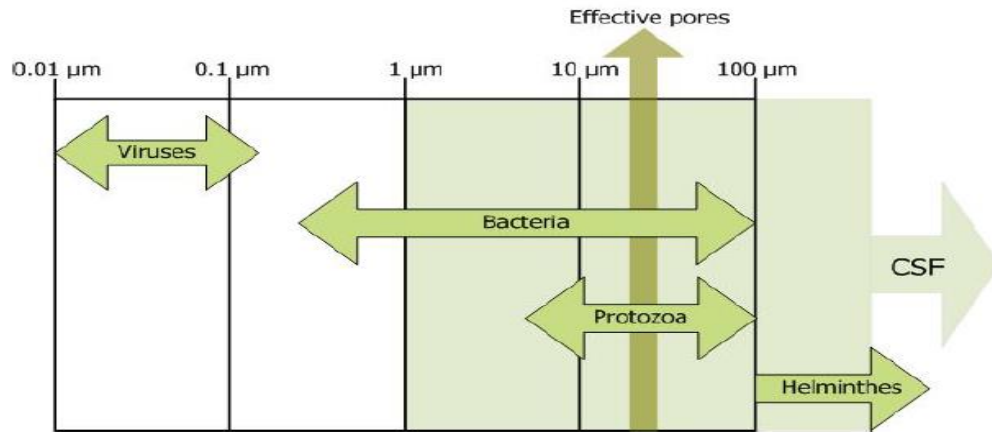


Figure 2. The Order of size (μm) of pathogenic microorganisms (Doris V. 2006).

Furthermore, with the addition of colloidal silver (a broad-spectrum antimicrobial) the filters have 100% effectiveness in tests for removal of *E. coli* (Bogdanchikova et al., 1992). Studies have also shown that silver is a potentially strong anti-viral compound (Gallieret al., 2011). Current ceramic water filter technology fulfills many of the water purifier requirements like affordability, acceptability, and filtering efficiency (Potters without Borders, 2012). Economically, the component clay and organic burnout material are both readily available across the developing world, creating sustainable and reliable local supply chains (although research may need to be done to ensure that clay in different areas can be used to form working filters) (Michael et al., 2013). The colloidal silver that helps to eliminate viruses is not locally-sourced and can be a bottleneck to scale-up. However, in areas where waterborne viruses such as hepatitis are not a concern, the filter element by itself does a satisfactory job of removing protozoan and bacteria (Yang and Tsai, 2008).

Ceramic filters membrane has been attractive to the researchers in the last decade due to their superior thermal and chemical stability, better mechanical strength, high resistance to acid and base and good defouling properties (Bottino et al., 2001). The successful applications of ceramic filters for the wastewater treatment were found in the chemical industry, metal industry, textile industry, food and beverage (Jedidi et al., 2009). The use of clay and fly ash as the raw material for crack-free ceramic membranes showed good performance for the treatment of textile wastewater and heavy metal from aqueous solutions (Fang et al., 2011, Nasir Subriyer, 2013).

Ceramic membranes made from clays and phosphates were suggested to be used as a previous clarification step in textile water treatment (Palacio et al., 2009). In another study, simple ceramic filters manufactured from clay soil and rice can be applied to remove more than 95% of iron through oxidation, co-precipitation, and filtration (Shafiquzzaman et al., 2011).

Unlike chemical or thermal disinfection, ceramic filters do not significantly change water taste or temperature, but it reduces turbidity (Clasen et al., 2004). They have a potentially long useful life of 5+ years (Campbell, 2005) with proper care and maintenance, although manufacturers may recommend regular replacement of the filter element every 1-2 years'. The ceramic filter surface is regenerated through periodic scrubbing to reduce surface deposits that slow down filtration rates.

A clay water filter has many advantages due to its lightweight, portable, low-cost, requires no chemicals, and is simple to use; it can be produced locally, using naturally available clay and other materials. The pore size and surface charge of ceramic water filter determine its ability to remove particles and pathogens from water (Bielefeldt et al., 2010). The effort of this research project was to develop a ceramic water filter from locally available materials for household water treatment and study the efficiency of the filter in removing microorganisms, coagulants and chemical contaminants from water.

2.3. Physical Characteristics of Ceramic Filter

Material behavior is determined by its properties so that the filter material will be characterized. The parameters chosen to characterize the material are the material porosity, pore size distribution, flow rate, surface charge, microstructure, and total pore area, etc. It is thought that these parameters contribute to the understanding of the filter discharge and the removal efficiency of pathogenic microorganisms.

2.3.1. Mechanisms and working principles of ceramic filter

2.3.1.1. *Mechanism of Filtration*

The phenomenon that takes place when the influent water passes through the ceramic filter pores is mechanical screening, sedimentation, adsorption, chemical activity, and biological activity. Mechanical screening is removing relatively larger size particles compared to the pore size of the filter. Sedimentation is retaining suspended particles on the surface of the filter. The suspended particles and dissolved substances are retained in the filter element by adsorption. After they are adsorbed, the particles will chemically convert into an insoluble form or decompose to simple non-toxic substances. Biological activity is the other mechanism of filtration due to the interaction of microorganisms with the filter element during filtration (Huisman, 1996).

2.3.1.2. *Mechanical Filtration*

Mechanical filtration is the process of removing particles from water with regard to their size. The contaminants are physically prevented from moving through the filter by screening them out with very small pores. The porosity of the filter is the fraction of the volume that is occupied by void space. It was suggested that filters work by additional mechanisms to mechanical screening, including sedimentation, diffusion, and adsorption (Huisman, 1996, Van Halem, 2006).

2.3.1.3. *Removing Microorganisms*

Removing microorganisms from the source water is one of the main tasks of the ceramic filter. The common indicator microorganisms are E.coli, fecal coliform and total coliform. There are several factors which play a great role in removing microorganisms in ceramic filtration like, the pore size of the filter, diffusion, and tortuosity of the filter. High tortuosity means a prolonged distance that water takes to exit from the filter element. One process of removing microorganism is by blockage of pore and organisms that are larger in size than the pore will retain from flowing through the outermost membrane layer (Doulton, 2009). Particles that are smaller than the average pore size will not necessarily run through the entire membrane. There is a possibility that they will adsorb on the ceramic or become blocked when larger particles plug up on the pores.

Filters with smaller pores have a higher removal efficiency of microorganisms (Oyanedel and Smith, 2008).

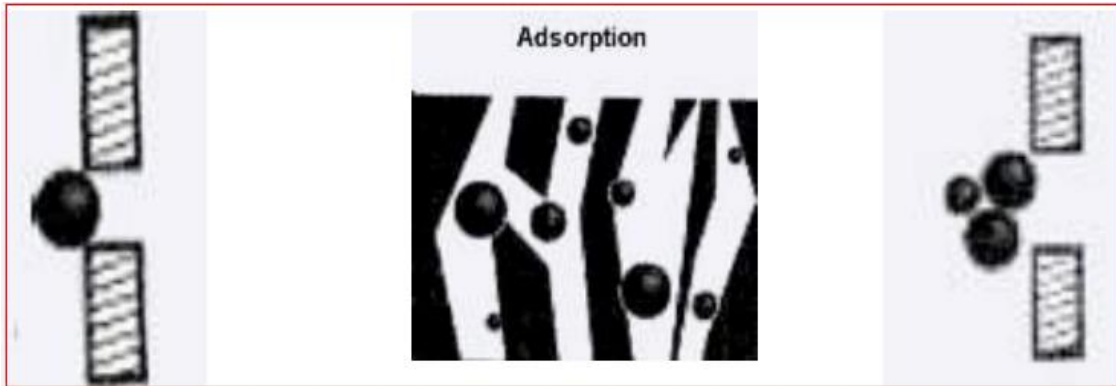


Figure 3. Mechanism of removing microorganisms (Molly, 2009).

2.3.1.4. Retention and Release of Metallic Compounds

Clay minerals have a negative surface charge. The composition of clay is a mixture of silicate, aluminate, and ferrate. The interaction of the anions in the clay surface and cations in aqueous solution can form an electric double layer that is the case for the retention of cations in a ceramic filter. Stem suggested that the electrified solid-liquid interface includes both the rigid Helmholtz layer and the diffuse one of Gouy and Chapman (Yakub et al., 2012). The other mechanism is adsorption and precipitation of metal ions as hydroxides or carbonates. The responsible factors that contribute for the retention or release of metals in the ceramic filter are changes of the ionic strength of the system, change in the acidity of the system, and formation of complexes (Yong, 2001). The leaching of the compounds from the clay filter element and the precipitation of calcium ion in the filter element was reported by (DHV Raadgevend Ingenieursbureau , 1983).

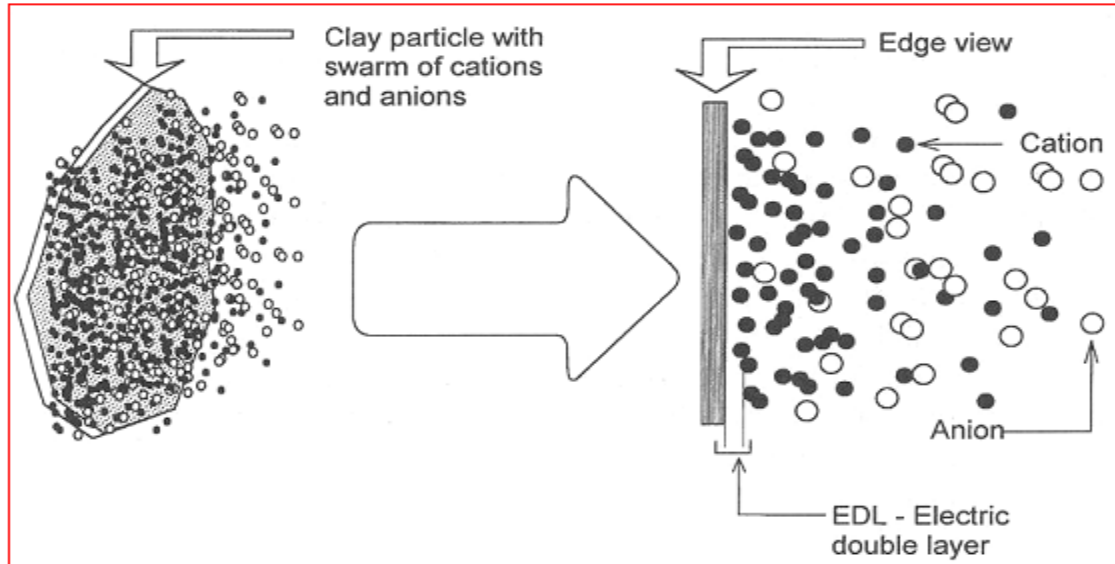


Figure 4. Schematic diagram of clay mineral particle with cations and anions (Yong, 2001).

2.3.2. Porosity

The total porosity of a solid is defined as the volume of voids divided by the total volume of the solid. Since porosity is a measure of the volume of empty space in a solid, filters showing a greater porosity will allow more water to pass through the ceramic body. Filter mix ratios are adjusted to achieve acceptable flow rate ranges, adding more burnout to the mixture if it is observed to be smaller (Hagan et al., 2009). However, increasing the pore size may compromise the mechanical screening phenomenon during filtration. Ceramic pores result from the burnout of organic materials mixed with the clay at high temperature before the sintering process. Pores can be also classified according to their accessibility to surroundings Fig.5. The pores communicating with the external surface are named open pores, like (b), (c), (d), (e) and (f). They are accessible for molecules or ions in the surroundings. Some may be open only at one end (b and f). They are then described as blind (i.e. dead-end) pores. Others may be open at two ends through pores, (e). If the porous solids are insufficiently heated, parts near the pores' outer shell collapse, thus inducing closed pores that have no communication to the surroundings. Closed pores (a) are also a product of insufficient evolution of gaseous substance. (K. Kaneko, 1994). Although the closed pore is not associated with adsorption and permeability of molecules, it influences the mechanical properties of solid materials. Interconnected pore space is more effective one because it is continuous throughout the filter and the dead-end pore is

interconnected only on one side of the filter, therefore, its effect is temporary on the discharge of water(Xiaolong and Yi, 2005).

Pores are also classified according to size into three categories; micropores (pore diameter smaller than 2 nm), mesopores (pore diameter 2 – 50 nm) and macropores (pore diameter larger than 50 nm) (Sing et al., 1985). There are different techniques of measuring the porosity of the materials, some of the methods are mercury porosimetry, nitrogen gas adsorption, and water vapor adsorption methods (Yakub 2012. van Halem, 2006).

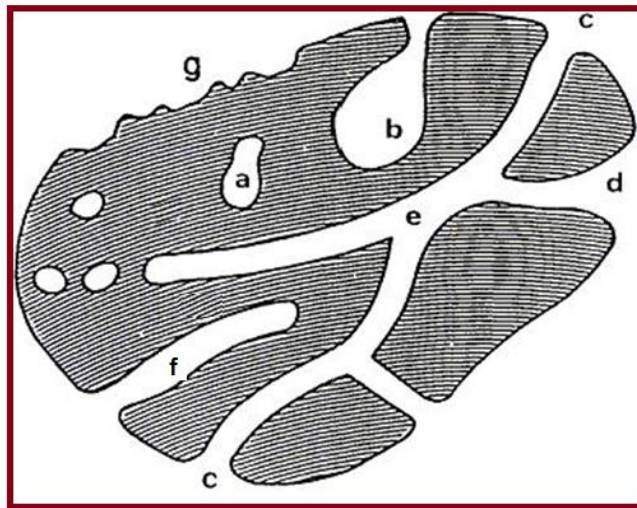


Figure 5. Schematic pores classification, according to their availability to surroundings (modified from IUPAC, 1994) a - closed pores, b, f - pores open only at one end, c, d, g – open pores, e - open at two ends (through) pores.

2.3.3. Flow Rate

Flow rate testing is an important quality assurance step which indicates the rate at which water passes through the ceramic filters per unit time. The acceptable flow rate of ceramic water filter is greater than one liter per hour in order to fulfill a family’s daily needs, but the flow rate must be low enough that the water passing through the ceramic filter has sufficient contact time in order to maximize pathogen removal (The Ceramics Manufacturing Working Group, 2011).

(Lantagne, 2001, Lantagne et al, 2009) reviewed filter manufacturing processes in several developing countries: a factory in Nicaragua accepts filters with flow rates between 1 and 2 liters per hour. However, tests of the Aqua-Pure factory filters in the Dominican Republic operate

below 2 liters per hour on average, consistently achieving 99% bacteria removal for flow rates below 1.7 liters per hour. Another study conducted in Nicaragua revealed the flow rates between 0.13 and 3.5 liters per hour. The flow rate of different ceramic filters that are currently in use is listed in the table 1 under section 2.3.

The flow rate can be adjusted in the manufacturing process by changing the ratio of combustible material to clay, increasing the combustible material used (which will result in larger pore sizes), or by changing the firing temperature in the kiln (Gensburger, 2011).

Gensburger's study, which examined filters manufactured in Cambodia, found a linear relationship between flow rate and quantity of burnout materials used. The same study found a strong correlation between the maximum firing temperature and the filter flow rate.

In another study ceramic filters of the configuration 70 percent clay and 30 percent combustible materials were the most efficient within optimum flow rate, tolerable turbidity, and pH level and zero bacterial counts which meets the World Health Organization's drinking water quality standard (Martins and Emmanuel, 2011). (Molly K, 2009, Biruk A, 2016) also reported a better performance for 65% clay to 35% burnout ratio filter.

The maximum flow rate 0.44 ± 0.11 ml/cm²/h for the filter with the ratio 60:40 of clay: coconut-shell charcoal, within the acceptable range for turbidity, coliform bacteria, and *Escherichia coli* were reported by (Watcharaporn et al., 2014).

Ceramic water filters designs (clay to sawdust ratio 60:40, 55:45, 50:50 and 45:55) fired at 950 °C for five hours had total *E. coli* removal efficiency of 99.99, 99.98, 99.97 and 86.76 percent respectively, and the results of this study suggest that the mean flow rate for a properly functioning filter (50% sawdust) fired at 950 °C is 1.7 L/h (Ndungu, 2009).

Many studies address the implications of flow rate for newly manufactured filters, filter clogging and changes in flow rate and efficacy over time are also of interest. (Bloem et al, 2009) investigated their mid-term effects, finding that filters with a higher initial flow rate show a larger decrease in flow rate over a 6-month period, although these filters maintain a higher flow rate than the filters with a lower initial flow rate, with negative effects on pathogen removal

efficiency. (Bloem et al., 2009) again performed a study that showed ceramic filters still reducing *E. coli* up to 44 months in use with no relationship between bacteria removal and time in use.

2.4. Raw Materials for Ceramic Filters

The main raw materials required for the manufacture of ceramic water filters are clay, grog, bone char, and the burnout material. The properties of porous ceramic materials are highly dependent on the properties of the raw materials, the volume ratios of the raw materials and sintering temperature (Sakka, 2003).

2.4.1. Clay

The term clay refers to a naturally occurring material composed of primarily finely grained minerals with grain size less than 2microns, which become plastic at appropriate water contents and will harden when dried or fired (Al-Ani and Sarapaa, 2008). Clay is one of the major important raw material in the manufacture of ceramic water filters. Pure clay does not occur naturally, they contain different clays and associated minerals (Ouahabietal., 2014). Clay minerals form an important group of the phyllosilicates or sheet silicate family of minerals, which are distinguished by layered structures composed of polymeric sheets of SiO_4 tetrahedral linked to sheets of $(\text{Al, Mg, Fe})(\text{O, OH})_6$ octahedral. The arrangement and composition of the octahedral and tetrahedral sheets account for most of the difference in their physical and chemical properties (AlAni and sarapaa, 2008). These properties determine the ability to work with clay and its usefulness for certain purposes. Plasticity is a very important property for the clay to be used in the manufacture of ceramic filters. Different applications require different plasticity (Nardo, 2005). Plastic clays (such as ball clays) can be rolled into a rope-like shape and wrapped around a thumb without breaking (Mukwasibwe, 2005). There are a number of different types of clay including kaolin, ball clay, stoneware clay, high aluminum clay, bentonite, brick clays, etc (Grimshaw, 1971). Ball clay is the preferred type for making ceramic filters because it is very plastic and has a high green mechanical strength [Obwoya, 2003). Plasticity is also affected by composition, wetness, aging, and bacteria. Plasticity can be increased by adding more plastic clays, fillers, and fluxes. Aging the clay body increases the plasticity by allowing the clay particles time to be thoroughly wetted (Kato, 1981). Some potters allow their clay to age

for 2-3 weeks before use. Bacteria increase the activity of the mix which increases the workability and plasticity with time.

2.4.1.1. Structure of Clay Minerals

Clay is known to be natural, earthy, fine-grained materials, which develop plasticity when mixed with a limited quantity of water. They are composed principally of silica, alumina, and water often with iron, alkali or alkaline earth metals (Bailey and Brindley, 1979, Nguetnkam et al., 2008). Clays consist of small particles of dimension 3 μm diameter and are adsorbents used to filter or remove solids and color in oils (Houdry et al., 1938). Clays have differing but inter-related structures. The differences in clay structures arise from the way the silica tetrahedra and alumina octahedra align in the structure as well as the differences in the number of the polyhedra and other ions present in the entire structure. The kaolinite has a single tetrahedral silica sheet and single octahedral alumina sheet, a combination which repeats itself indefinitely (fig.6a& b). The crystal structure consists of unit layers, which are stacked on one another and held together finally by hydrogen bonding among the hydroxide ions of the octahedral sheet of one layer and the oxygen of the tetrahedral sheet of the adjacent layer. Kaolinite is a clay mineral with the chemical composition $\text{Al}_2\text{Si}_2\text{O}_5(\text{OH})_4$ or $\text{Al}_2\text{O}_3 \cdot 2\text{SiO}_2 \cdot 2\text{H}_2\text{O}$ (Kerr, 1952). Within each layer, there is a repetition of structure and therefore it is referred to as a unit cell. The distance between a certain plane in the layer and the corresponding plane in the next layer is referred to as the basal or d-spacing. The lower layer is the octahedral sheet which is composed of alumina (Al, O, OH) while the upper layer is the tetrahedral sheet composed of silica (Si, O, OH). It is a non-expanding mineral and therefore is unable to absorb water into the interlayer position. This makes kaolinite to swell on wetting and shrinks on drying. In pure form, kaolinite has a melting point of 1770°C and a melting point between 1200 and 1450°C in a clay form due to the presence of highly fluxed feldspar.

An illite is a group of micas of the igneous and metamorphic rocks that have a unit layer composed of octahedral sheets sandwiched among tetrahedral sheets. Presence of potassium ions among these sheets results in increased thickness of the layer. The chemical formula is given as $(\text{K}, \text{H}_2\text{O})(\text{Al}, \text{Mg}, \text{Fe})_2(\text{Si}, \text{Al})_4\text{O}_{10}[(\text{OH})_2, (\text{H}_2\text{O})]$ but there is considerable ion substitution (Bain and Nadeau, 1986). It occurs as aggregates of small monoclinic grey to white crystals (Gates, 2002).

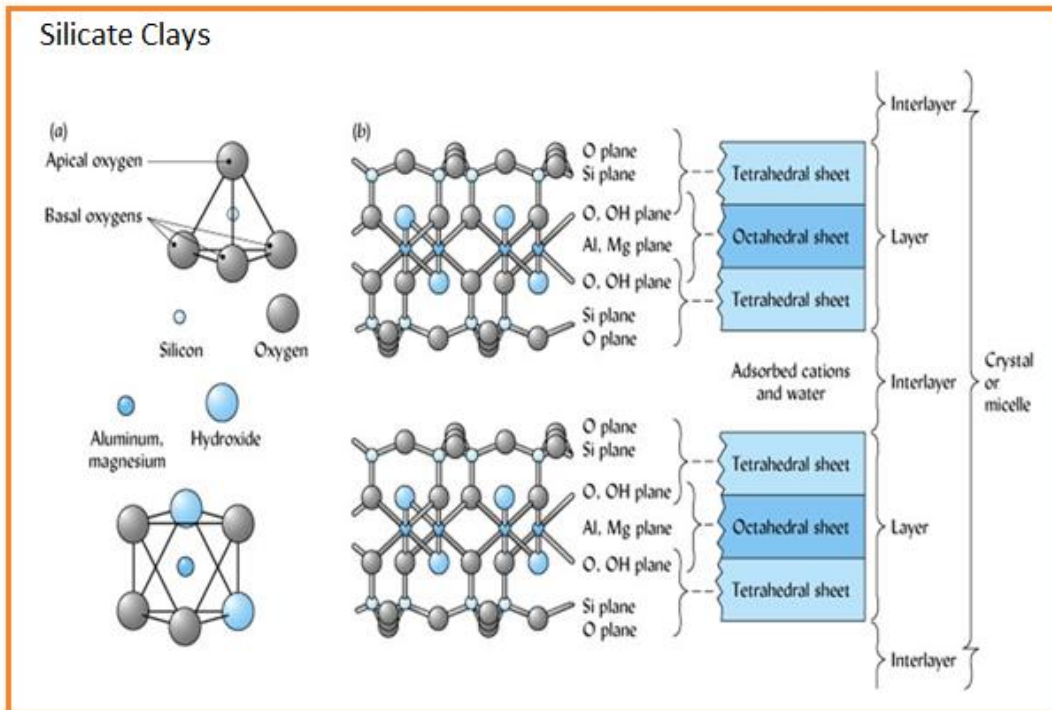
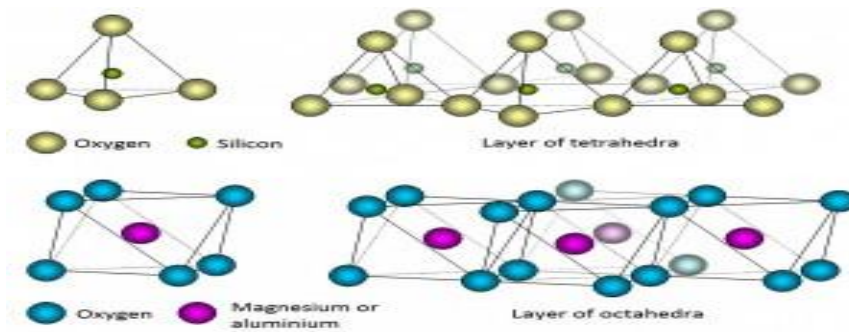


Figure 6 a): A single Si–O tetrahedron and the structure of the tetrahedral sheet and a single Al–O octahedron and the structure of the octahedral sheet. b) Schematic representation of the structure of 2:1 layer clay.

The montmorillonites are made of an alumina octahedral sheet between two silica tetrahedral sheets. Nontronite is the iron (III) rich member of the smectite group of clay minerals. Nontronites typically have a chemical composition consisting of more than ~30% Fe_2O_3 and less than ~12% Al_2O_3 ignited basis. A typical structural formula for nontronite is $\text{Ca}_5(\text{Si}_7\text{Al}_8\text{Fe}_2)(\text{Fe}_{3.5}\text{Al}_4\text{Mg})\text{O}_{20}(\text{OH})_4$. The dioctahedral sheet of nontronite is composed mainly

of trivalent iron (Fe^{3+}) cations, although some substitution by trivalent aluminum (Al^{3+}) and divalent magnesium (Mg^{2+}) does occur. The tetrahedral sheet is composed mainly of silicon (Si^{4+}). On the basis of relative percentages of aluminum, silicon and alkali metals or alkaline earth metals, the clays studied can be asserted to satisfy the formulae and structures (Deer et al., 1992).

Table 2. Chemical composition and crystallography of some clay minerals.

	Kaolinite	Pyrophyllite	Mica
Chemical formula	$\text{Al}_2\text{Si}_2\text{O}_5(\text{OH})_4$	$\text{Al}_2\text{Si}_4\text{O}_{10}(\text{OH})_2$	$\text{KA}_3\text{Si}_3\text{O}_{10}(\text{OH})_2$
Mineral formula	$\text{Al}_2\text{O}_3 \cdot 2\text{SiO}_2 \cdot 2\text{H}_2\text{O}$	$\text{Al}_2\text{O}_3 \cdot 4\text{SiO}_2 \cdot \text{H}_2\text{O}$	$\text{K}_2\text{O} \cdot 3\text{Al}_2\text{O}_3 \cdot 6\text{SiO}_2 \cdot 2\text{H}_2\text{O}$
Crystal class	Triclinic	Monoclinic	Monoclinic
Space group	P_1	C_2/c	C_2/c
Density	$2.6\text{g}/\text{cm}^3$	$2.8\text{g}/\text{cm}^3$	$2.8\text{g}/\text{cm}^3$
c-Lattice parameter	2.7Å	18.6Å	20.1Å

2.4.2. Burnout materials

Burnout materials are added to the clay to increase the porosity. The most used materials are carbonaceous materials. When the mass is fired the carbonaceous matter burnout, leaving corresponding pore spaces so that the porosity of the fired mass is roughly proportional to the volume of carbonaceous matter added. The main combustible materials are hardwood sawdust, cork seeds, naphthalene and occasionally fine ground coke (McCallister, 2005), flour, corn husks and rice husks (Katherine et al., 2008). Petroleum waste products may also be used, however, they burnout at higher temperatures than wooden sawdust (Kaminska and Valuikевичius, 2005). Sawdust of wood consists of volatile oils and small quantities of mineral content. The mineral matter in sawdust wood consists mostly of salts of calcium, potassium, and magnesium. Ash is formed from mineral matter during combustion and gasification. The ash yield has a very small proportion of 0.1% to 1% by volume which has little effect on the porosity of the ceramic, and during combustion, the mineral ions oxidize and volatilize or form particulates (Ragland et al.,

1991). Rice husks are not the preferred choice because it has a low heating value and is characterized by high ash content (18-22% by weight) (Bharadwaj et al., 2004).

2.4.3. Grog

Grog is fired clay, used to strengthen the ceramic body, reduce plasticity and shrinkage, and aid drying. Grog is available in a variety of sizes from very fine to coarse. The coarse sizes can be used to add texture to clay bodies. In the case of highly plastic clays, the grog usually enhances some characteristics of the unfired body, such as the permeability, which facilitates the drying stage. However, its addition can be detrimental to the porosity and mechanical strength of the final ceramic product. The amount of the grog added into the ceramic filter body will be convenient for both the processing and the quality of the ceramic product. Moreover, these materials facilitate the drying stage as well as the breakdown reactions that occur during the firing stage. Thus, for very plastic clays it may be necessary to add non-plastic material to improve the process conditions (Faustine and Obwoya, 2014, Obwoya, 2003).

2.4.4. Bone Char

Bone char is made of animal bone that charred (burnt) and crushed. It was one of the earliest media suggested for fluoride removal from water (HWTFR, 2011, Gitahi, 2012). It was not widely implemented due to the unpleasant taste of treated water. However, in 1988 the WHO proclaimed bone char to be an applicable technology for developing countries. The steps for preparing bone char include charring, crushing, sieving, washing, and drying. Bone char from any animal needs to be carbonized at a temperature of 400 to 500°C with a controlled air supply (Harmon and Mjengera, 2001). The charred bones are then crushed either manually or by using a crushing machine. For households and small communities, bone char media can be used in different kinds of filters. Bone char media needs to be renewed or regenerated periodically. Regeneration can be done using caustic soda or NaOH (Christoffersen, 1990).

2.5. Water Quality

Water quality describes the chemical, physical and biological conditions of drinking water (WHO, 2017). Chemical ingredients or physical parameters in drinking water are generally considered to have less influence on human health than microbial contaminations. Chemical compounds in drinking water are primarily present in very low concentrations and may cause

long-term health issues through the continual intake of small dosages. But, physical parameters are able to directly affect acceptability aspects of drinking water. They can lead to significant changes in appearance, odor, and taste; so that the consumers may possibly consider the drinking water as un-enjoyable. While turbidity in water does not directly cause health problems, it normally indicates poor quality or treatment failures. Water with high dissolved solids or salinity has a high electrical conductivity value, which may be unacceptable to consumers. Excessive hardness may not acceptable to consumers. This work includes research on the removal efficiency of microbial, chemical and physical parameters that are potentially dangerous for human health after long- or short-term consumption like an indicator organism (*E. coli*), fluoride, nitrite, hardness, iron, turbidity, and conductivity of the filtered water using ceramic filters developed for this work.

2.5.1. Indicator Organisms

In most household water treatment systems, the focus of research has been microbial removal. Removing pathogenic microorganisms from water is one of the main uses of ceramic filters. The organisms in the influent and effluent are measured to determine the removal efficiency of the filters. Detecting pathogenic microorganisms is complex and risky; therefore the use of 'indicator' organisms is introduced. Criteria for an 'indicator' organism in water bacteriology have been formulated as follows: it should always be present whenever a pathogen is present, and preferably in much larger numbers; it should only be present in the same source as the pathogens and should not multiply in the aquatic environment; its persistence in the natural environment or resistance to water treatment processes should be similar to that of the pathogens of concern; enumeration should be simple, accurate and inexpensive (Gray, 2003, Gerba, 2000). The bacterium *E. coli* is a Gram-negative, facultative anaerobe, non-spore forming bacillus with the width of 0.5 μm and 3.0 μm length (Chengwei Luo, S2011). *E. coli* itself is found in largest numbers in the intestinal flora of human and animals. *E. coli* is analyzed separately from coliform bacteria. *E. coli* appears exclusively with fecal contamination. Because of this, it serves as a direct indicator organism for fecal contaminations in drinking water (WHO, 2003). The WHO and others recommend that there should be no detectable amounts of *E. coli* in 100 ml of drinking water (APHA, 1978, BGOSHU, 2000, Scheutz et al., 2005 and WHO, 2011).

2.5.2. Turbidity of Water

Turbidity in drinking water is primarily caused by the presence of suspended particles of inorganic or organic matter. Often microorganisms attach to these suspended particles and decrease drinking-water quality. Some ingredients which cause turbidity can also affect taste, odor, and appearance as well as cause possible health issues.

Turbidity not only affects the overall appearance, but it can also be seen as an indicator for potential chemical or microbial contamination of drinking water (WHO, 2011). The WHO recommends turbidity of one NTU and up to 5 NTU is allowed (Lechevallier *et al.*, 1981). Light scattering by transparent isotropic media is accurately described by a macroscopic fluctuation theory first formulated by Einstein. Turbidity, τ , is dependent on fluctuations in the refractive index (or the dielectric constant) in volume, V , according to the equation

$$\tau = \frac{32\pi^3 V n^2 \langle (\delta n)^2 \rangle}{3\lambda_o^4} \dots\dots\dots 2.1$$

where λ_o is the wavelength of the incident radiation in a vacuum, $\langle (\delta n)^2 \rangle$ is the fluctuation average in the refractive index n . In an absorbing media, the refractive index is complex and therefore $\langle (\delta n)^2 \rangle$ can be replaced by $\langle (\delta n)^2 \rangle + \langle (a_c)^2 \rangle$ where a_c is the imaginary part of the complex refractive index, the absorption coefficient a_c must be much smaller than the real part if one is to be able to detect any scattered light (Miller, 1977).

The Turbidity of water can be measured using either an electronic turbidity meter, turbidity tube or spectrophotometer, and its units are Nephelometric Turbidity Unit (NTU), Jackson Turbidity Unit (JTU) or Formazin Attenuation Unit (FAU) depending on the method of measurement. The units are nearly equal. The detailed description of how turbidity is measured using the methods and advantages over each other is given by (Marty *et al.*, 2007).

2.5.3. Electrical conductivity

The electrical conductivity of water (EC), is a measure of the ability of water to conduct an electric current. It is usually measured in situ and expressed as micro siemens per centimeter ($\mu\text{S} / \text{cm}$). The electrical conductivity is as an indicator of the presence of salt and other impurities in water sample

usually pure water has low conductivity. It is effectively a surrogate for total dissolved solids and sensitive to variations in dissolved solids. The higher the level of dissolved solids (minerals, nutrients, etc.), the greater the ability of the water to pass an electrical current and, thus, the higher the conductivity value (Schiefer, 2003). The conductivity of most freshwater ranges from 10 to 1,000 $\mu\text{S}/\text{cm}$ but may exceed 1,000 $\mu\text{S}/\text{cm}$, in polluted waters (UNESCO/WHO/UNEP, 1996). High or low ECs in drinking water generally do not harm human health, but they can affect the taste in a negative way (WHO, 2011). The EC is an important parameter used to assess the cleaning success of the filtration system.

2.5.4. Iron

Ferrous iron is often called clear water iron because it is clear when poured. Carbon dioxide acts on iron in the ground to form soluble ferrous bicarbonate. The WHO recommends a concentration of 0.3 mg/L for ferrous iron and 1.0 mg/L for total iron. Iron concentrations higher than the WHO recommendation are responsible for causing the reddish brownish color to the water, staining laundry and giving the water some sour taste but do not present any health hazard.

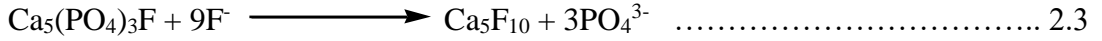
2.5.5. Fluoride

Fluoride is an ion of the element fluorine and it is the most reactive element of the halogen family. The WHO recommends a general standard for the concentration of fluoride in water, which ranges from 0.5 to 1.5 mg/L. Optimum fluoride concentration (about 1 mg/L) in drinking water is good for dental health and proper bone development. However, intake of excess fluoride (beyond 1.5 mg/L, WHO guideline) for a long period can result in the incidental fluorosis. Low concentration of fluoride in drinking water has been considered beneficial to prevent dental fluorosis, skeletal fluorosis, and bone fractures.

The beneficial and harmful effects of fluoride are based on the possible ion exchange reactions between hydroxide and fluoride ions in the calcium hydroxyl-phosphate, the main skeletal structure compositional material, the replacement of hydroxide ions with fluoride ions, is given by equation which results in more acid resistant structure fluoroapatite.



Fluoroapatite being more resistant to acid attack compared to hydroxyapatite a protective to the teeth enamel against acid from foods. This prevents dental fluorosis. Excessive fluoride intake, however, may enhance the reaction to go beyond replacement of hydroxide.



In this reaction, ion exchange occurs between phosphate and fluoride ions. The resultant compound, calcium decafluoride, is a very hard and brittle material not appropriately suited for the functions of the skeletal structure (Thole, 2011). The occurrence of high fluoride concentration in drinking water and the risk of fluorosis associated with using such water for human consumption is a problem faced by many countries, such as Saudi Arabia, Sri Lanka, the Rift valley countries in East Africa (Alabdulaaly et al., 2013, Dissanayake, 1991, Jianhua and Hui, 2012, Rango et al., 2012). The main methods used in defluoridation from aqueous solutions are membrane techniques and adsorption techniques: alumina-based adsorbents, clays, and soils fired clay pot and iron oxide (Fan et al., 2003, Huang et al., 2011, Kofa et al., 2017, Kefyalew et al., 2012). The adsorption techniques have been found to be the most effective and widely used because of its low maintenance cost and even appreciable fluoride removal at low concentrations. Using hydroxyapatite (HA)-Clay filters, (Yakub et al., 2013) were able to demonstrate high fluoride removal rate.

2.5.6. Nitrite

The contamination of surface water and groundwater with nitrate and nitrite has been considered in most urban and rural areas of the world. Pollution of underground and surface water in rural areas are due to human activities including agricultural activities (Mahvi et al., 2013) and diffusion from industrial processes and disposal of solid waste (Wakida, 2005) are the most common sources of nitrate and nitrite pollution. Nitrite accumulates in agricultural watersheds where farmers spread fertilizers and animal manures on cropland. The primary health hazard from drinking water with nitrate-nitrogen occurs when nitrate is transformed to nitrite in the digestive system (Robillard et al., 2006). The nitrite oxidizes iron in the hemoglobin of the red blood cells to form methemoglobin, which is short of the oxygen-carrying ability of hemoglobin.

This creates the condition known as methemoglobinemia, that is the iron in the blood, hemoglobin (Fe^{2+}) changed into its oxidized form, Fe^{3+} ((Adam, 1980). Higher concentrations of nitrite are indicative of pollution by industrial wastewater or agricultural run-off. The USEPA established a maximum contaminant level (MCL) of 1 mg/L nitrite-nitrogen in drinking water to help the prevention conditions, including blue baby syndrome in infants (WHO, 1985). Different optimized methods such as nano-filtration (Yousefi et al., 2016) and ion exchange resins (Shahbaziet al., 2010) in wastewater have been studied by researchers to reduce levels of these contaminants.

2.5.7. Hardness

Hardness in water refers to existing divalent ions, such as iron, manganese, calcium, and magnesium. Among them, calcium and magnesium are known as the dominant species for water hardening (Yanet et al., 2008). Most of the water resources should be treated for purification before consumption. In some countries, groundwater is the main safe drinking water resource (Bruggen and Vandecasteele, 2003). In some cases, the resource does not satisfy to the desirable levels regarding their chemical properties, such as hardness, nitrate contamination, heavy metals, soluble iron, etc. (Teixeira and Rosa, 2006). Water hardness can appear problematic in some cases; it can also be considered an important aesthetic parameter. The WHO guideline values are given for the concentration of calcium 100-300 mg/L and magnesium 200 mg/L in drinking water (Appendix K).

Table 3. Chemical, *E.coli*, and Physicochemical Risk Categories of drinking water summary.

Parameter	Risk Categories			
Iron	Low: <0.3 mg/L	Moderate: 0.3-1.0 mg/L	High: >1.0 mg/L	
Turbidity	Low: <1 NTU	Moderate: 1-5 NTU	High: >5 NTU	
Fluoride	Low: <0.5 mg/L	Moderate: 0.5-1.5 mg/L	High: >1.5 mg/L	Very high: >3 mg/L
Hardness	Soft: < 60 mg/L	Moderately hard: 60-180mg/L	Hard: 180-300 mg/L	Very hard: 300 mg/L
Electrical conductivity	Low: <150 µS/cm	Moderate: 150-500 µS/cm	High: 500-800 µS/cm	Very high: >800 µS/cm
<i>E. coli</i> Range (CFU/100 mL)	Low: 0	Moderate: 1-10	High : 10-100	Very high: >100

3. METHODS AND MATERIALS

3.1. Description of the Study Area

The study was conducted at Adama Science and Technology University, Department of Applied Chemistry which is located in Oromia national regional state east of Ethiopia 99 Km away from Addis Ababa with an average altitude of 1712 m above sea level. Ceramic water filters were developed by collecting clay sample from Kechene, Mariam River. Kechene Woreda is located in Addis Ababa administrations of Gullalle sub-city Woreda 6 at 38⁰45'0"E and 9⁰3'30"N. Water sample was collected from Modjo River, which located 75Km East of Addis Ababa the capital city of Ethiopia, which is geographically situated in between 39⁰ 05' E – 39⁰ 4'E longitudes and 8⁰ 34' – 9⁰ N latitudes. Microbial tests, fluoride, turbidity, and conductivity determination were done at OSHO (Oromo Self Help Organization) fluoride technology center, Modjo, filter elements firing, flow rate and total porosity determinations were conducted in Adama Science and Technology University chemistry department laboratory, phase and functional group analysis were done at Addis Ababa University Science Faculty chemistry department, total silicate analysis was conducted at Ethiopian Geological Survey laboratory, BET and microstructural analysis were done in Indian Institute of Technology KANPUR, materials testing laboratory.

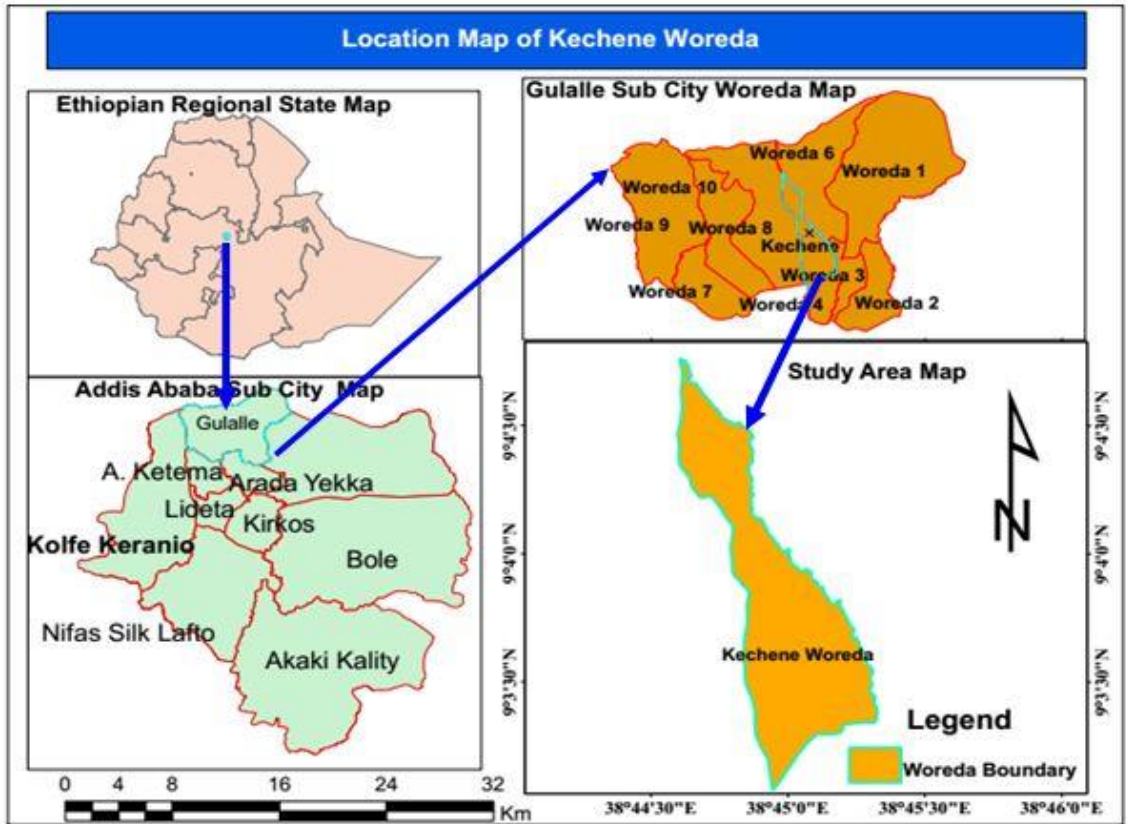


Figure 7. Clay soil sampling area (Kechene).



Figure 8. Photograph of the Water sampling area (Modjo River).

3.2. Ceramic Water Filter preparation process

The clay material collected was dried for two weeks to remove the water and crushed with wooden mortar and pestle, ground and sieved using a sieve with 0.75mm to obtain finer particles. The sawdust was also, dried, ground and sieved with 0.3 mm sieve to isolate the large particles of the sawdust. The Grog used for this work (fired clay without burn out materials) was prepared from fresh dried and sieved clay fired at 800°C for 2hrs (Molly 2009). The first kind of 24 selected filters was made from clay, grog and sawdust while the second kind of 15 filters was made from clay, grog, sawdust and animal bone that charred at 400°C as indicated in Table 4.

For the preparation of different batches of the ceramic filter; sieved clay powder, grog, and sawdust materials were taken in the required proportion for the production of ceramic filters according to the early developed procedure (Hagan et al., 2008). Clay, sawdust, and grog were mixed for more than one hour in dry. Then, water was added consistently on a dry mixture of clay, sawdust, and grog through mixing for 5hrs and aged for 3days. The blends were again mixed in wet by wedging and rolling to get a homogenous uniform mixture and the wet mixture was divided into blocks. The percentage of sawdust, clay, grog, and sintering temperature were varied in different batches of the ceramic filter designs. The blocked clay mixtures were molded into frustum shape at Kechene women pottery cooperation, Addis Ababa by using a 2-ton car jack. The manufactured filter element has a 10.0cm top radius, 15.0 cm height, 5.0 cm bottom radius, and 1.10cm wall thickness.

The shaped filters were allowed to sun dry for about two weeks. Once the filters were completely dried they were taken to Adama Science and Technology University, Applied Chemistry Post Graduate Laboratory and then sintered in muffle furnace at 800°C, 850°C, 900°C, 950°C and 1000°C for a period of 6 hours gradually starting from room temperature as depicted in figure 9. Afterward, the filters were left to cool gradually until the temperature reached room temperature. Once cooled, the filters were soaked in distilled water for 24 hours before starting the flow rate experiments. The selected filters were washed with distilled water, dried in an oven, packed properly in plastic bags to protect them from any contamination and made ready for the different tests.

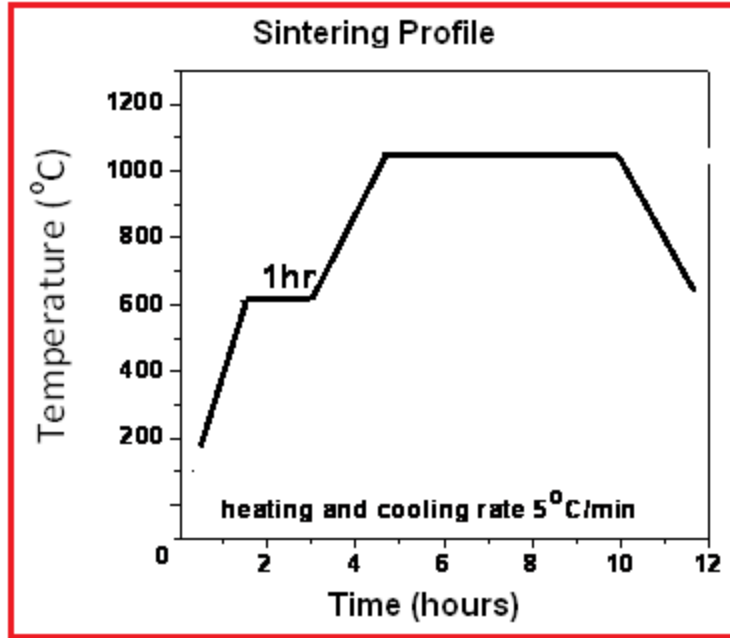


Figure 9. Firing summary used for ceramic filter sintering.



Figure 10. Some of the shaped and sintered filter elements produced.

Table 4.Filters developed with different designs.

Batch code	Filter Design	%Clay(v/v)	%Grog(v/v)	% Sawdust (v/v)	Bone Char	Sintering Temperature (°C)
First kind of filters (clay, sawdust, and grog)						
A [F1-F4]	C(800-950)-50-15-35	50	15	35	No	800-950
B[F5-F8]	C(800-950)-60-15-25	60	15	25	"	800-950
C[F9-F12]	C(800-950)-70-15-15	70	15	15	"	800-950
D[F13-F15]	C(800-900)-70-10-20	70	10	20	"	800-900
E[F16-F18]	C(900-1000)-70-5-25	70	5	25	"	900-1000
F[F19-F21]	C(900-1000)-75-5-20	75	5	20	"	900-1000
G[F22-F24]	C(900-1000)-80-5-15	80	5	15	"	900-1000
Second kind of filter designs (clay, sawdust, grog & bone char)						
BONE Char	C(800-950)-50-15-35	50	15	35	5%	800-950
Bone char	C(800-950)-60-15-25	60	15	25	5%	800-950
Bone char	C(800-950)-70-5-25	70	15	15	5%	800-950
Bone char	C(1000)-(70-85)-5-(25-15)	70-85	5	15-25	5%	1000

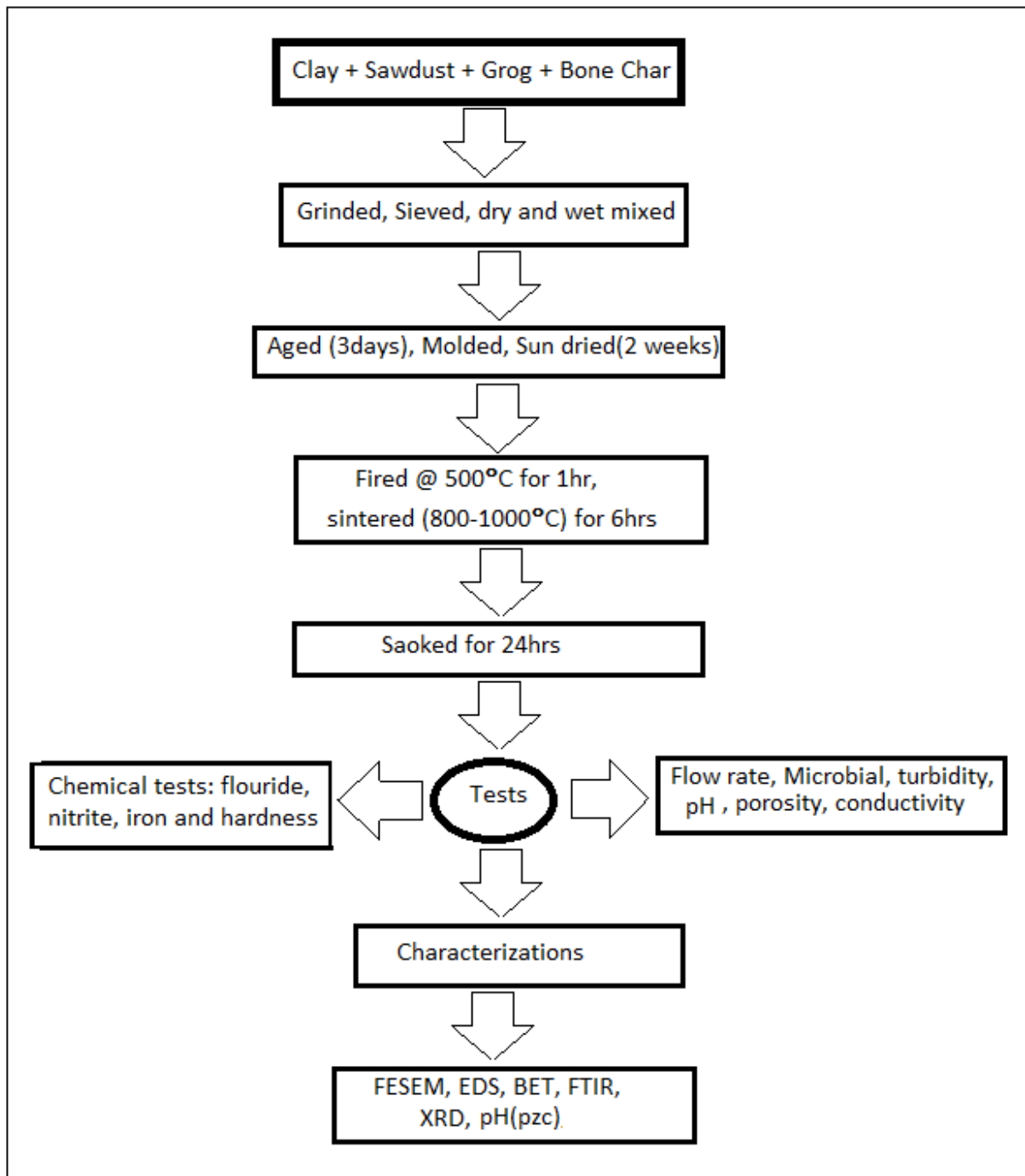


Figure 11. The flow chart for the filter production process and testing.

3.3. Ceramic Filter Test

3.3.1. Flow Rate

Flow rates were measured from the water source with the turbidity of 58NTU as the input for the filter. Flow rate testing is an important quality assurance step which indicates the rate at which water passes through the filter element. So, the produced filters for this work were fully immersed in water and soaked for 24 hours to ensure full saturation of filters at the beginning of the test and to achieve standardized results. Once soaked, the filters were transferred onto a flow testing rack. Each of the filters was filled to the brim with water. Once the filter was filled to the brim, a timer was started for one hour. The filter was filled with influent and repeatedly re-filled to the brim level for 1 hour. After an hour, the filter was removed from the rack and the flow rate of each filter was measured with a measuring cylinder. Finally, the flow rate of the selected filter was recorded in terms of L/h and the obtained data were analyzed (Rayner, J. 2006). The same procedure was used to measure the flow rate of each filter at different time intervals: 15, 30, 45 and 60 minutes.

3.3.2. Escherichia coli

The water used for the bacterial test was collected from Modjo River which is contaminated with pathogenic bacteria (Kenesa Chali, 2017) by purposive sampling techniques (Ilker.E et al., 2016), and taken to Oromo Self Help Organization/ OSHO Laboratory which is found in Modjo Town. Sufficient amount of contaminated water sample collected from the river was diluted with sterilized water by 1:100 ratios (i.e., 1ml of contaminated raw water was added to 99ml sterilized water) due to the high concentration of E.coli in 100ml of raw water.

3.3.2.1. *The Sampling Process*

The sample bottles were cleaned thoroughly with a suitable detergent and hot water, repeatedly rinsed with hot and distilled water. The sample bottles were sterilized for an hour at a temperature of 170°C, loosen caps before autoclaving to prevent distortion. The sterilized bottle was opened; it was held by the lower part and was submerged to a depth of about 20 cm with the mouth facing slightly upwards and filled with sample water leaving ample airspace in the bottle (about 2.5 cm) to facilitate mixing by shaking before the examination. The bottle was capped and placed in a clean plastic bag and transported to OSHO Laboratory for the *E. coli* test.

3.3.2.2. Incubation of the *E. coli* Plate

The 10mL syringe was used to draw water from diluted water sample for *E. coli* test. The syringe was sterilized by sucking hot water, and after 10 seconds the water was discarded to the discharge vessel. The filter paper holder was pasteurized by submerging its upper part in the hot water and the water of the filter paper holder was drained to the discharge vessel. A clean glass was also sterilized in the same manner. The pasteurized glass was filled with the water to be analyzed. A sterilized filter paper was taken with pasteurized forceps holding it by the edge and was placed on the pasteurized filter paper support. The filter paper support was closed with the cap carefully and tightly to avoid leakages during filtration. The 10mL water sample was drawn from the water sample by the syringe and put on the filter paper then the syringe was fixed with the filter paper support and then the syringe handle was pulled slowly to filter the 10mL water sample through the filter paper; finally the filtered water was discarded into the discharge vessel. The filter paper support was opened and the filter paper was removed carefully from the filter paper holder by pasteurized forceps. The filter paper was placed carefully on the *E. coli* plate to avoid air pockets between the nutrient path and the filter paper and covered tightly, marked then placed in an incubator for 24 hrs of incubation at a temperature of 35°C. After 24 hrs the number of blue spots (*E.coli* colonies) was counted and recorded a total of about 25 in a 10mL diluted water sample. *E. coli* concentration for 100mL of a water sample is counted by multiplying the count of the 10mL sample by 10 (Arora and Arora, 2008).

Finally, the numbers of *E. coli* density and removal efficiency of the ceramic filters were calculated according to (Anwar, 2011) and expressed as CFU/100ml:

$$\% R.E, \eta = 100 \left(1 - \frac{NtF}{NtB} \right) \dots\dots\dots 3.1$$

Where, NtB, is the number of *E. coli* before in 100 ml of raw water and NtF, is the number of *E. coli* in 100 mL of water after filtration.

3.3.3. Fluoride Removal Efficiency

In this test Ion-Selective Electrode (Orion Model 940 Expandable Ion Analyzer) was used to determine the fluoride removal efficiency of seven filters on the synthetic water samples. Two filters with the compositions of clay (50 and 60)% , grog 15% , sawdust (35 and 25)% that

sintered at 800°C respectively, one filter from 50% clay, 15% grog, 35% sawdust compositions sintered at 800°C, and three filters with clay (70, 75 and 80)%, grog 5%, sawdust (25, 20 and 15)% sintered at 1000°C respectively were prepared with 5% bone char for the fluoride removal efficiency investigations. Fluoride removal efficiency can be calculated by taking the fluoride concentration difference before and after filtration with a ceramic filter.

3.3.3.1. Preparation of TISAB

500ml distilled water was placed in a 1L beaker and 7g trisodium citrate ($\text{Na}_3\text{C}_6\text{H}_5\text{O}_7 \cdot \text{H}_2\text{O}$), 56gm sodium chloride and 2gm ethylenediaminetetraacetic acid (EDTA) were added to it and stirred to dissolve. To 57mL glacial acetic acid 5M sodium hydroxide was added until the pH reached 5.3 and transferred to a 1L volumetric flask and diluted with distilled water to the mark of the flask.

3.3.3.2. Calibration of the Electrode

20mL of fluoride solutions with different fluoride concentrations: 1mg/L, 2mg/L, 3mg/L, 4mg/L, and 5mg/L were prepared. 2mL TISAB was added to each solution. The potential reading of each concentration was taken and the graph of potential (E in mv) versus the logarithm of concentration (Log C in mg/L) was drawn then the slope of the graph and r^2 were calculated to check the accuracy of the measurement.

3.3.3.3. Sample Preparation and Fluoride Measurement

10mL of the sample was put into a 50mL plastic beaker and 10mL distilled water and 2mL TISAB were added. The sample solution was placed on a magnetic stirrer. The electrodes were immersed in the sample solution and the developed potential was measured while stirring on a magnetic stirrer. The electrodes remained in the solution until the millivolt reading was constant or no drift sign was visible on the liquid crystal display/LCD screen. The electrodes were withdrawn from the solution and rinsed with distilled water and blotted dry between readings (blotting may poison electrode if not done gently). The potential readings of all the samples were entered in an excel (spreadsheet) program and the potential reading was converted to concentration.

The potential developed in ISE and the concentration of F⁻ in the solution correlates using Nernst equation:

$$E = E^{\circ} - (2.303RT/zF) \log [F^{-}] \dots\dots\dots 3.2$$

Where: R is the gas constant (8.314 joules/mole); T is the absolute temperature (K); z is the charge of fluoride ion in the solution; E is the measured electrode potential in the solution; E^o is the standard potential of the reference electrode; F is Faraday's constant (96,500 coulombs/mole); and [F⁻] is the concentration of fluoride ion in a particular sample solution.

3.3.4. Conductivity

For the measurements of pH and conductivity of the filtered water using the ceramic media, the same water sample used for flow rate determination was used. The pH, conductivity, and turbidity of the water sample used before filtration for testing the efficiency of the developed filters were 8.2, 157 μs/cm and 58 NTU respectively. Standard solution of KCl was prepared with concentration and conductivity of 0.7455 ppm (1330 μs.cm⁻¹), 0.0746 ppm (133 μs.cm⁻¹), 0.0149 ppm (26.6 μs.cm⁻¹) to confirm the suitability of the instrument. A beaker was filled with 8ml of conductivity calibration solution and the probe of the conductivity meter was immersed into the beaker. The instrument (Conductivity Meter HI9033–Hanna) was turned on and the appropriate range of measurement was selected. The probe was tapped repeatedly on the bottom of the beaker and the solution was stirred to ensure that no air bubbles were trapped inside the sleeve. The calibration timer was turned on until the proper conductivity value was displayed at 25°C and the calibration was completed and the instrument was ready for use.

3.3.5. Turbidity Test

The turbidity removal efficiency of the ceramic filters was evaluated for the same water source that used for the flow rate test using the instrument CL52 D NEPHELOMETER (provided turbidity measurement in Nephelometric Turbidity units in a range of 0.1 to 400 NTU) (ASTM International, 2003a). The measurement was made before and after filtration of the collected water sample using CF to evaluate the removal efficiency of the prepared filter. Before measurement the turbidity meter was calibrated regularly using different calibration standards, bottled water (0.18 NTU) was used. The samples were transferred into special covet and placed

in the turbidity meter. Then, continue rinsing of covet with distilled water and gently wipes the outside part of covet by soft tissue. Finally, the turbidity removal efficiency (η), can be calculated using the equation:

$$\eta = 100 \left(1 - \frac{r_B}{r_A} \right) \dots\dots\dots 3.3$$

where: r_B - is the turbidity before filtration and r_F - turbidity after filtration.

3.3.6. pH

The pH of the raw water and filtered water samples were analyzed with pH Meter, Metrohm, (pH Electrode, Metrohm 6.0220.100) in OSHO laboratory. The pH meter was calibrated before sample determination using standard buffers. A magnetic stirrer was inserted inside the sample on a 50 ml beaker and the electrodes of the pH meter were submerged. Readings were recorded when the meter stabilized.

3.3.7. Zero point charge (pH_{zpc})

The pH at which the sorbent surface charge has a zero value is referred to as the point of zero charges (pH_{zpc}). The Isoelectric point or Zero point charge (pH_{zpc}) of the selected samples was measured by using the method described by (Duran-Valle, 2012). 0.1 M of 10 NaCl solutions having the initial pH values ranging from 1 to 12 with 1 increment was prepared in duplicate using 0.1M HCl and 0.1M NaOH. Then the solutions were filtered with C900-50-35-15 filter media. The final pH values of the twelve solutions were then measured and thereby calculation of ΔpH was made by subtracting the initial pH values from final pH values. The graph was drawn by plotting the initial pH values against ΔpH . From the graphs plotted, the pH_{zpc} (point of zero charges) of the adsorbent was determined.

3.3.8. Water Hardness Agents Removal Test

Water hardness removal efficiency of the ceramic filter elements was evaluated with complexation titration method by using EDTA and Eriochrome Black-T (EBT), the metal ion indicator (Kolthoff and Stenger, 1947). Magnesium solution was prepared by dissolving 4.6g $MgCl_2 \cdot 6H_2O$ in 500 mL conical flask with distilled water and transferred to 1000 mL volumetric flask and filled with distilled water up to the mark. Calcium chloride solution was prepared from 1.1g of solid $CaCl_2$ dissolving in a beaker of 500 mL with distilled water then transferred to 1000

a sharp endpoint through the complexation of the EBT indicator with the magnesium ions present.

3.3.9. Iron Removal Test

The purpose of this activity was to evaluate the iron removal efficiency of the selected ceramic filters from synthetic water using the method developed by (Basheer et al., 2011). The iron removal efficiency of ceramic filters was performed with single beam UV-visible spectrophotometer (XP-1000P, China, number 2000 to 8004) for synthetic water sample of 27.12mg/L concentration of iron (II). For the iron determination, a stock solution of Mohr's salt $[\text{Fe}(\text{NH}_4)_2(\text{SO}_4)_2 \cdot 6\text{H}_2\text{O}]$ 1000 ppm was prepared by dissolving 6.97 g of the salt in 500 mL beaker, then transferred to 1000 mL volumetric flask and filled to the mark. Standard solutions at different concentrations (30 ppm, 20 ppm, 10 ppm, 8 ppm, 6 ppm, 4 ppm, and 2 ppm) were prepared from the stock solution for the calibration of the UV-Visible spectrophotometer instrument. The concentration of 1,10 phenanthroline was 3 times the concentration of Mohr's salt because of 1mol of Mohr's salt for the formation of the orange-red color complex $[(\text{C}_{12}\text{H}_8\text{N}_2)_3\text{Fe}]^{2+}$ with 3 moles of 1,10 phenanthroline (Figure 12). The absorbance of the red complex produced was measured with a spectrophotometer at a wavelength of 510 nm. Hydroxylammonium chloride was used as a reducing agent for the conversion of iron (III) to iron (II) in the solution. Before UV determination 1mL HCl, 5 mL hydroxyl ammine, 3 mL sodium acetates, 5 mL 1,10 phenanthroline were added by taking 10 mL solution from each of the standard solutions, and the blank. Then, the solutions were filled up to mark with distilled water in 100 mL volumetric flask. The same procedure was followed for the determination of iron concentration before and after filtration.



Figure 12. Solutions prepared for UV-Visible spectrophotometer.

3.3.10. Nitrite Removal test

The nitrite removal test was conducted on synthetic water using single beam UV visible spectrophotometer (XP-1000P, China, number 2000 to 8004) on synthetic water using the method developed by(Afkhamiet al., 2004). The stock solution of 1000 ppm was prepared by dissolving 1.456 g sodium nitrite in 1000 mL volumetric flask and filled to the mark with distilled water. The standard solutions of (100 ppm, 10 ppm, 8 ppm,6 ppm, 4 ppm, and 2 ppm) were prepared from the stock solution for standardization of the instrument. A solution of 0.025 M Paranitroaniline and 0.025 M 1-naphthol were prepared from the mass of 1.726 g paranitroaniline and 1.802 g of 1-naphthol by dissolving in 1000 mL volumetric flask and filled up to the mark separately. Nitrite under acidic conditions is going through diazotization with para-nitroaniline in an ice bath and is formed a violet colored complex with 1-naphthol under basic condition. All the chemicals used were analytical reagents.



Figure 13. Solutions prepared for UV-Visible spectrometer of nitrite.

3.4. Composition analysis

For the determination of major and minor oxides complete chemical analysis (Analytical method LiBO_2 Fusion, HF attack, Gravimetric, Colorimetric, and AAS) of the raw clay and sintered filters were done at Geological Survey of Ethiopian Geochemical Laboratory, Addis Ababa. The results of chemical analysis were shown the percent of the major and minor oxides and Loss on Ignition (LOI).

3.5. FT-IR Analysis

A portion of the filter sample was pulverized to a fine powder in an agate mortar and pestle. A small portion of the material weighing approximately 2 mg was then ground and mixed thoroughly with 40 mg of dried potassium bromide (KBr). The powder was distributed evenly within the die by first rotating the plunger, and the assembly was placed in a press. A load of 10 tonnes was applied for 3 to 4 min to form a transparent KBr disc. The die was disassembled and the disc carefully removed and placed in a sample holder. The Perkin Elmer Spectrum 65 Spectrum BX FTIR (at Addis Ababa University, Department of chemistry, Ethiopia) was used. The beam splitters used were KBr for the mid-IR region 4000 to 400 cm^{-1} and the resolution was 4 cm^{-1} .

3.6. Powder X-Ray Diffraction (XRD)

X-Ray Diffraction (XRD) technique was used for phase identification of raw clay and the fired filter materials. The raw sample was roughly ground and its same portion was scanned by XRD which named as a bulk state (bulk). The clay particles obtained from bulk sediments placed in a large glass cylinder filled with water with addition of 5×10^{-4} mol/L sodium pyrophosphate as deflocculating agent then the suspension transferred in to large cylinder to settle in the water according to Stokes Law by sedimentation from suspensions and washed by pure water to remove the dispersing agent, dried and powdered for XRD analysis. Then the filtrate was dried and scanned by XRD which named as a normal state (normal). Finally this normal state of the sample (clay fraction $< 2 \mu\text{m}$) heat treated at $550 \text{ }^{\circ}\text{C}$ and scanned as heat treated state. For the present work XRD data have been taken for the prepared raw clay powders and fired filter powders with X-ray diffractometer (Bruker D8 Advance Diffractometer) at room temperature, using Nickel filtered $\text{Cu-K}\alpha$ radiation ($\lambda = 1.54 \text{ \AA}$), over the range of Bragg angles ($10^{\circ} \leq 2\theta \leq 80^{\circ}$) with a scanning speed of $2^{\circ} \text{ min}^{-1}$. The instrument was run at power settings of 40 KV and 30 mA and the powder samples were mounted into a top loaded circular sample holder to be rotated in the instrument at 50 rpm.

3.7. Field Emission Scanning Electron Microscopy (FESEM)

The Field Emission Scanning Electron Microscopy (FESEM) is a useful technique to study the topography, morphology, and composition of the materials with much higher resolution. In this work, the microstructural investigations of the sintered ceramic samples were made on the fractured surface of the sample using FESEM (JEOL-JSM-6610LV, Tokyo, Japan) after a thin layer of gold was coated by using Auto Fine Coater (JFC-1600) for 90 seconds. Energy Dispersive X-ray Spectroscopy (EDS) with the conjunction of FE-SEM was used to characterize the elemental composition of the analyzed volume.

3.8. The porosity of Ceramic Filters

3.8.1. Total porosity

The porosity of the ceramic filters was determined using the water absorption test (direct) method (D'ujanda, 2001) in Adama Science and Technology University Applied Chemistry Post

Graduate Laboratory. Three different samples weighing (50 g, 60 g, and 100 g) were taken and the average porosity of these three samples and the apparent porosity of a ceramic filter was determined. The samples were weighed when dry in the air then saturated in distilled water at room temperature for 24 hours. The water with the samples was then boiled for about two hours and allowed to cool to room temperature for another 24 hours. This was done to ensure that the air in the open pores of the filter samples was replaced by the distilled water. The soaked samples were weighed under distilled water, then removed and the surface was wiped with tissue paper and weighed in air. The weight of the wire was subtracted from the value obtained while determining the weight of the sample suspended in water. Apparent porosity was then calculated using the expression given below.

$$P = 100 \left[\frac{W_{saturate} - W_{dry}}{W_{saturated} - W_{underwater}} \right] \dots \dots \dots 3.5$$

Where; $W_{saturated}$ is the weight of the sample when saturated in water, W_{dry} , is the weight of the dry sample and $W_{underwater}$, the weight of the sample underwater.

3.8.2. Specific surface area and pore size distribution analysis

Brunauer–Emmett–Teller (BET) nitrogen physisorption measurements were performed at 77K using an ASAP 2000 absorptiometer (Micromeritics, USA). The samples (~400 mg) were degassed at 473K for 24 hours prior to the sorption experiment. The total pore volume, V_{tot} , was measured as the adsorbed amount of N_2 at P/P_0 values near to 0.99 allowing the surface area to be calculated by the BET equation. The pore size distribution was determined by the Barrett-Joyner-Halenda (BJH) method applied to the N_2 desorption isotherm branch.

3.9. Data Analysis

One way analysis of variance (ANOVA) was used to test if there are significant differences in porosity, flow rate, E.coli, hardness, and nitrite removal efficiencies, due to the variation of the ratio of raw materials and sintering temperature among different filters at ($p = 0.05$) and the correlation among variables (Miller and Miller, 2010). The data analysis was done by SPSS version 23 software and excel 2007.

4. RESULTS AND DISCUSSION

4.1. Flow Rate Test

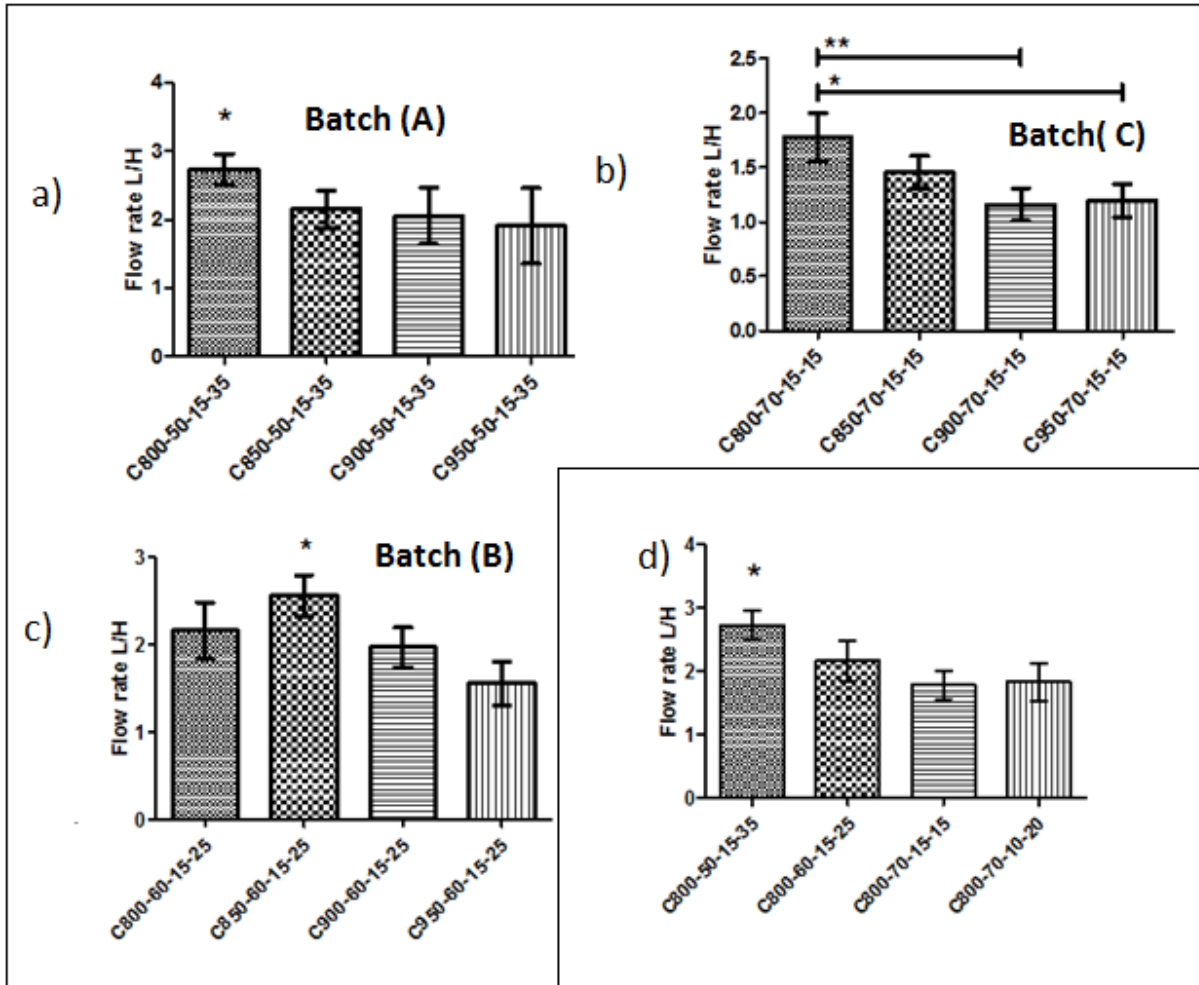
Flow rates were measured from the same source water with the turbidity of 58NTU as the input for the filter. Figures 14(a-d), 15(e-h) and Appendix A, summarized the results of the flow rate experiments. The results in Appendix A depicted as the flow rate of the ceramic filters were affected with ratios of clay, sawdust, grog as well as the sintering temperatures of the filter elements. The average flow rate values of ceramic filters with the composition of clay (50%), grog (15%) and sawdust (35%), decreased with increase in sintering temperature; 2.73 ± 0.23 L/h, 2.15 ± 0.28 L/h, 2.05 ± 0.41 L/h and 1.91 ± 0.55 L/h respectively as shown on the fig.14a. Increasing the sintering temperature of the ceramic filter body reduces the pore volume or pore size, and increases the density of the filter elements. The flow rates result of C(800-950)-50-35-15 filter designs showed the inverse relationship between sintering temperature and flow rate.

The flow rates of filters with designs; C800-50-15-35, C800-60-15-25, C800-70-10-20 and C800-70-15-15 were 2.73 ± 0.23 , 2.16 ± 0.32 , 1.83 ± 0.30 and 1.78 ± 0.22 , respectively. These results showed a decrease in flow rate with the decrease of burnout materials at a fixed sintering temperature (800°C). According to Lantagne 2001a, pore size and total porosity of the filter element depends on the amount of burnout material added to the clay. For this reason, the flow rate results revealed, filters with high burnout materials and sintered at low temperature have a relatively large flow rate in comparison with filters with high sintering temperature. This might be observed due to the formation of more isolated and interconnected pores in the ceramic filter body (Liang et al., 2006, .Molina et al., 2005).

As shown on the Fig.14c, the flow rate of the filter in the same group decrease with the increase in the sintering temperature with the exception of the filter made with 60% clay, 25% sawdust, 15% grog and fired at 850°C (Filter C850-60-25-15) that was the fastest filter (2.56 ± 0.24 L/h) in the group (Fig.14c).

The average flow rate of filter designs: C800-50-15-35 (2.73 ± 0.23 L/h), C850-60-15-25 (2.56 ± 0.24 L/h), and C900-70-5-25 (2.94 ± 0.38 L/h) (Table 5) were relatively good as per the potters for peace recommendation. The average flow rate range of the filter designs produced by

this team are ranged from 1.16 ± 0.15 liter per hour to 2.94 ± 0.38 liter per hour, which is in the range recommended by potters for peace (Rayner.J, 2006). This might be due to the proper mixing process of the raw materials, the ratio of raw materials used, and optimized sintering profile used during the preparation of the filters element.



* indicates the p value is < 0.05 (the statistical difference is significant), while ** indicates the p value is < 0.01 (the statistical difference is more significant).

Figure 14. (a-d). The flow rate of ceramic filter designs of Batch A, B, C and mix (d).

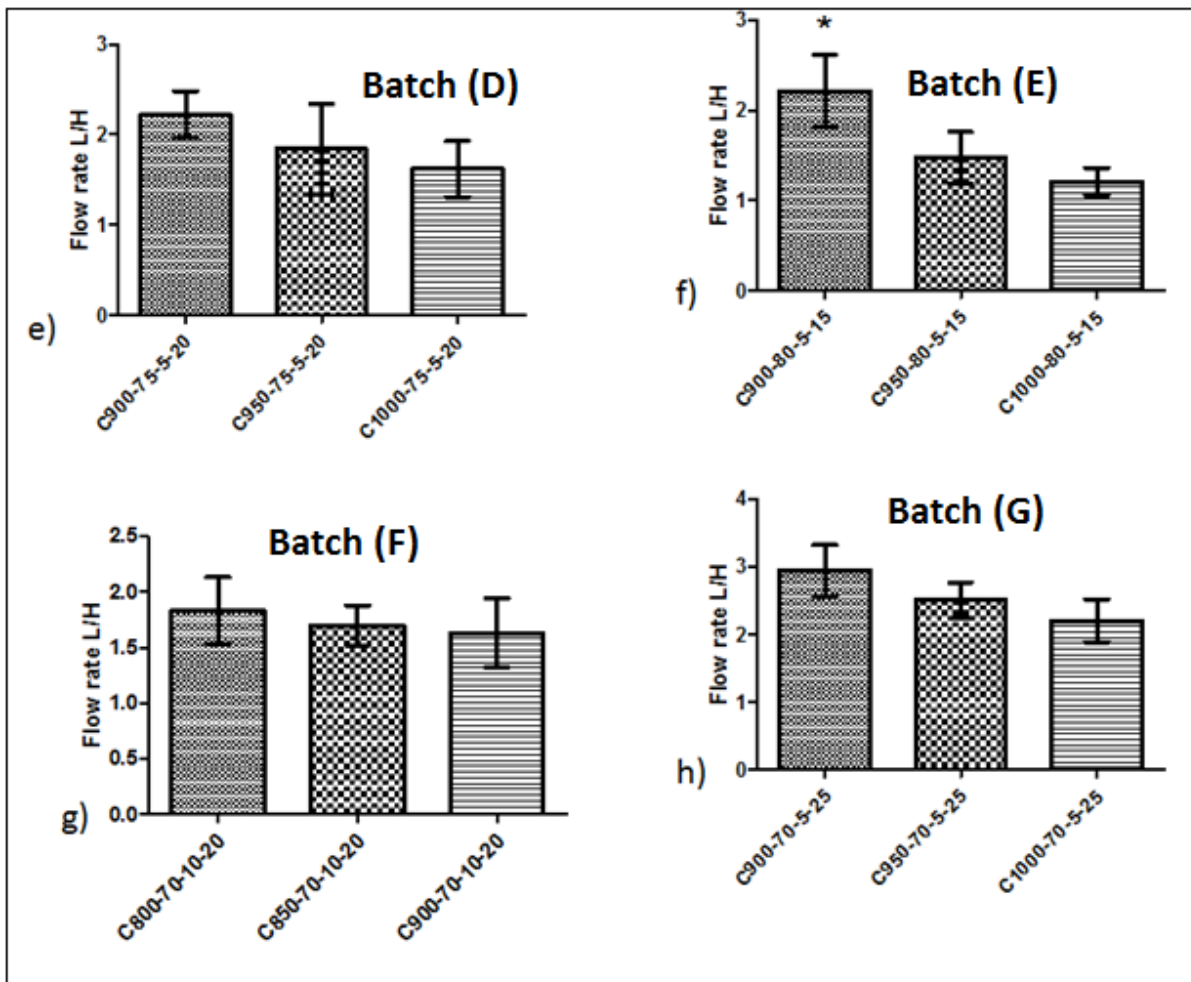


Figure 15(e-h). The average flow rate of ceramic filter designs of Batch D, E, F, and G.

Table 5. Test results of flow rate for filters with different ratios of clay, grog and sintered at 900 and 950°C.

Filter Code	Sintering temperature, percentage of (clay, grog, and sawdust)	Flow rate (L/h)
F7	C900-60-15-25	1.97±0.23
F16	C900-70-5-25	2.94±0.38
F8	C950-60-15-25	1.56±0.25
F17	C950-70-5-25	2.50±0.27

Moreover, filters with C900-70-5-25 and C950-70-5-25 designs were derived from filters C900-60-15-25 and C950-60-15-25 by reducing the percentage of grog from 15% to 5% and increasing clay from 60 % to 70 % by keeping the percentage of sawdust and sintering temperature constant. The average flow rate of F7, F16, and F8, F17 were increased from 1.97 ± 0.23 to 2.94 ± 0.38 and 1.56 ± 0.25 to 2.50 ± 0.27 respectively. These flow rates change observed, on filters with a low percentage of grog and a high percentage of clay were due to the low porosity of grog than the clay. According to (Abiriga and Obwoya Kinyera, 2014) the introduction of grog or fired clay was found to improve the mechanical properties of the filters, although if so much proportion of it is added the flow rate is lowered. Table 6 showed the influence of the amount of sawdust and grog on the flow rate of the ceramic filters. The rate of water flow is higher for filters with a high proportion of sawdust and low grog in the filter compositions. According to (Dies, 2003), interconnected pores are formed when the green body of the filter with precise proportions of sawdust are fired.

Table 6. Test results of flow rate for filters with different ratios of grog and sawdust.

Sintering temp, % (clay, grog, and sawdust)	Filter code	Flow Rate (L/h)
C800-70-15-15	F9	1.78 ± 0.22
C800-70-10-20	F13	1.83 ± 0.30
C850-70-15-15	F10	1.46 ± 0.15
C850-70-10-20	F14	1.70 ± 0.18
C900-70-15-15	F11	1.16 ± 0.15
C900-70-10-20	F15	1.63 ± 0.31
C900-70-5-25	F16	2.94 ± 0.38

At the 0.05 level, the data drawn for flow rates were significantly different in flow rate for groups of ceramic filters with percentage composition of clay, sawdust and binder : 60%, 25%, 15% ($P = 0.0103$), 70%, 15%, 15% ($P = 0.0073$) and 50%, 35%, 15% ($P = 0.0153$). The mean flow rate P-values of ceramic water filters with composition: 80%, 5%, 15% ($P = 0.1254$), 70%, 15%, 15% ($P = 0.6725$), 70%, 25%, 5% ($P = 0.0822$) and 75%, 20%, 5% ($P = 0.2154$) were

found to be greater than 0.05 and thus, failed the test. The flow rate results of multiple tests on 12 selected ceramic filters were listed in Table 7. The obtained results for the flow characteristics experiments showed that the developed filters are porous and free from major fractures. The flow rate of the ceramic clay filter is basically dependent on the nature of the pores in the filter fired body and the crack formed during sintering (Hangan et al., 2009).

Table 7. The flow rate of twelve ceramic filters in a 15 minutes interval in (L/h).

Filter Design	15min	30min	45min	60min
C800-50-15-35	0.60	1.17	1.81	2.54
C850-50-15-35	0.56	1.09	1.59	2.13
C900-50-15-35	0.51	1.03	1.49	2.09
C950-50-15-35	0.42	0.90	1.41	1.86
C800-60-15-25	0.63	1.19	1.59	2.11
C850-60-15-25	0.57	1.15	1.79	2.41
C900-60-15-25	0.52	0.99	1.39	1.97
C950-60-15-25	0.37	0.78	1.11	1.60
C800-70-15-15	0.50	0.95	1.36	1.81
C850-70-15-15	0.39	0.74	1.05	1.45
C900-70-15-15	0.32	0.61	0.89	1.16
C950-70-15-15	0.28	0.53	0.83	1.23

4.2. Porosity Test

The variation of apparent porosity results with temperature, % clay, % grog, and % sawdust ratios are summarized in Appendix B. The relative percent porosity range of C(800-950)-50-15-35, C(800-950)-60-15-25 and C(800-950)-70-15-15 were 35.89-40.32 %, 30.37-32.95 % and 27.62-30.65 %. According to the reports by (Simonis and Basson, 2012, Yakub, 2012) total porosity of ceramic water filter are in the range of 34 % to 46 %. Filters with more combustible materials have more void space and the total porosity of the fired filter is roughly proportional to the volume of combustible material added. The results presented on figures 16 (a-d) and 17(e-h), exhibited the apparent percent porosity of ceramic filters of different groups. Different porosities were recorded for a filter of different designs as indicated in figure 16 and 17. Filters with the same sawdust-to-clay ratio, sintered at low sintering temperatures in their respective group

relatively showed the better apparent percentage porosity. According to (Joong and Kang, 2005), sintering ceramic filter at higher temperature reduces the void space in the ceramic filter by eliminating the isolated and interconnected pores. The ANOVA results of porosity showed that there is a significant difference between different filter groups ($p = 0.00$) at 95% confidence level, this could be due to the impacts of sintering temperature, different percentage ratios of clay, grog, and sawdust used for the preparation of each ceramic filter. According to (Doris van, 2006), ceramic filters with total porosity range of 30-38% are free from the fracture.

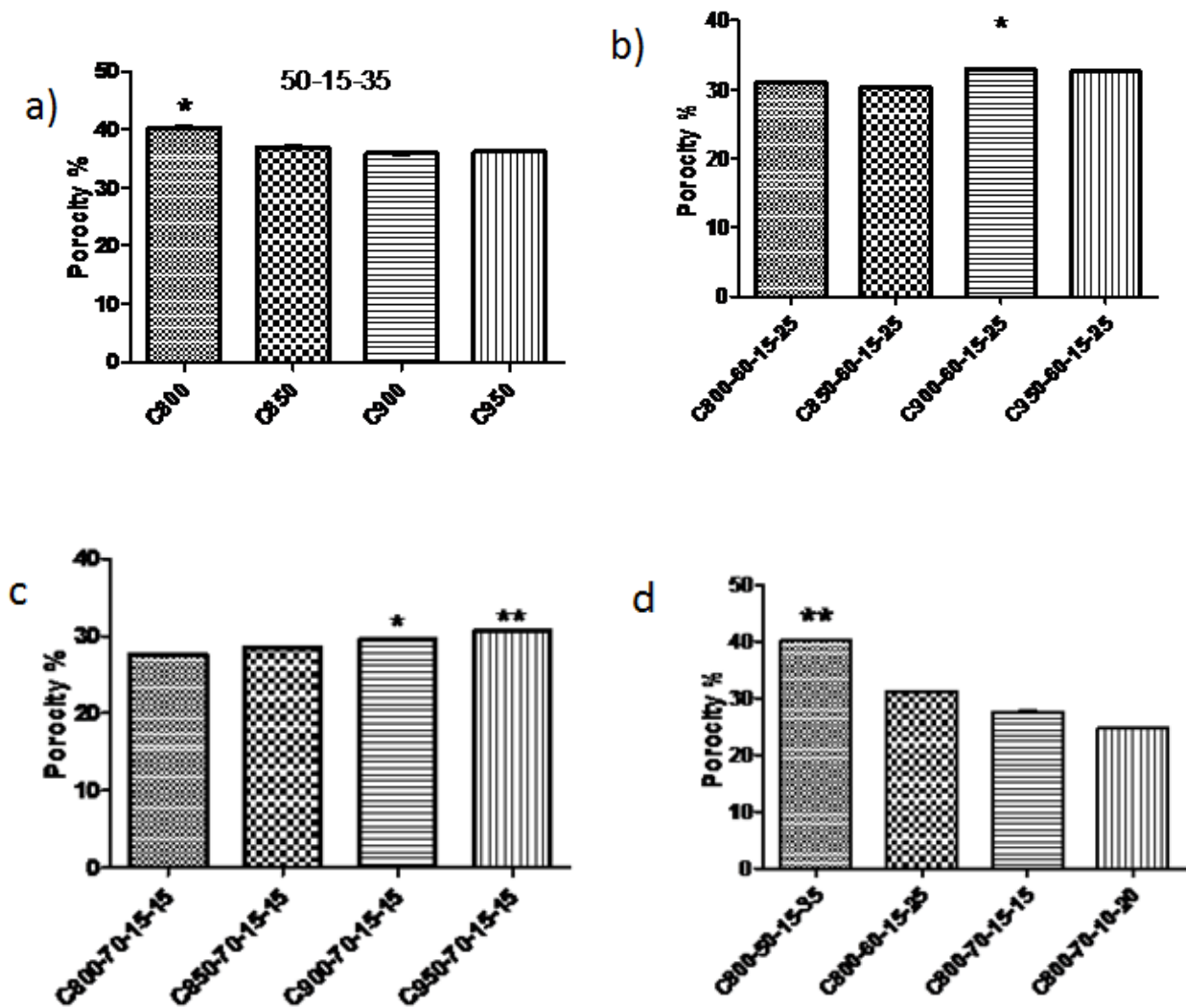


Figure 16. (a-d). The average porosity of ceramic filter designs of Batch A, B, C, and D.

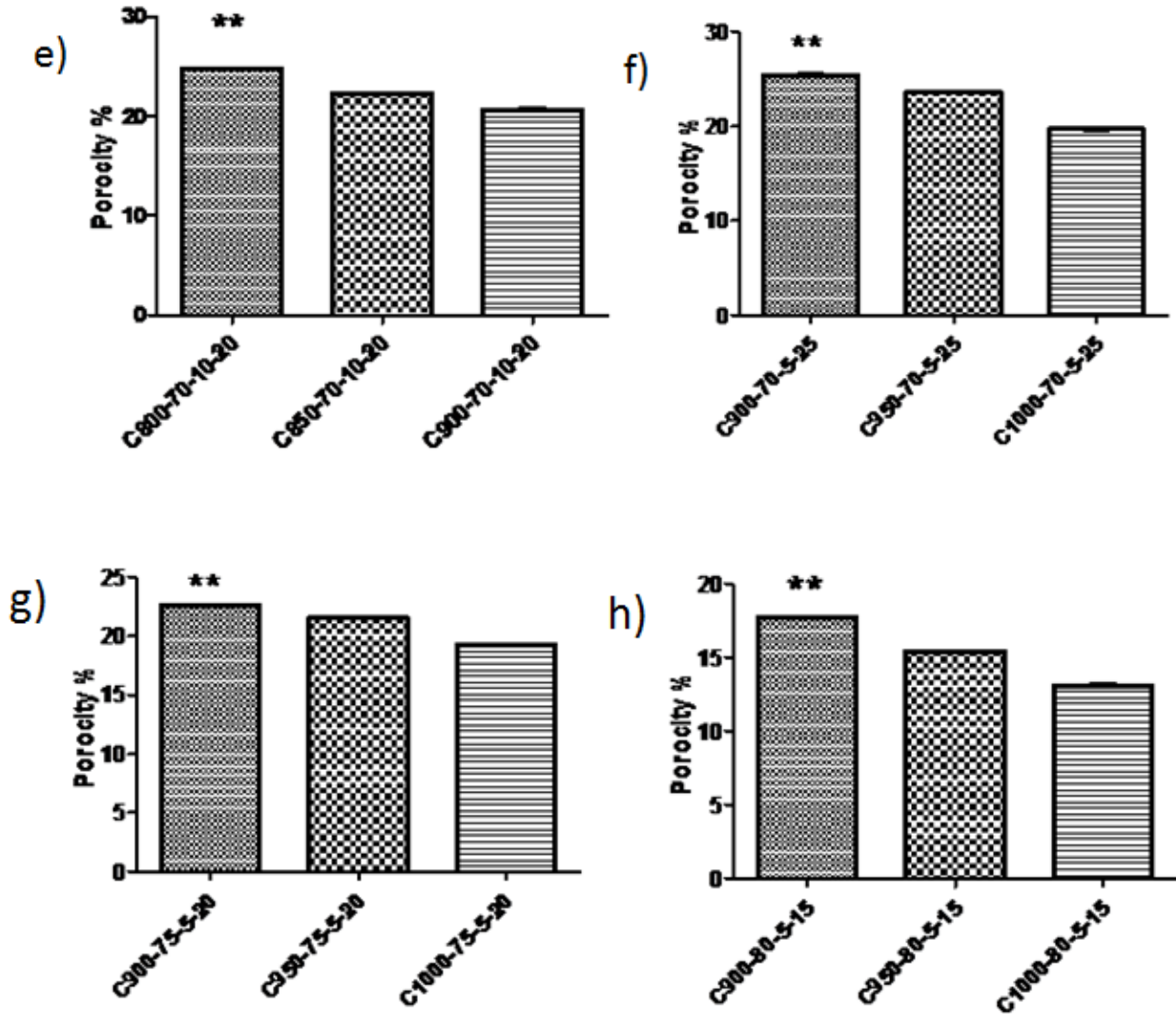


Figure 17. (e-h). The total porosity of ceramic filter designs of Batch, E, F, G, and H.

4.3. Escherichia coli Removal Efficiency

E. coli filtration experiments were performed on all filters with contaminated water which had more than 250 CFU (Colony Forming Unit) *E.colis* bacteria detected in 100 ml. As indicated in Table 8, the number of the colony of *E.coli* bacteria after filtration in all the filtrates expressed in terms of percentage reduction of *E.coli* bacteria removal denoted the microbial removal efficiency of the ceramic filters were ranged from 85.47 ± 0.57 % to 99.87 ± 0.23 %. The filters with less than 99% removal efficiency were termed as high-risk filters according to the WHO water risk categories.

Filter Designs like C900-50-15-35, C950-50-15-35, C900-60-15-25, and C900-70-15-15 had zero *E.coli* per 100 ml, and according to the WHO water risks categories, they are termed as risk-free filters. Ceramic water filters with interconnected pores and average pore diameter less than the size of bacteria are more efficient in removing microbial from bacterially contaminated water sources (Clasen et al., 2007). Among the developed ceramic water filters for this project, filters: C900-50-15-35 (99.6±0.40%), C950-50-15-35 (99.73±24%), C900-60-15-25 (99.87±0.23%), and C900-70-15-15 (99.6±0.40%) have better efficiency in removing microbial from bacterially contaminated water sources. Only four designs from the developed filters met the WHO standard for water treatment. According to (Yakub *et al.*, 2013) Neither *E. coli* nor other bacteria should be detectable in 100 ml of drinking water. From statistical ANOVA analysis, there were significant variation in the *E.coli* removal efficiency of ceramic filters of : C800-50-35-15, C850-60-25-15, C950-70-15-13, C900-70-10-20, C900-70-5-25, and C900-70-15-15 ($p < 0.05$).

Generally, the trends pointed out, the increase of the microbial removal efficiency of the filters with the increase in the percentage composition of clay plus grog and firing temperature. The lower removal efficiency registered were mainly for filters with a high amount of burnout materials at low sintering temperature in their respective batch and rarely observed on filters that sintered at high temperatures (Lantagne et al., 2009). The later one might be occurred due to the poor mixing condition of burnout material with clay and grog. This is most likely lead to the formation of cracks and heterogeneous pores with different sizes that can allow the *E. coli* with filtrates during filtration as it was observed microstructure analysis of SEM images of filters in the next section.

Table 8. The % microbial removal efficiency of the ceramic filters with different Design.

Batch Code	Filter Designs	Trail 1(%)	Trail 2(%)	Trail 3(%)	Mean ± SD
A[F1-F4]	C800-50-15-35	96.0	95.6	96.0	95.87±0.23
	C850-50-15-35	97.60	98.00	98.40	98±0.40
	C900-50-15-35	99.20	99.60	100	99.6±0.40
	C950-50-15-35	99.60	99.60	100	99.73±24
B[F5-F8]	C800-60-15-25	98.80	97.60	100	98.97±1.22
	C850-60-15-25	94.40	86.40	89.60	90.33±3.36
	C900-60-15-25	100	100	99.60	99.36±0.55
	C950-60-15-25	99.60	99.20	98.80	98.99±1.90
C[F9-12]	C800-70-15-15	97.60	97.60	98.00	97.73±0.23
	C850-70-15-15	98.40	97.60	98.80	98.27±0.61
	C900-70-15-15	100	99.20	99.60	99.6±0.40
	C950-70-15-15	99.60	95.60	96.40	97.2±2.12
D[F13-F15]	C800-70-10-20	98.80	95.60	96.40	96.93±1.67
	C850-70-10-20	95.60	92.00	90.00	92.53±2.84
	C900-70-10-20	95.20	94.30	92.90	94.13±1.16
E[F16-F18]	C900-70-5-25	90.40	85.50	88.00	87.97±2.45
	C950-70-5-25	95.60	96.40	95.60	95.87±0.46
	C1000-70-5-25	98.40	96.40	98.00	97.6±1.06
F[F19-F21]	C900-75-5-20	94.00	92.00	92.00	92.67±1.15
	C950-75-5-20	97.20	94.80	96.00	96±1.20
	C1000-75-5-20	88.80	84.00	86.40	86.4±2.40
G[F2-F24]	C900-80-5-15	86.40	84.40	85.60	85.47±0.57
	C950-80-5-15	94.40	89.60	91.20	91.73±2.44
	C1000-80-5-15	96.80	95.20	93.20	95.07±1.80

4.4. The microstructure of Ceramic Filters

In this section, the microstructures of selected ceramic filters with different performance were investigated. The microstructure is one of the physical properties of ceramic materials and the major factor that affects the mechanical properties, flow rate, microbial removal efficiency and porosity of the filter element. Images obtained by scanning electron microscopy techniques, for this work can be considered for quality control of the ceramic filter body. Hence, the FESEM micrograph images of composite ceramic filters design with different efficiency were discussed in this section.

4.4.1. The Micro-structure of ceramic C(800-950)-60-15-25 filters

In this work, the microstructures of a ceramic filter with composition of 60 % clay, 15 % grog and 25 % sawdust, sintered at 800, 850, 900 and 950°C with the same dwelling time and uniform heating and cooling rate investigated with FESEM were displayed on figure 18. It has been claimed that the microstructure of the ceramic materials can be affected by the sintering profile (Zereffa and Seghne, 2018).

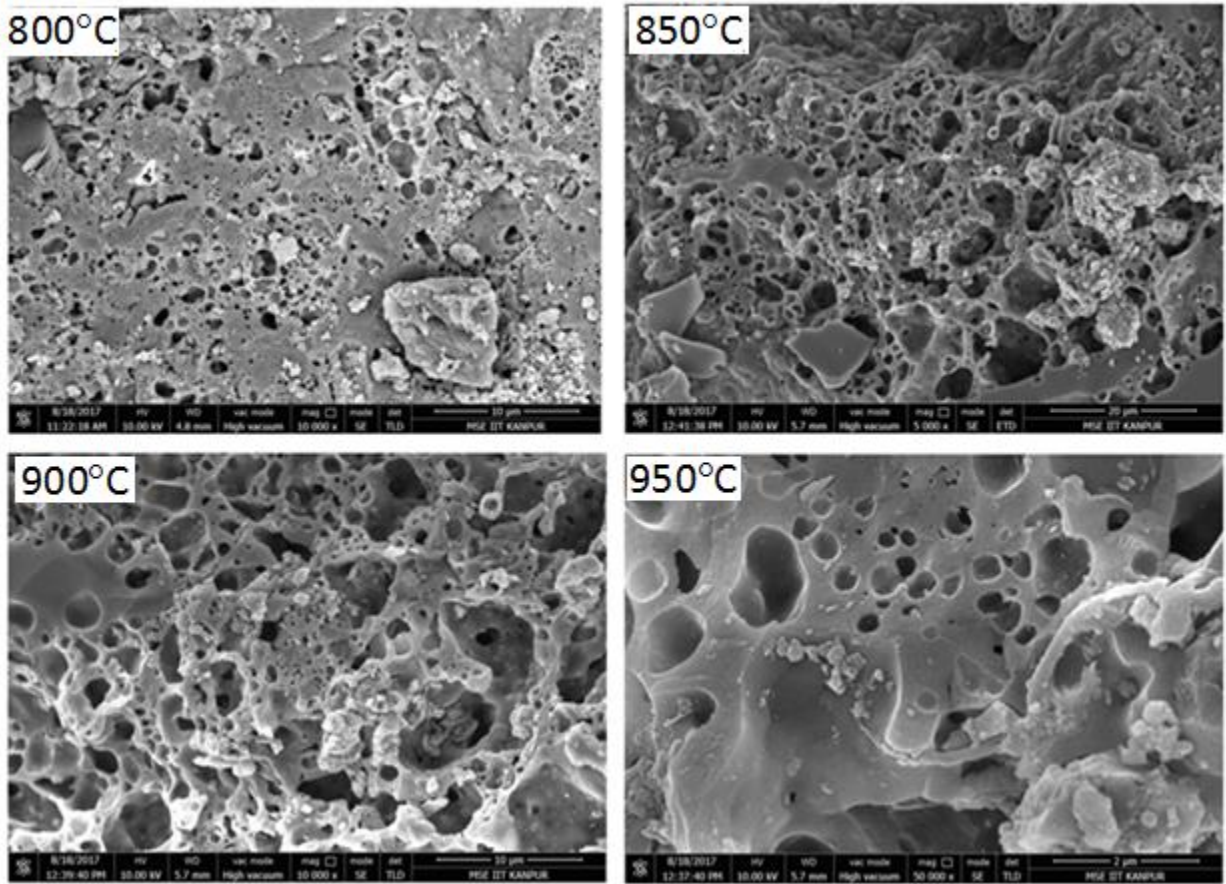


Figure 18. SEM micrographs of the fractured surface of C60-15-25 sintered at 800, 850, 900 and 950°C.

As it was observed from the FESEM images, Figure 18, there were changes on the microstructures of the filters with the change in sintering temperature. The porosity of the ceramic filter developed slightly changed with an increase in sintering temperature for the same composition of clay and burnout as it is mentioned in section 4.2. Moreover, Fig-18 revealed the effect of sintering temperature on the microstructure of the filter element that is more apparent on the filter sintered at 950°C. The flow rate results of these filters revealed the influence of sintering temperature.

The average flow rate of filter designs: C800-60-15-25 (2.16 ± 0.32 L/h), C850-60-15-25 (2.56 ± 0.24 L/h), C900-60-15-25 (1.97 ± 0.23 L/h) and C950-60-15-25 (1.56 ± 0.25) as indicated in Appendix A were relatively good as per the potters for peace recommendation (Potters without Borders, 2012). A filter that sintered at 850°C exhibited the fastest discharge. High flow rate, ~

2.5 L/h, was obtained by low total porosity filter (C850-60-15-25) which might be due to the absence of dead and isolated pores in the filter body. This is might be as the temperature increases, there is a networked pore formed when the combustible materials burn off by leaving the ceramic filter body. As indicated on the FESEM images the pore size increased with the increase in sintering temperature, caused by the overlapping of small pores. Hence, the FESEM micrograph images of the mentioned composite ceramic filters confirmed as sintering temperature highly influence the performance of the filters.

4.4.2. The Micro-structure of a ceramic filter with 5% grog

In this section, the microstructural characterization of ceramic filters with 5% grog and different designs were discussed. In the first case, ceramic filter with C900-70-5-25 design characterized with a high average flow rate of about 2.94 ± 0.38 L/h and low percentage E Coli removal efficiency ($87.97 \pm 2.45\%$) as it was discussed in section 4.1 and 4.3. The microbial removal efficiency of filters with a different design developed with a low percentage of grog (5%) was below the recommended standard (Potters without Borders, 2012). The Microstructure analysis of C900-70-5-25 design at different magnifications (Fig.19) revealed the presence of a small number of big size interconnected pores that allow *E.coli* with filtrate during filtration. This is might be one of the main reasons for the high flow rate and poor filtering effects.

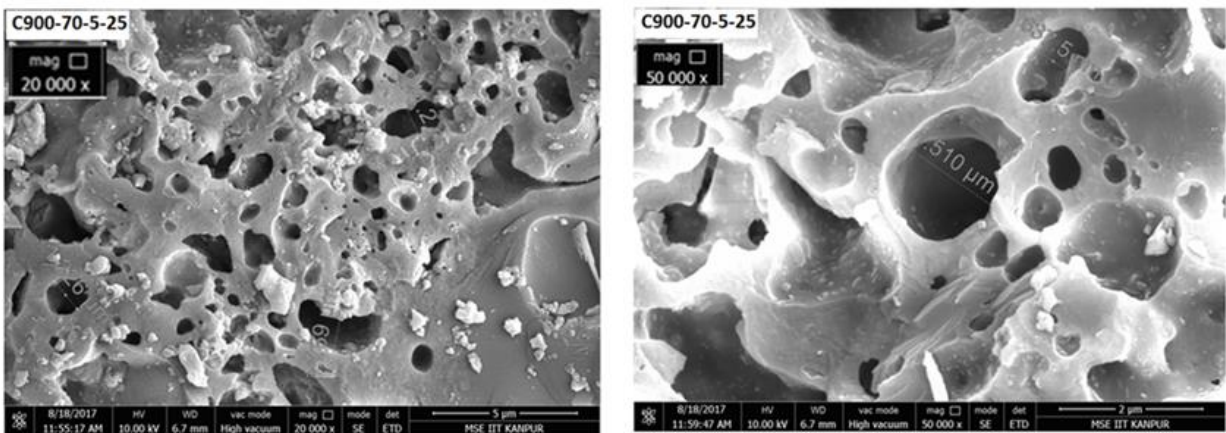


Figure 19. FESEM micrographs of porous media of C900-70-5-20 fractured surface at different magnifications.

In the second case, for filters with fixed low percentage of grog (5%), and a reduced amount of burnout materials or sawdust (20% and 15 %), their relative percentage of *E. coli* removal efficiencies were declined: C900-75-5-20 (87.97 ± 2.45 %) and C900-80-5-15 (85.47 ± 0.57 %). The typical microstructure of the ceramic filter designs with C900-75-5-20 and C900-80-5-15 (figure,29)confirmed the existence of cracks that result with high flow rates observed and poor *E. coli* removal efficiency, figure 20.

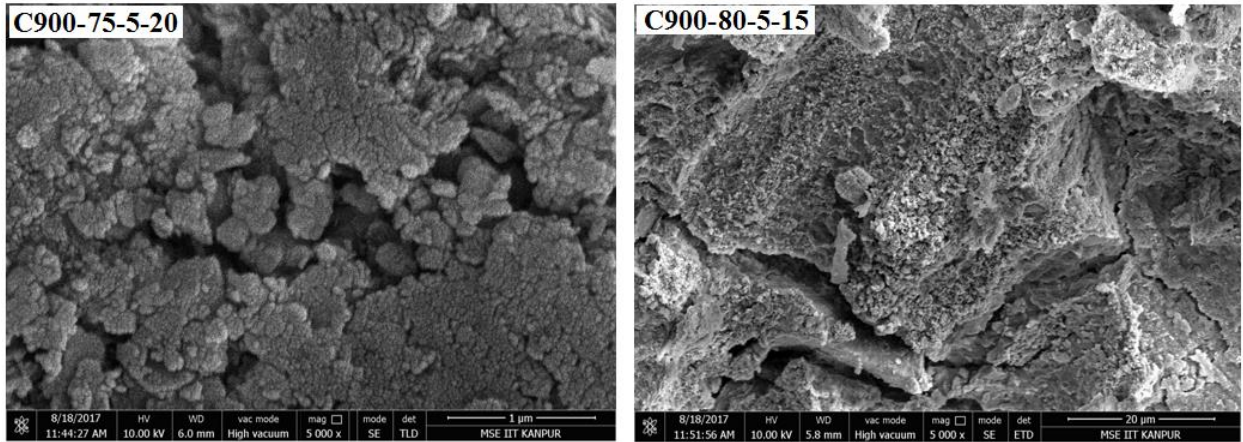


Figure 20. The Microstructures of ceramic filters C900-75-5-15 and C900-80-5-15 designs.

4.4.3. The Micro-structure of ceramic filter C900-50-15-35 design

The *E. coli* removal efficiency of C900-50-15-35 filter design (99.6 ± 0.40 %) and its flow rate (1.91 ± 0.55 L/h) are in the suggested standard. The FESEM images of the sintered ceramic filter scanned at different magnifications confirmed the formations of the porous ceramic filter. Figure 21(a-b) revealed the presence of smaller size homogeneous pores in the sintered ceramic filter materials. Although, at higher magnification (Fig.c and d), the number of isolated and interconnected pores, the kinds of pores in porous materials that contribute to the filtration process were observed. This property guide to the hypothesis that these materials could be used as a water filter.

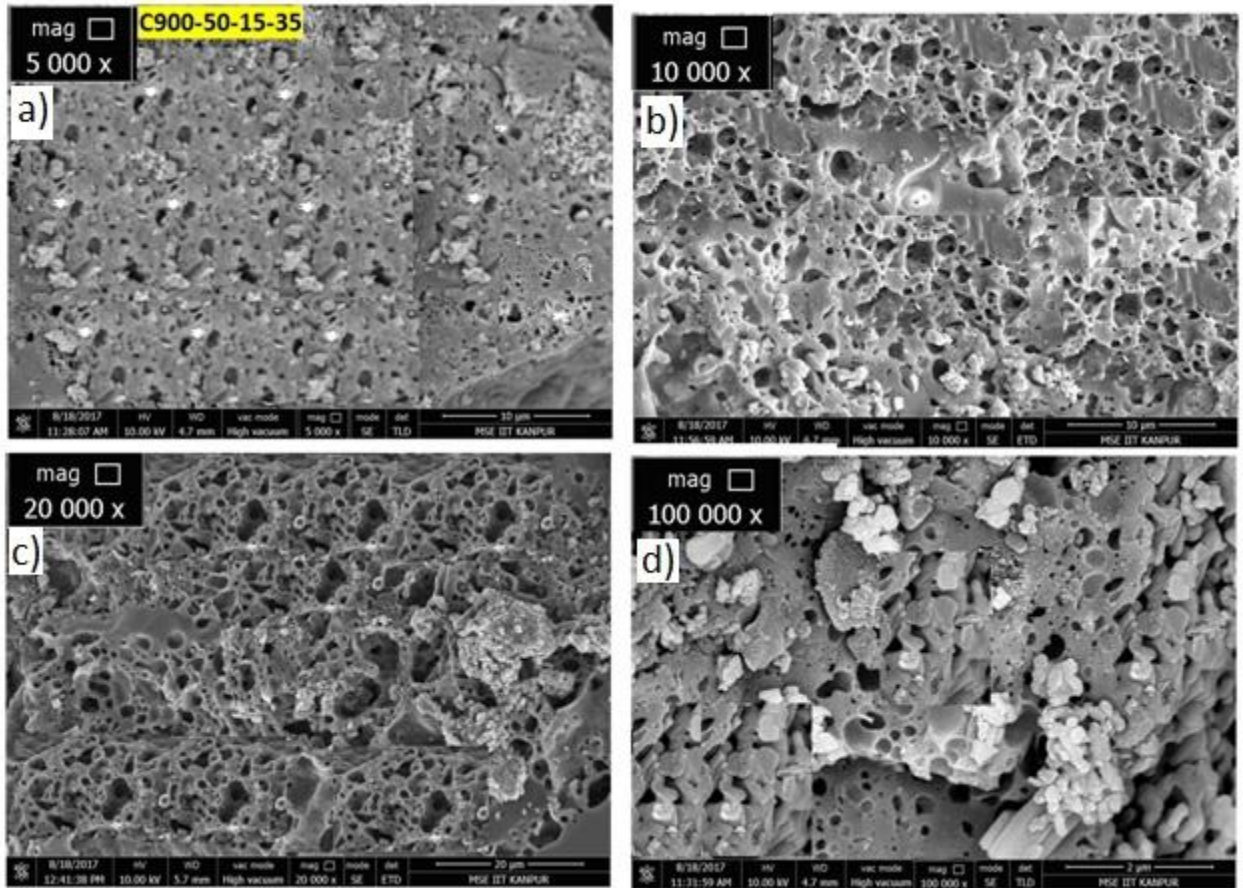


Figure 21(a-d). FESEM: The Microstructures of a ceramic filter with C900-50-15-35 design micrographs at different magnifications.

4.4.4. The Micro-structure of other ceramic filters design

It is noticed from the FESEM micrographs of C900-70-15-15 and C850-70-10-20 composite ceramic filters, both filters are porous with different types of pore and pore diameter, Fig.22. The image of C850-70-10-20 revealed the presence of many two ends open pores with large diameters while that of C900-70-15-15 contains many one end closed pores with large diameter and very fine interconnected pore with small diameters. C900-70-15-15 filter has better *E.coli* removal efficiency ($99.6 \pm 0.40\%$) while, C850-70-10-20 filter has low removal efficiency ($92.53 \pm 2.84\%$).

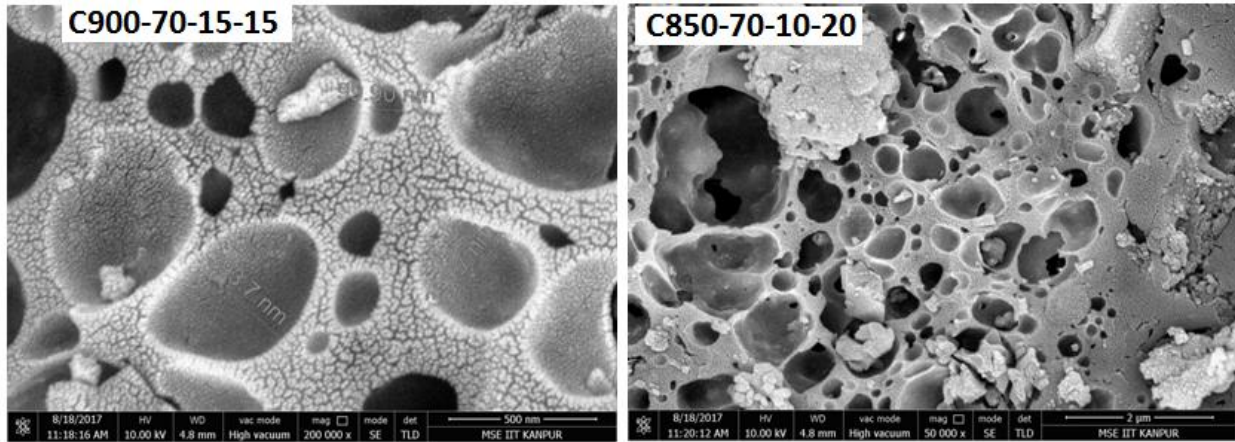


Figure 22. FESEM micrographs on fractured surface of C900-70-15-15 and C850-70-10-20.

4.5. BET Analysis of the sintered ceramic filter

By analyzing the adsorption isotherms of nitrogen on the porous ceramic filters surface with increasing relative pressure, the BET surface area, pore size, and volume were determined. Figure 23, shows the adsorption and desorption isotherms of optimized C900-50-15-35 ceramic filter design. From the figure, it can be observed that the adsorption and desorption isotherms are not the same for a specific region of relative pressure. This phenomenon is known as a hysteresis loop and is commonly exhibited in the mesoporous adsorbent. With the adsorption and desorption isotherms characteristics, the observed isotherms can be classified as the Type IV isotherm in accordance with the IUPAC isotherm classification (Sing et al., 1984). The mesoporous structure of the ceramic filter element makes it a potential adsorbent material. The distribution of pore sizes and the textural parameters obtained by low-temperature nitrogen adsorption for sintered C900-50-15-35 were listed in Table 9. The pore size distribution of C900-50-15-35 filter design, are in the ranges of 20-180 Å, with an average pore size distribution of 4.83 Å. From the Multipoint BET analysis, in the 0.025 to 0.30 range of relative pressure (P/P_0), the linear plot with a correlation coefficient of 0.99 was determined, with the positive slope of 5.45. The distribution of pore sizes (diameters) of sintered C900-50-15-35 was also depicted in figure 24.

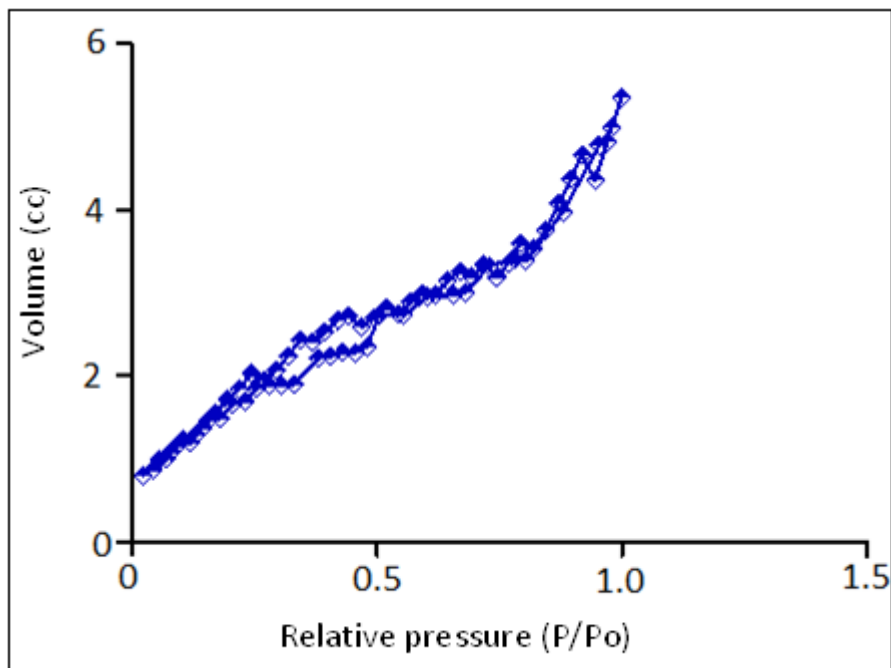


Figure 23. Adsorption and desorption Isotherm of composite filter C900-50-15-35.

Table 9. Textural parameters obtained by low-temperature nitrogen adsorption for sintered C900-50-15-35.

BET Surface Area	6.183 m ² /g
Slope	5.45.2
Y - Intercept	18.03
Correlation Coefficient	0.994384
C	3.123
Multipoint BET	6.183 m ² /g
Langmuir Surface Area	1.109 m ² /g
Total Pore Volume	0.008308 cc/g
Average Pore Diameter	48.3 Å

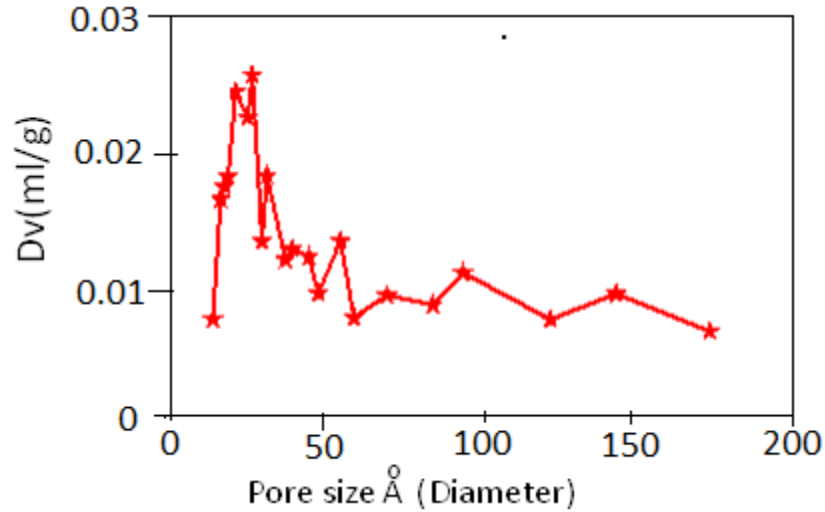


Figure 24. Pore size distributions of sintered composite filter C900-50-15-35.

The calculation of specific surface area (BET), total pore volume (V_t) and average pore diameter (D_p) based on the Brunauer-Emmett-Teller (BET) method for three sintered filters were listed in Table 10. It can be seen that the total porosity and pore surface area in ceramic filter C950-50-15-35 and C900-50-15-35 samples are the higher. Pore surface area of C950-50-15-35 sample is 1.18 times larger than that of C900-50-15-35, but the porosity in C900-50-15-35 is 2.52 times higher than C950-50-15-35. In other words, the higher porosity and smaller pore diameter in C900-50-15-35 than other samples, corresponding to the presence of a large number of pores with relatively small pore diameters. The filter design C900-60-15-25 has the smallest surface area and pore volume which are $0.717 \text{ m}^2/\text{g}$ and $0.0023 \text{ cm}^3/\text{g}$, respectively. These parameters are quite small among other selected samples. Due to its low average pore diameter (4.83 nm) and large total pore volume (0.0083 cc/g), C900-50-15-35 filter has better flow rate ($2.01 \pm 0.41 \text{ L/h}$) and *E. coli* removal (99.60%), while the other two filters have high *E. coli* removal efficiency (> 99%), but less flow rate.

Table 10. BET surface area and Barret-Joyner-Halenda (BJH) pore volume and diameter.

Filter design	S_{BET} (m ² /g)	V_t (cc/g)	D_p (nm)
C900-60-15-25	0.717	0.002	11nm
C950-50-15-35	7.30	0.0033	18nm
C900-50-15-35	6.2	0.0083	4.83nm

SBET: BET pore surface area, Vt: Total pore volume , Dp: Average pore diameter.

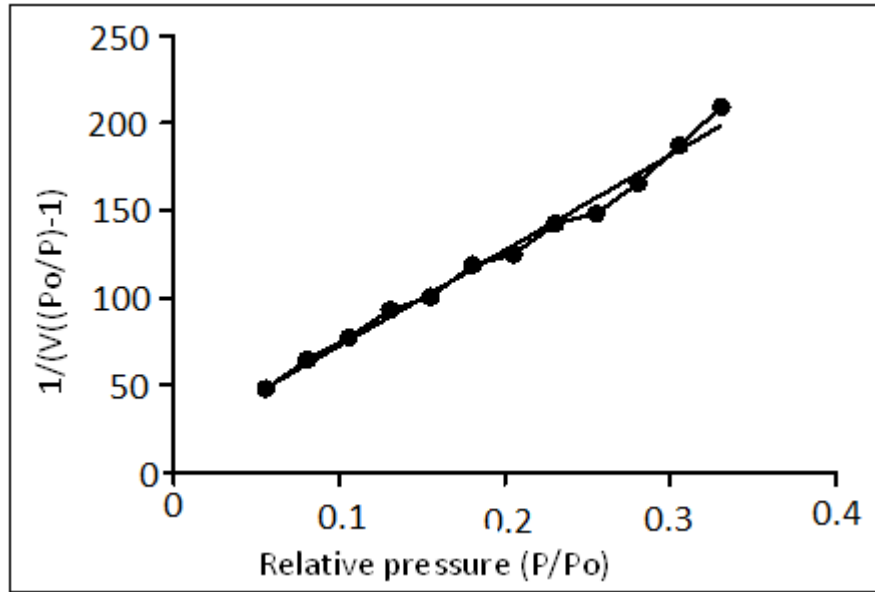


Figure 25. Multipoint BET plot for C900-50-15-35 filter.

4.6. Chemical Analysis

Table 11 and 12 indicated the compositional analysis results of raw clay, sintered filter with and without bone char before and after used for hardness, iron, and *E. coli* removal tests. The chemical composition of the raw and sintered clay ceramic filter results revealed that the raw clay essentially consists of Si and Al. The amount of alkalis oxides are also more noticeable in the raw clay while the contents of alkalis earth metal oxides are high in the sintered filters with bone char. The color of the sintered clay material is red; it is due to the presence of a relatively high amount of iron (8.2%). The composition of the sintered clay is different from that of the raw clay, characterized by a significant increase of Al and Si due to the addition of grog

(or sintered clay without burnout). The relatively high amount of Al_2O_3 and low content of alkaline oxides, which serve as fluxes, indicate that the clay came from typical kaolinitic clay. The results showed that the major composition of the filter material is SiO_2 (58.12%), Al_2O_3 (23.58%) and Fe_2O_3 (8.22%). 1.44 % of CaO , 0.72% of MgO , 2.12% of Na_2O and 0.72% of K_2O were found in the sintered filter before usage. The amount of silica, SiO_2 is large compared to the other oxides. This indicates the filter material is composed of high silica clay. The high percentage of P_2O_5 (2.46%) and CaO (2.80%) in the filter with bone char were due to the presence of Ca and P in hydroxyapatite of the bone char. The decreased in the percentage of loss on ignition (LOI) value in the sintered filter was indicated the loss of different materials during firing (Johari et al., 2011). The mineral kaolinite, one of the constituents of clay ($\text{Al}_2\text{O}_3 \cdot 2\text{SiO}_2 \cdot 2\text{H}_2\text{O}$), decomposes at low temperature (550°C) into metakaolinite ($\text{Al}_2\text{Si}_2\text{O}_7$) by losing water molecules. Additionally, the $\text{SiO}_2/\text{Al}_2\text{O}_3$ ratio: 2.16, 2.46 and 2.48 of the three samples are above that of 1.18 associated with kaolinite, indicates an excess of SiO_2 in the form of free quartz.

Table 11. (%)chemical composition of raw clay, fired ceramic filter with and without bone char.

Item	SiO_2	Al_2O_3	Fe_2O_3	CaO	MgO	Na_2O	K_2O	MnO	P_2O_5	TiO_2	H_2O	LOI
Raw	47.32	21.88	11.6	0.44	<0.01	4.18	1.48	<0.01	0.07	0.31	2.20	11.55
Fired	58.12	23.58	8.2	1.40	0.72	2.12	0.72	0.06	0.10	0.41	0.23	2.68
Fired BC	55.42	22.32	10.24	2.90	0.74	4.00	0.69	0.08	2.46	0.27	0.09	2.54

The EDX analysis of sintered ceramic filter (figure 26 and Table 12) confirmed the presence of major elements: Si, Al, Fe, Mg, Ca, K and Na. It also revealed the presence of carbon which might be due to the remaining of carbon in the filter body from sawdust in the form of activated carbon. Trace toxic heavy metals like Pb, Cd, Hg, and As which could have negative impacts on human health are not found in the sintered ceramic filter.

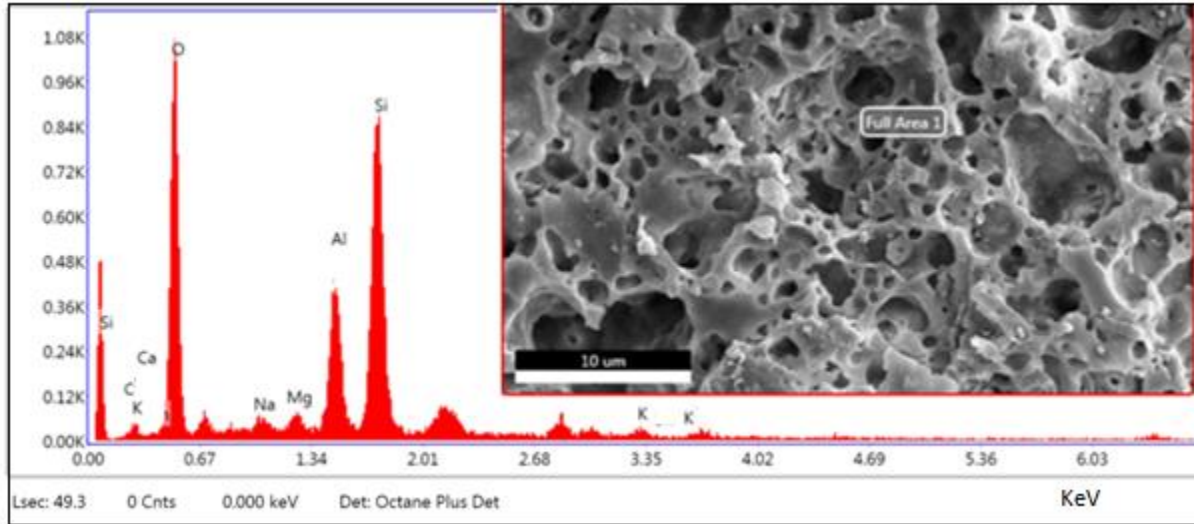


Figure 26.EDS spectrum of C950-50-15-35 ceramic filter.

In addition, the chemical analysis results of the filter used for hardness and iron removals showed more concentration of Ca^{2+} , Mg^{2+} , Fe^{+2} , Fe^{3+} , Si^{+4} and less ion concentration of Na^{+} and K^{+} . This might be due to the ion exchange reactions between the ions in the solutions and filter surface during filtration. The energy dispersive spectrometry (EDS) analysis (Appendix C) revealed the presence of elements like copper, tin, and carbon in the ceramic filter surface that used for contaminated water analysis. This might be due to the adsorption of other ions on the surfaces of ceramic filter elements from the contaminated water during filtration.

Table 12. Chemical composition (%) of the filter before and after hardness removal.

Compound	SiO_2	Al_2O_3	Fe_2O_3	CaO	MgO	Na_2O	K_2O	MnO	P_2O_5	TiO_2	H_2O	LOI
Fresh filter	58.12	23.58	8.2	1.40	0.72	2.12	0.72	0.06	0.10	0.41	0.23	2.68
Used Filter	55.03	22.02	11.64	3.60	2.50	1.00	0.20	0.08	0.46	0.27	0.09	2.01

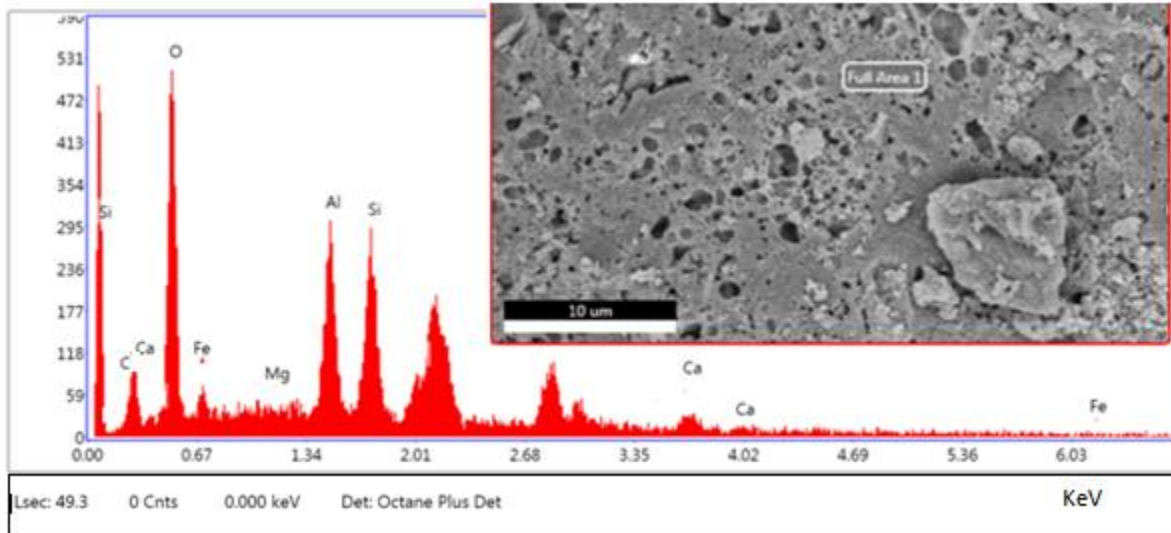


Figure 27. EDS spectrum of the sintered ceramic filter after used for hardness and iron removal tests.

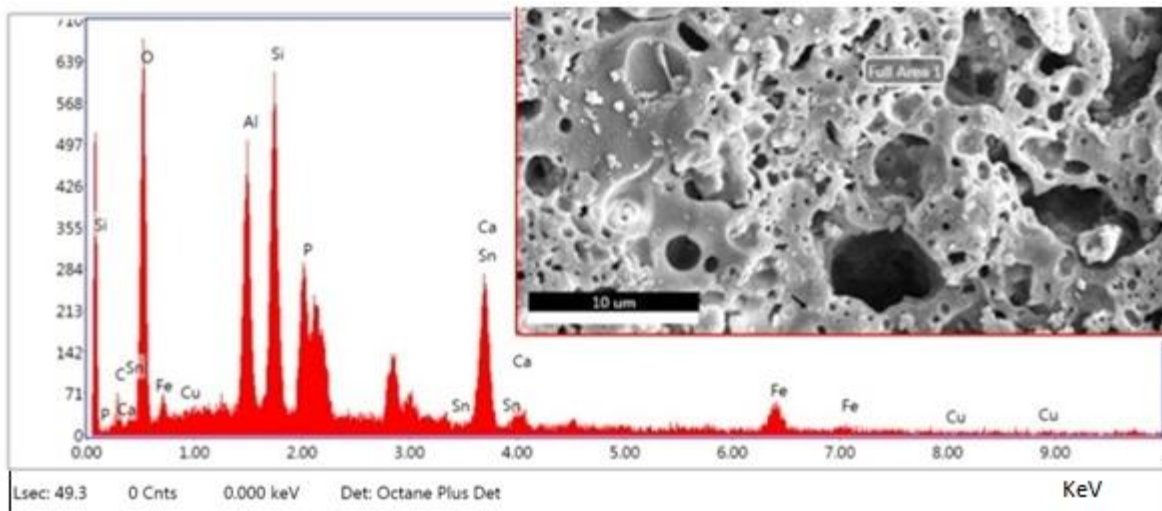


Figure 28. EDS spectrum of sintered ceramic filter used for *E.coli* removal from Mojo river.

4.7. XRD Analysis

The raw claysample was ground and its some portion was scanned by XRD which named bulk state (bulk).The clay particles obtained from bulk sediments placed in a large glass cylinder filled with water with addition of sodium pyrophosphate as deflocculating agent, then the suspension transferred in to large cylinder to settle in the water according to Stokes Law by sedimentation and washed by pure water to remove the dispersing agent, dried and powdered for

XRD analysis. Then, the filtrate was dried and scanned by XRD which named as a normal state (normal). Finally, this normal state of the sample (clay fraction $< 2\mu\text{m}$) heat treated at $550\text{ }^{\circ}\text{C}$ and scanned as heat treated state. Figure 29 (a and b) shows the XRD pattern of the raw clay and fired ceramic filter. The major peaks of raw clay are associated with peaks of kaolin (K) ($2\theta = 12, 25.08$ and 26), Quartz (Q) ($2\theta = 20, 35.08$), illite (I) ($2\theta = 21, 25$) and Hematite (H) ($2\theta = 36$ and 62). The XRD pattern of fired filter peaks are related Quartz ($2\theta = 21, 26, 50$), Mullite (M) ($2\theta = 33$), illite ($2\theta = 35$), Hematite ($2\theta = 36$ and 62). The absence of kaolinite at high sintering temperature above $600\text{ }^{\circ}\text{C}$ is due to the formation of metakaolinite from kaolinite or phase transformations, which is an amorphous material and, consequently, displays no XRD peaks (Carty et al., 1998). From XRD analysis the compositions of membrane before sintering reflections of illite, kaolinite, and quartz were observed from the literature. In the sintered samples, no reflection of kaolinite was found due to transformation to metakaolinite. For membrane sintered at $950\text{ }^{\circ}\text{C}$, reflections of illite, mullite, and quartz ($\text{Na}_2\text{O}, \text{Al}_2\text{O}_3, 2\text{SiO}_2$) were found. Quartz reflections did not change significantly. A critical observation of the peaks at higher temperature revealed that there is significant phase transformation occurs at $950\text{ }^{\circ}\text{C}$. The XRD diffraction graphs indicate no change in the peak trends corresponding to quartz thereby inferring that quartz phase is not at all affected by sintering of inorganic materials within the temperature.

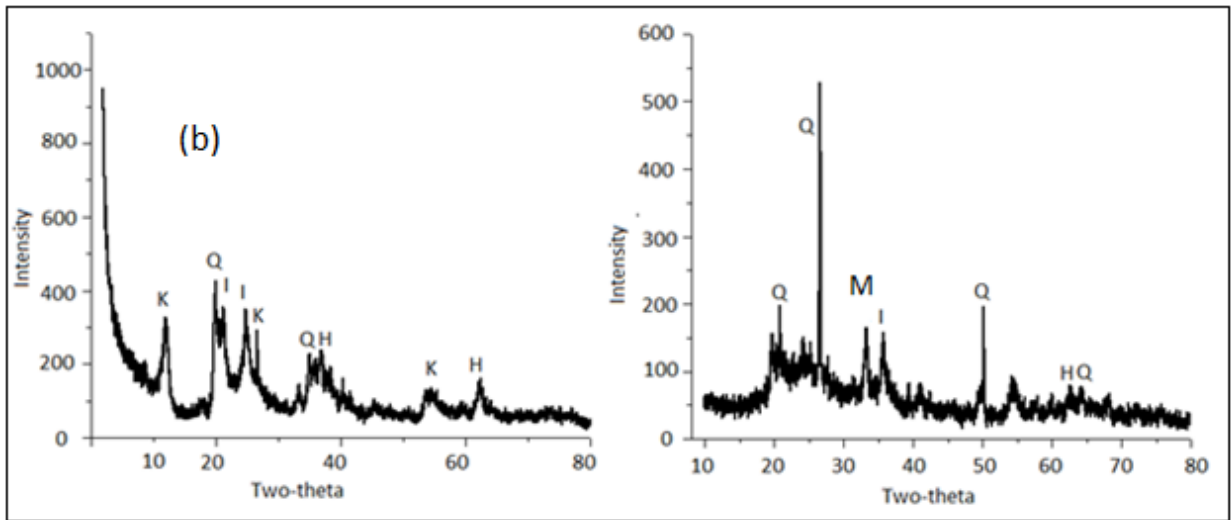
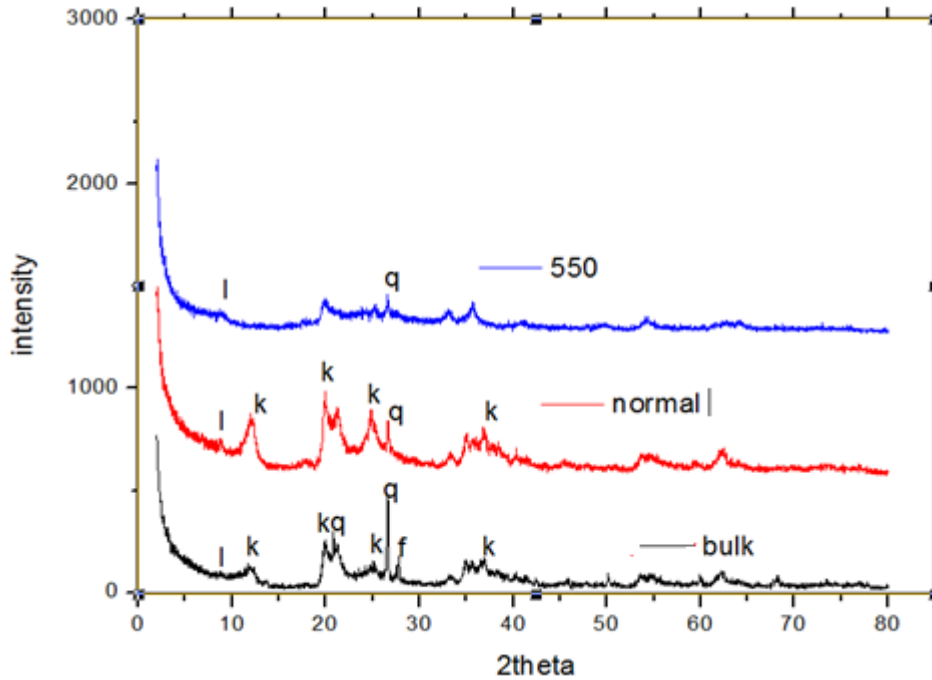


Figure 29. (a) XRD patterns of raw bulk, normal and heated clay at 550°C (b) XRD patterns of raw clay and sintered filter C950-50-15-35.

4.8. FT-IR Analysis

FTIR studies of the filters help in the identification of various forms of the minerals present in the raw clay and filter elements Figures (30-31). In the IR studies, the coupled vibrations are appreciable due to the availability of various groups. Most of the bands such as 3696cm^{-1} , 3622cm^{-1} , 3450cm^{-1} , 1033cm^{-1} , 917cm^{-1} , 795cm^{-1} , 692cm^{-1} , 533cm^{-1} , 466cm^{-1} show the presence

of kaolinite (Franco, 2004). The vibrations observed at 917 cm^{-1} indicates the possibility of the presence of hematite (Farmer V, 1974). Whereas 3622 cm^{-1} , $\sim 1631\text{ cm}^{-1}$, 1033 cm^{-1} are also indicative of gypsum and $\sim 693\text{ cm}^{-1}$ shows the possibility of the presence of calcite (Ghosh et al., 2010). A strong band at 3696 cm^{-1} , 3622 cm^{-1} and 3450 cm^{-1} indicate the possibility of the hydroxyl linkage. However, broadband at 3450 cm^{-1} and a band at 1633 cm^{-1} in the spectrum of clay suggest the possibility of water of hydration in the sample.

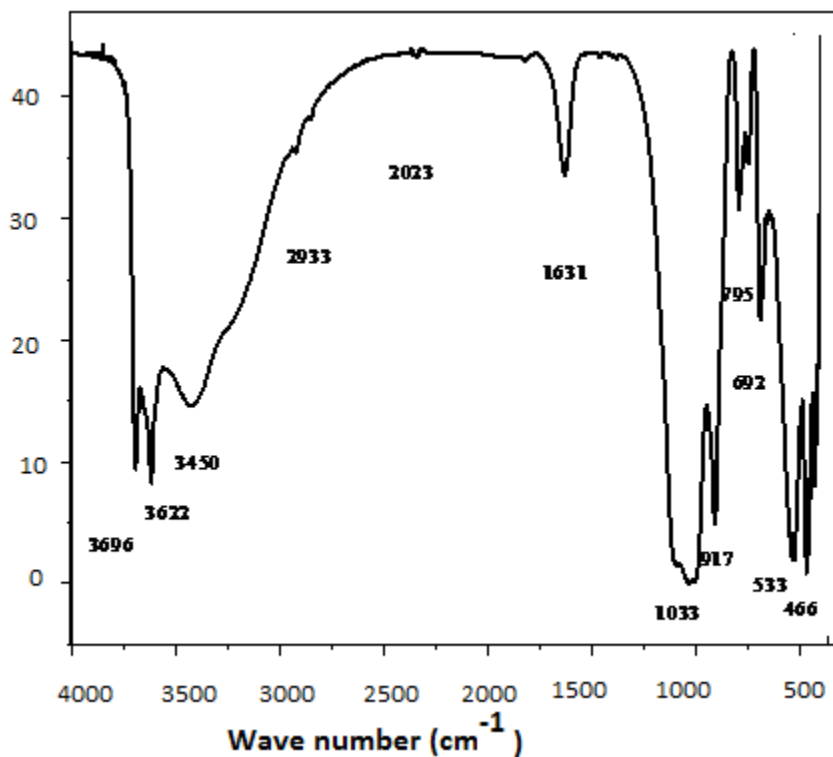


Figure 30. The FT-IR spectrum of raw clay.

On the FT-IR spectrum of C800-50-15-15 with 5% bone char mix, the Si-O stretching vibrations were observed at $\sim 792\text{ cm}^{-1}$, $\sim 693.4\text{ cm}^{-1}$, $\sim 538.8\text{ cm}^{-1}$ and $\sim 468.9\text{ cm}^{-1}$ showing the presence of quartz (Eslami et al., 2008). PO_4^{3-} stretching mode of vibration characterized by a strong band in the $1000 - 1150\text{ cm}^{-1}$ range. The peaks observed around at 1042 and 961.5 cm^{-1} are due to the presence of P-O bonds in the phosphate group. Thus, the presence of PO_4^{3-} group in hydroxyapatite is confirmed from the IR studies. The bending vibration of PO_4^{3-} was observed by bands located at 536 cm^{-1} . The OH groups on the filter surface can involve in the sorption of

cations. Ion exchange and electrostatic interaction were suggested as the main mechanisms involved in the sorption of ions on filter surfaces. The FTIR studies of filters with different designs revealed the influence of the sintering temperature of the ceramic filters functional group as indicated in Figures 32 and 33.

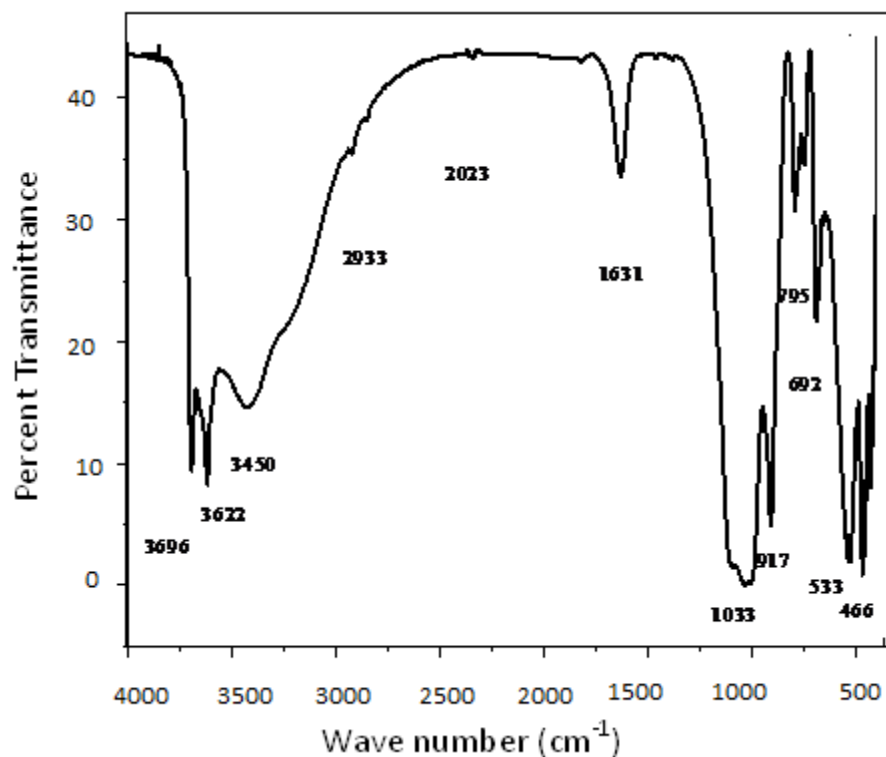


Figure 31. FTIR Spectrum of sintered C800-50-15-35 ceramic filter.

The FT-IR spectra analysis also revealed the differences between the functional groups in the filter before and after filtration of the NaF solution. It was observed that the hydroxyl groups present on the filter surface were mainly involved in the sorption of fluoride. Anion exchange and electrostatic interaction were suggested as the main mechanisms involved in the sorption of fluoride on the filter. The changes in the stretching frequency of fluoride-treated filter material compared to untreated filter material confirm the chemical modification.

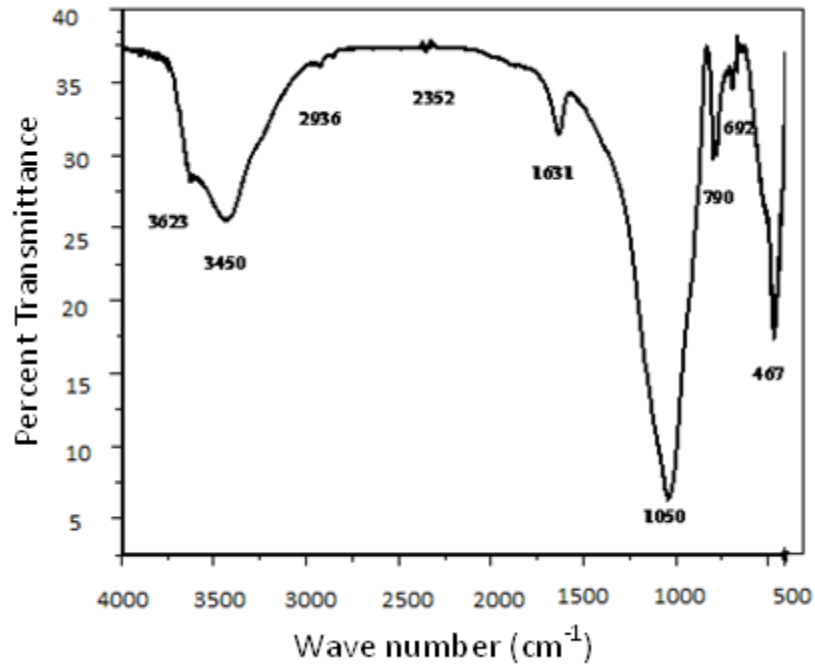


Figure 32. The FT-IR spectrum of C900-50-35-15 with 5% Bone Char.

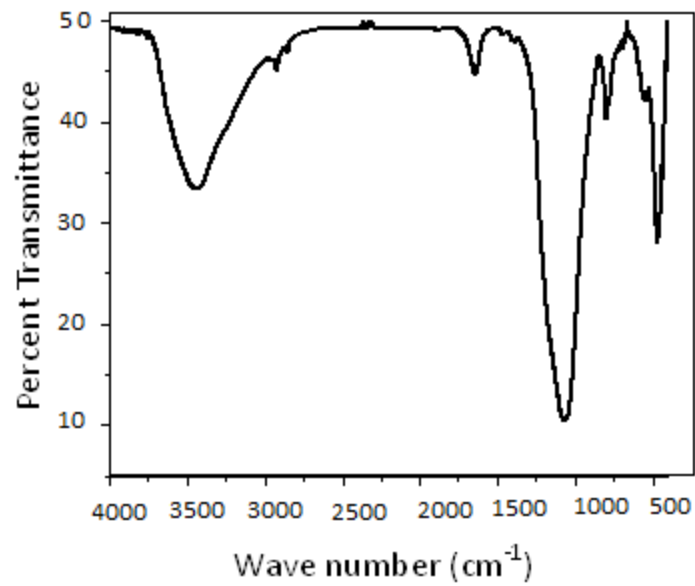


Figure 33. The FT-IR spectrum of sintered filter C1000-80-5-15.

4.9. Removal Efficiency of Hardness Agents

The removal efficiency of water hardness agents by ceramic filters was evaluated by preparing the solution of calcium chloride and hydrated magnesium chloride. Nine filters with different designs were randomly selected based on the raw materials clay, sawdust, and grog percentage ratios and sintering temperatures. The results listed in Table 13 contain ceramic filters removal efficiency of Mg^{2+} and Ca^{2+} . The removal of calcium and magnesium ions might be due to the ion exchange on the ceramic surface, formation of precipitation as oxides and hydroxides of these cations. The central cations in clay structure, aluminum, and silicon with higher charge might be replaced with a lower charge like magnesium and calcium by leaving net negative charge. The results in Table 13 indicate, water hardness removal efficiency of the filter elements increased with a decrease in the percent composition of burnout (Table 13). There was no significant difference for different design ceramic filters for water hardness agents (Mg^{2+} and Ca^{2+}) removal efficiency, ($p > 0.05$) and ($p > 0.05$), respectively (Appendix D and E). According to the works of (Babafemi and Yinusa, 2015, Birendra and Pandey, 2014), a ceramic filter developed from sawdust and clay can remove 50.8% hardness and 96% iron from stream water. The highest adsorption capacity towards Ca^{2+} and Mg^{2+} ions were achieved at neutral pH.

Table 13. The removal efficiency of water hardness agents with initial concentrations of Mg^{2+} (546 ppm) and Ca^{2+} (393 ppm) before filtration.

Design	Filter code	Clay + Grog	Concentration of Mg^{2+} and Ca^{2+} after filtration (ppm)		Percent removal efficiency (%)	
			Mg^{2+}	Ca^{2+}	Mg^{2+}	Ca^{2+}
C850-50-15-35	F2	65	250±2.64	278.6 ±1.44	55	29
C850-60-15-25	F6	75	220±1.73	190.05±0.5	60	52
C850-70-15-15	F10	85	145±10	120±0.86	73	69
C900-50-15-35	F3	65	199.5±2.1	116 ±1.32	64	70
C900-60-15-25	F7	75	144±1.32	115.1±0.1	74	71
C900-80-5-15	F22	85	170.3±0.60	90±1.32	69	77
C950-50-15-30	F4	65	210±2.64	166±1.32	62	57
C950-60-15-25	F8	75	151.2±1.05	140±1.73	72	64
C950-80-5-15	F23	85	210.5±0.5	95±0.91	61	76

4.10. Iron Removal Efficiency

The iron removal efficiency of the ceramic filter was determined by comparing the concentration of iron in the raw and filtered water after the ceramic filtration of sample water. The concentrations were calculated from a calibration plot prepared from a series of standard iron solutions. The comparable removal efficiency of iron has been observed for all ceramic filters as it can be observed in Table 14. There is a slight decrease in the removal efficiency with the decrease in the percentage of sawdust and sintering temperature in the production of filter elements, this might be related with the amount of activated carbon media or adsorbent left in the ceramic filters and cations formed in the ash during sintering. Adsorption of cations might be affected by the surface area contact of adsorbent and adsorbate surface area in contact increase for highly porous ceramic filters. The interaction between a negatively charged clay surface and the cations in the pore water could be generated an electric double layer. This was an important phenomenon and it could be described in terms of the retention of the cation in the pore. The central ions of clay structure might be replaced by others in changing the environment like the pH of water in the ceramic pores. With relative to the report by (Nasir Subriyer, 2013) the filters developed for this project are slightly less efficient in removing iron from aqueous water. The iron removal efficiency of the filters developed by this group was (67-81) %, which is relatively low (Babafemi and Yinusa, 2015, Birendra and Pandey, 2014), and the amount of iron in the filtrate is in the range of 5.25-9.05 mg/L is still above the WHO recommended concentration for iron. Clays, including kaolinite and metakaolinite, compete for ions (Inglezakis et al., 2010) through the capillary penetration of the iron solution into ceramic porosity, followed by adsorption on surfaces of aluminosilicates and ion exchange for clays. During the ion exchange process, ions replaced some of the ions on surfaces of metakaolinite as confirmed with X-ray elemental analysis in section 4.6

From statistical ANOVA test, there is no significant difference in iron removal among the ceramic filters formed from different percentage composition of clay and burnout materials, $p=0.191$, Appendix-F. But, the Post Hoc result showed that there is a difference between filters with filter codes F2, F6, F10 and F4, F8, F23 with ($p = 0.925$ and 0.198) respectively.

Table 14. The Iron removal efficiency of the filters from initial concentration (27.12 ppm) at room temperature.

Design	Code	The concentration of iron in the filtered water (ppm)	% Removal
C850-50-15-35	F2	5.69±0.18	79.02
C850-60-15-25	F6	5.82±0.02	78.54
C850-70-15-15	F10	7.08±0.10	73.89
C900-50-15-35	F3	5.39±0.02	80.13
C900-60-15-25	F7	5.25±0.18	80.64
C900-80-5-15	F22	9.05±0.13	66.74
C950-50-15-35	F4	5.09±0.02	81.23
C950-60-15-25	F8	5.63±0.06	79.24
C950-80-5-15	F23	7.4±0.26	72.80

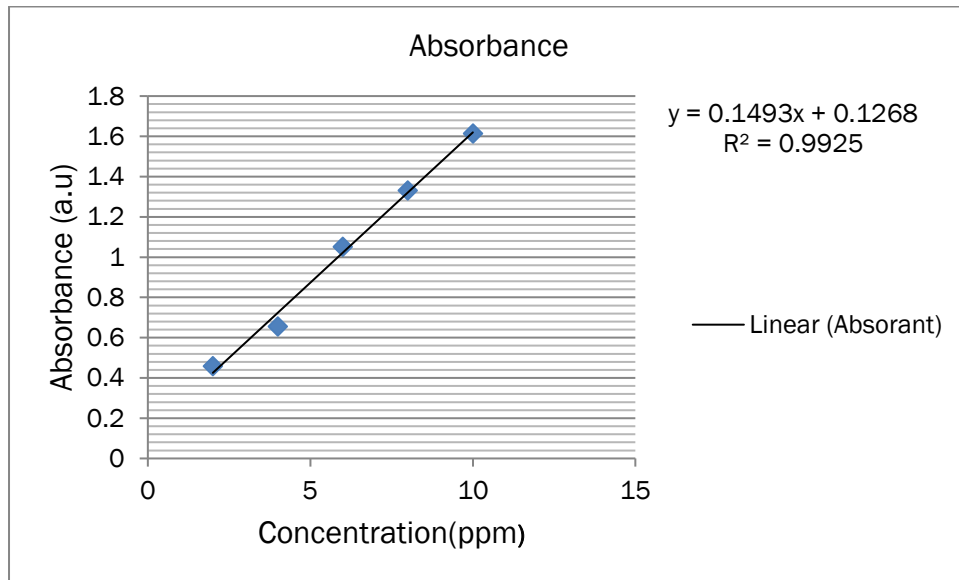


Figure 34. The calibration graph for the determination of the Iron concentration.

4.11. Nitrite Removal Efficiency

The concentrations of the nitrite before and after filtration were calculated from a calibration curve prepared from a series of standard nitrite solutions (Figure 31). Ceramic filter design C850-50-15-35 has minimum removal efficiency of 63.26% of nitrite from water solution while filter design C950-50-15-35 has 91.94% (Table 15). The removal efficiency trend of the selected filters increased with an increase insintering temperature. The statistical ANOVA test showed there is a significant difference between the ceramic filters composed of different percentage of clay to sawdust, $p=009$, AppendixG. The Post Hoc analysis also confirms the existence of great significant difference in removal efficiency of nitrite between ceramic filters group (F2- F6-F10), (F3-F7-F22) and filter group (F3-F7-F22), (F4-F8-F23) which were sintered by 50°C temperature differences. The nitrite removal mechanism of the ceramic filters might be by the exclusion within the pores of the ceramic filters related to size (Naddafi et al., 2005, Watcharaporn, 2014). The filters fired at high temperature showed high nitirite removal efficiencies and met the WHO recommended limit less than 1.0 mg/L.

Table 15. The nitrite removal efficiency of the ceramic filters from 4 mg/L original concentration at room temperature.

Filter Design	% Sawdust	Filter Code	$[NO_2^-]$ in filtrate (mg/L)	Removal efficiency(%)
C850-50-15-35	35	F2	1.4696	63.26
C850-60-15-25	25	F6	1.2664	68.34
C850-70-15-15	15	F10	1.0772	73.07
C900-50-15-35	35	F3	0.7532	81.17
C900-60-15-25	25	F7	0.3948	90.13
C900-80-5-15	15	F22	0.3616	90.96
C950-50-15-35	35	F4	0.3224	91.94
C950-60-15-25	25	F8	0.2524	93.69
C950-80-5-15	15	F23	0.3576	91.06

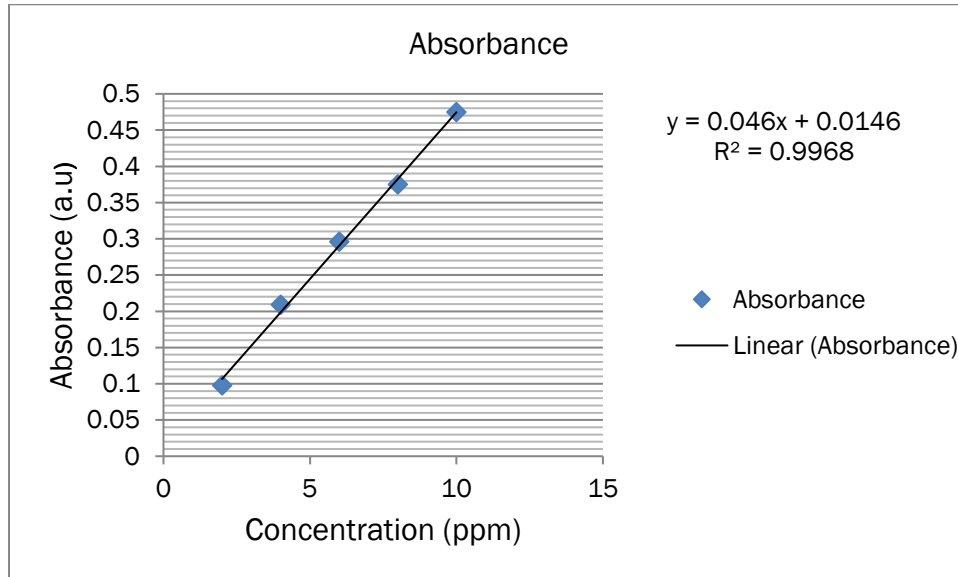


Figure 35. Calibration graph of the determination of nitrite concentration.

4.12. The Efficiency of the ceramic Filters towards Fluoride Removal

Selected filters used for fluoride removal test and the results are listed in Table 16. The main methods used in defluoridation from aqueous solutions are ion exchange and adsorption techniques. Seven selected filters were used including three (i.e. C1000-70-5-25, C1000-75-5-20 and C1000-80-5-15) filters fired at high temperature, 1000°C. On average, the ceramic filters reduced the original content of 10 mg/L in the untreated water sample to 0.68 mg/L in the filtered water which is greater than 95% removal efficiency. The filters fired at lower temperature showed high fluoride removal efficiencies: C800-50-15-35, C800-60-15-25, C800-70-15-15 and C850-50-15-35 with fluoride removal efficiencies of 96.8%, 98%, 97.7%, and 98.2% respectively, which met the WHO recommended a limit of 1.5 mg/L. At lower temperature, a small number of hydroxide ions are removed from the filter surface, and high amount of fluoride ions and hydroxide ions exchange between the water and the filter, which increased the removal efficiency of the filter. The high fluoride removal efficiency of ceramic

filters sintered at low-temperature results might be due to the exchangeable hydroxyl ions from clay, bone char, and activated carbon media in the ceramic body.

Table 16. Fluoride removal efficiency in percent from 10 mg/L of aqueous solution at pH of 8.

Filter Design	Bone Char (%)	Filter code	Fluoride removal efficiency, %
C800-50-15-35	5	F1	96.8
C850-50-15-35	5	F2	98.2
C800-60-15-25	5	F5	98.0
C800-70-15-15	5	F9	97.7
C1000-70-5-25	5	F18	85.0
C1000-75-5-20	5	F21	83.8
C1000-80-5-15	5	F24	79.0

4.13. Turbidity Removal Efficiency of the Filters

Table: 17 represents the results in turbidity removal efficiency of the nine ceramic filters. The turbidity of the source water used for analysis was the same throughout the filtration, 58 NTU (Nephelo Turbidity Unit). The turbidity removal efficiency of the selected filters was varied from 84.48% to 100%. Many drinking waters sources achieved low levels of turbidity (0.1 NTU),(EPA. 2009). The European standards for turbidity state must be not more than 4 NTU. The WHO established that the turbidity of drinking water should not be more than 5 NTU, and should ideally below 1 NTU. As listed in Table 17 the turbidity removal efficiency of filters F1, F2, F5, F6, and F7 are in the recommended limit of 5 NTU of the WHO. The turbidity removal efficiency of a filter was affected by different factors such as the porosity of the filter element and the turbidity of the source water. The Table also indicates the relationship between the percentage composition of the clay and sawdust used for the production of the ceramic filter elements with turbidity removal efficiency. The ceramic pot manufactured with PFP has the potential to reduce turbidity between 30% to 100% as reported by (Lantagne et al., 2006). ANOVA statistical analysis of turbidity removal efficiency indicates that there is a significant

difference in turbidity removal efficiency of the ceramic filters having a different percentage composition of clay to sawdust and fired at 800, 850 and 900°C temperatures ($p = 0.009$).

Table 17. Turbidity removal efficiency of selected filters from source water with 58 NTU.

Design	Sample code	The turbidity of water after filtration	Turbidity removal efficiency (%)
C800-50-15-35	F1	3.77NTU	93.5
C800-60-15-25	F5	0.2NTU	99.65
C800-70-15-15	F13	7.13NTU	87.7
C850-50-15-35	F2	2.61NTU	95.5
C850-60-15-25	F6	1.03.NTU	98.3
C850-70-10-20	F14	5.8 NTU	90
C900-50-15-35	F3	4.64NTU	92
C900-60-15-25	F7	3.95NTU	93.5
C900-70-10-20	F16	9.00NTU	84.48

4.14. Conductivity and pH Analysis of Filtrate with Ceramic Filters

Thus, for this assessment, the same water sample used for flow rate determination was used. The pH, conductivity, and turbidity of the water sample used before filtration for testing the efficiency of the developed filters were 8.2, 157 $\mu\text{s}/\text{cm}$ and 58 NTU respectively. Ceramic filters were evaluated for conductivity and pH changes after filtration and all the ceramic filters could be reduced conductivity and pH of the source water. Electrical conductivity is directly related to the number of ions present in a given solution (Adhena et al., 2015). The pH value of the source water was relatively high and it was decreased after filtration in all the ceramic filters (Table 18). Higher pH conditions could enhance the adsorption of positively charged ions. The statistical ANOVA test showed there is a significant difference between the ceramic filters of F1, F5, F13 ($p = 0.01$) and F2, F6, F14 ($p = 0.00$), but, there was no significant difference between filters with codes F3, F7, and F16 ($p = 0.012$), Appendix H, in pH change before and after filtration. While, the statistical ANOVA test showed there is a significant difference

between the ceramic filters of F1, F5, F13 ($p = 0.00$) and F2, F6, F14 ($p = 0.00$) and F3, F7, F16 ($p = 0.00$) in conductivity changes before and after filtration (Appendix I).

Table 18. Average \pm SD pH,and conductivity values after filtration using ceramic filters.

Filter Desgin	Ceramic code	pH	Conductivity ($\mu\text{s}/\text{cm}$)
C800-50-15-35	F1	7.8 \pm 0.04	142 \pm 0.32
C800-60-15-25	F5	7.4 \pm 0.13	138 \pm 0.23
C800-70-15-15	F13	7.3 \pm 0.05	108.5 \pm 0.41
C850-50-15-35	F2	7.6 \pm 0.04	140 \pm 0.15
C850-60-15-25	F6	7.2 \pm 0.02	101 \pm 0.30
C850-70-10-20	F14	7.3 \pm 0.03	101.5 \pm 0.25
C900-50-15-35	F3	7.0 \pm 0.01	96.3 \pm 0.18
C900-60-15-25	F7	6.9 \pm 0.12	98 \pm 0.38
C900-70-10-20	F16	7.2 \pm 0.08	130 \pm 0.29

4.15. Zero point Charge (pH_{PZC})C900-50-35-15 filter

The pH_{PZC} result indicated the surface of C900-50-35-15 composite filter was neutral at 8.5 (Sunil and Arti, 2012). As shown in Table 19 and, Figures 36 and 37, the prepared ceramic filter has a high pH point of zero charges ($\text{pH}_{\text{PZC}} \sim 8.5$). This indicates the adsorption affinity of many positively charged particles and anion exchange including fluoride ions would be feasible in the WHO recommended range for drinking water (Doke et al., 2013).

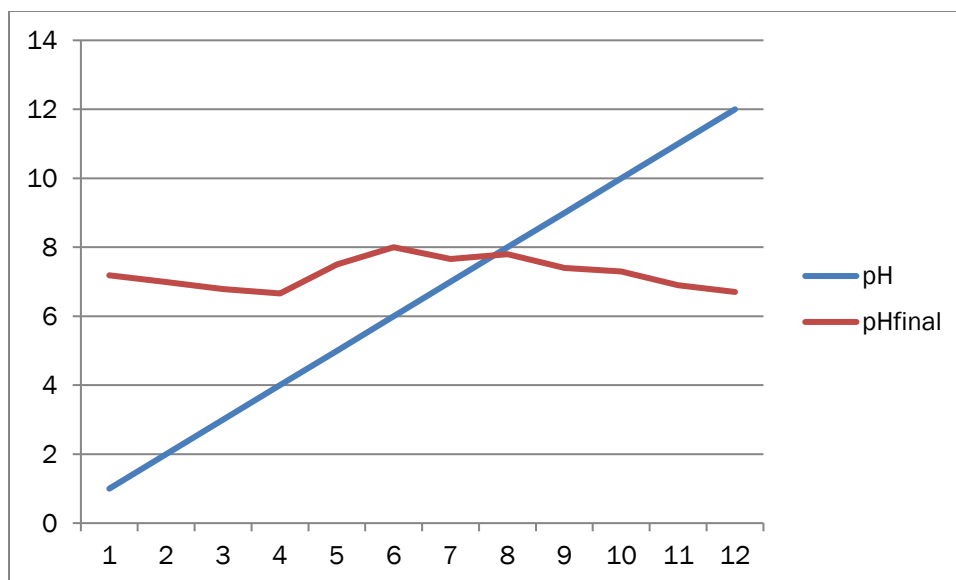


Figure 36. pH_i vs pH_f intersects of pH pzc.

Table 19. Experimental data for determination of zero point charge.

Initial (pH)	Final (pH)	ΔpH	Initial (pH)	Final (pH)	ΔpH	Initial (pH)	Final(pH)	ΔpH
1	7.19	6.19	5	7.5	2.5	9	7.4	-1.6
2	6.99	4.99	6	8.0	2.0	10	7.3	-2.7
3	6.79	3.79	7	7.66	0.66	11	6.9	-4.1
4	6.66	2.66	8	7.8	0.2	12	6.7	-5.3

The presence of basic functional groups such as hydroxyl on the surface of the ceramic filter from different raw materials used for the filter preparation: activated carbon of sawdust, hydroxyapatite of bone char and aluminates in the fired clay. The net surface charge of the filter under pH_{pzc} is positive, while it is negative above pH_{pzc}. Therefore, the knowledge of this value helps in deciding at which pH value one should work during adsorption studies. The pH of all the filtered water solutions from low pH to high pH (or pH1-12) was in the WHO recommended pH range (6.7-8) (Appendix J), which revealed that the composite filter is resistant to acid and base (Bottino et al., 2001).

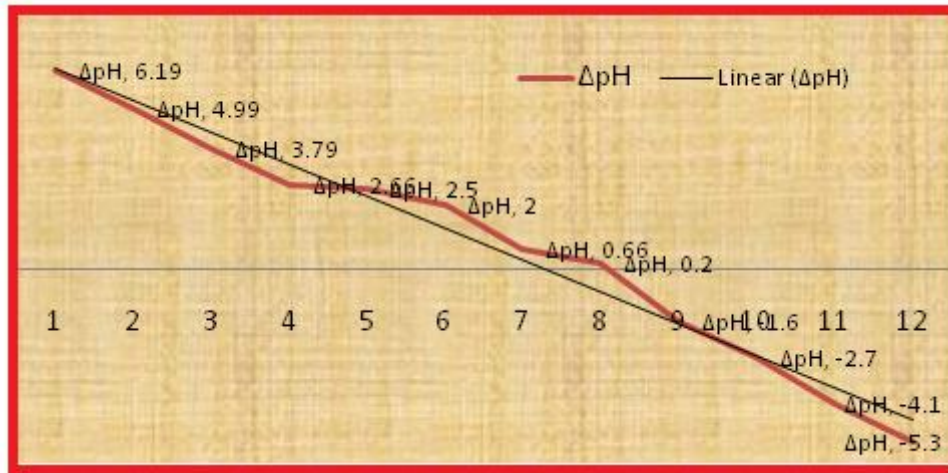


Figure 37. Graph of ΔpH versus the initial pH of the C900-50-35-15 filter to determine pH_{pzc} .

5. CONCLUSIONS

Ceramic water filtration is one of the points use water treatment methods to provide an immediate solution and solve the problem of contamination of water. In this research finding, ceramic filters were developed with different compositions of clay, sawdust, grog, and animal bone char and fired at a different temperature in the laboratory scale. The efficiency of the developed ceramic filters was assessed for different parameters like flow rate, porosity, turbidity, *E.coli* removal efficiency, cations (calcium, magnesium, and iron) and anions; (nitrite and fluoride) removal efficiency. The pH and conductivity water before and after filtration were also evaluated for a different design of filter elements. The average flow rate range of the filter designs produced by this team are ranged from 1.16 ± 0.15 to 2.94 ± 0.38 liter per hour, which is in the range recommended by potters for peace. Among the developed ceramic water filters for this project, filters: C900-50-15-35 (99.6 ± 0.40 %), C950-50-15-35 (99.73 ± 24 %), C900-60-15-25 (99.36 ± 0.55 %) and C900-70-15-15 (99.6 ± 0.40 %) have better efficiency in removing microbial from contaminated water sources. The average total percentage porosity, BET surface area and average pore diameter determined for ceramic filter design, C900-50-15-35, were 36%, $6.183 \text{ m}^2/\text{g}$ & 4.83 nm respectively. The porosity of the filter; C950-50-15-35 (36.33 ± 0.05), its flow rate (1.91 ± 0.55), nitrite (70.00 ± 0.22 %) and fluoride (96.8 ± 0.41 %) removal efficiency are in WHO standard. The EDS analysis results of the filter elements used for hardness and iron removals showed the ion exchange reactions between the filter elements and contaminated water.

6. RECOMMENDATIONS

The following points are recommended for further investigation; Investigation of the effectiveness of the ceramic filter in removing organic pollutants, toxic heavy metals like arsenic, chromium, and lead from contaminated water, and other pathogens mainly viruses.

REFERENCES

- Abebe, W.(2010): Health hazards of fluoride as related to Ethiopia: a review of some relevant issues for preventive approaches., *Ethiop E-J Res Innov Foresight*; 2(1):5: 9–18.
- Adam, J.W.H. (1980): Health aspects of nitrate in drinking-water and possible means of denitrification, *Water SA*, 6: 79-87.
- Afkhami, A., Masahi, S., Bahram, M. (2004): Spectrophotometric determination of nitrite based on its reaction with p-nitroaniline in the presence of diphenylamine in the micellar media, *Bull. Korean Chem. Soc*, 25(7): 1009-1011.
- Akaahan, T. J., Oluma Hyacinth, O. A., Sha’Ato, R. (2010): Physico-chemical and Bacteriological Quality of Water from Shallow Wells in Two Rural Communities in Benue State, Nigeria. *Pakistan Journal of Analytical and Environmental Chemistry*, 11: 73-78.
- Alabdulaaly, I. I., Zarah, A., Khan, M.A. (2013): Occurrence of fluoride in ground waters of Saudi Arabia, *Applied Water Science*, 3: 589-595.
- Anwar K., Amir H., Amir W., Shazmeen Z., Ghulam M. (2011): Qualitative and quantitative analysis of drinking water samples, *International Journal of the Physical Sciences*, 6(33): 7480 – 7489.
- APHA (American Public Health Association)/AWWA (American Water Works Association/ WEF (Water Environment Federation) (1978): Standards methods for the examination of water and wastewater 20th edition Washington, DC.
- ASTM International.(2003a): D1889–00 Standard test method for turbidity of the water, in *ASTM International, Annual Book of ASTM Standards, Water and Environmental Technology*, v. 11.01, West Conshohocken, Pennsylvania.
- Arora, D.R., and Arora, B. (2008). *Textbook of Microbiology*. 3rd ed., CBS Publisher, New Delhi.
- Azoru-ra, C. A. (1994): A Study of the Composition and Mechanical Strength of Ugandan Clays, *MSc Dissertation, Makerere University*.

Babafemi, A., and Yinusa, D. (2015): Formulation of Ceramic Water Filter Composition for the Treatment of Heavy Metals and Correction of Physiochemical Parameters in Household Water. Ado-Ekiti, Nigeria Scientific Research Publishing Inc. Art and Design Review, 3: 94-100.

Bain, C.D., and Nadeau, P.H. (1986): Composition of Some Smectites and Diagenetic Illitic Clays and Implications for Their Origin. Clays and Clay Minerals, 34: 455-464.

Bailey, S.W., and Brindley, G.W. (1979): Structure of Basic Clay Mineralogy Groups. Clay Mineral, 27: 238-239.

Basheer, K. A., Segun, A., Hussein, K. O., and Ximba B. J. (2011): Spectrophotometric determination of iron (III) in tap water using 8-hydroxyquinoline as a chromogenic reagent, African Journal of Biotechnology, 10(71): 16051-16057.

Bharadwaj, A., Wang, Y., Sridhar, S., and Arunadhalan, V.S. (2004): Pyrolysis of rice husk. Current science journal, 87(7):981-6.

Bielefeldt, AR., Kowalski, K., Schilling, C., Schreier, S., Kohler, A., Summers, RS. (2010): Removal of the virus to protozoan sized particles in point-of-use ceramic water filters. Water Research; 44(5): 1482-88.

Birendra, S., and Pandey, I. (2014): Determination of Calcium and Magnesium in Clinker, Cement & Fly, Ash Based Cement by EDTA without Using Masking Reagents, International Journal of Advanced Research in Engineering and Applied Sciences, 3 (4):9-17.

Biruk, A. (2016): Construction and Evaluation of Homemade Ceramic Pot Filter for Domestic Drinking Water Purification in Developing Countries: A Perspective Review Article, International Journal of Emerging Technology and Advanced Engineering, 6: 10-25.

Bloem, S.C., van Halem, D., Sampson, M.L., Huoy, L.S. and Heijman, B. (2009): Silver impregnated ceramic pot filter: flow rate versus the removal efficiency of pathogens. International Ceramic Pot Filter Workshop. Atlanta, Georgia.

Bogdanchikova, N. E., Kurbatov, A. V. , Tret'yakov, V. V., and Rodionov, P. P. (1992): Activity of colloidal silver preparations towards smallpox virus, *Pharmaceutical Chemistry Journal*, 26(10):778-779.

Bottino, A., Capannelli, C., Del Borghi, A., Colombino, M., Conio, O.(2001): Water treatment for drinking purpose: ceramic microfiltration application, *Desalination*, 141: 75-79.

Brown, J. M.(2007): Effectiveness of ceramic filtration for drinking water treatment in Cambodia, Ph.D. Thesis, Department of Environmental Sciences and Engineering, the University of North Carolina at Chapel Hill.

Brown, J., Sobsey, M., & Proum, S. (2007): Improving household drinking water quality: Use of ceramic water filters in Cambodia. WSP Field notes. Phnom Penh, Cambodia: WSP.National Academy of Sciences. Ceramic filtration.

Bruce Grey Owen South Health Unit. (2000): The investigative report on the Walkerton outbreak of waterborne gastroenteritis.

Bruggen, B.V.D., Vandecasteele, C. (2003): Removal of pollutants from surface water and groundwater by nanofiltration: an overview of possible applications in the drinking water industry, *Environ. Pollut*, 122: 435–445.

Campbell, E. (2005): Study of Life Span of Ceramic Filter Colloidal Silver Pot Shaped Model. Agua Solutions, Managua Nicaragua.

Carty, W.M and Senapati, U.(1998): Porcelain-Raw Materials, Processing, Phase Evolution, and Mechanical Behavior, *Journal of the American Ceramic Society*, 8: 3-20

Cath, T.Y., Childress, A.E., Elimelech, M. (2006): Forward osmosis: principles, applications, and recent developments. *Journal of Membrane Science*, Volume 281(2): 70-87.

Chengwei Luo, S. T. (2011): Genome sequencing of environmental *Escherichia coli* expands understanding of the ecology and speciation of the model bacterial species. *Proceedings of the National Academy of Sciences*.

Christoffersen, J., Christoffersen, M. R., Larsen, R., Moller, I. J. (1990): Regeneration of bone char used in defluoridation of water supplies. Unpublished paper, Medicine–chemical institute, Panum Institute, Copenhagen.

Clemens, R., Kjell, B., Bjørn, F., Zenebe, M., Redda, T.H., Ulrich, S.(2003): Drinking water quality in the Ethiopian section of the East African Rift Valley I—data and health aspects, *The Science of the Total Environment*, 311:65–80.

Clasen, T.F., Brown, J., Collin, S., Suntura, O., and Cairncross, S. (2004): Reducing diarrhea through the use of household-based ceramic water filters: a randomized, controlled trial in Rural Bolivia, *Am Trop Med Hyg*, 73(4):790-795.

Clasen, T. G., Garcia, P., Boisson S., & Collin, S. (2005): Household-based Ceramic Water Filters for the Prevention of Diarrhea: A Randomized, Controlled Trial of a Pilot Program in Colombia. *A.M. J.Trop, Med Hyg*, 73(4): 790-79.

Clasen, T., Schmidt, W., Rabie, T., Roberts, I., Cairncross, S. (2007): Interventions to improve water quality for preventing diarrhea: a systematic review and meta-analysis.*BMJ*, 334(7597) : 782-790.

Deer, W.A., Howie, R.A., and Zussman, J. (1992): *An Introduction to the Rock-Forming Minerals*. 2nd Edition, Longman, London, 496-502.

Desalegn, A., Sissay, M. and Tesfaye, G. (2013): Microbiological Quality of Drinking Water Sources and Water Handling Practices among Rural Communities of Dire Dawa Administrative Council, *Int.J. Curr.Res.Rev*.1: 29-54.

DHV Raadgevend Ingenieursbureau BV, ‘Het kalk-koolzuurevenwicht opnieuw bezien1983): , Amersfoort, The Netherlands.

Dies, W.R.(2003): Development of a ceramic water filter for Nepal, Masters of Engineering Thesis, MIT Department of Civil and Environmental Engineering. Cambridge, MA.

Dissanayake, C.B. (1991): The fluoride problem in the groundwater of Srilanka-environmental management and health, *International Journal of Environmental Studies*, 38: 137-155.

- Doek, S., Simon, B., Dik, B. and Bas, H. (2007): Particle Removal from Surface Water with Ceramic Microfiltration. Leeuwarden: The Netherlands.
- Doke, M. K., Amol Chavan, R. Nalawade, Ejazuddin M. (2013): Kinetics and Equilibrium Isotherm for adsorption of Basic Blue 9 Dye onto Activated Charcoal prepared from Bhagar Seed Husk, *J. Matter and Environmental Science*, 3: 374-383.
- Doris, V. (2006): Aqua for All Post bus 1072 3430 BB Nieuwegein Department of Water Management Faculty of Civil Engineering Delft University of Technology, Kiwa Water Research Groningerhaven: 1- 76.
- Doulton, D. (2009): Water Filter Ceramic Candle & Cartridge Technologies.
- D'ujanda, F. (2001): Modeling the Porosity Dependence of the Electrical Conductivity of Kaolin”, Ph.D. Thesis, Makerere University.
- Du Preez, M., Conroy, R. M., Wright, J. A., Moyo, S., Potgieter, N., Gundry, S.W. (2008): Use of Ceramic Water Filtration in the Prevention of Diarrheal Disease: a Randomized Controlled Trial in Rural South Africa and Zimbabwe. *American Journal of Tropical Medicine and Hygiene*, 79 (5): 696-701.
- Duran-Valle C. J. (2012): Techniques Employed in the Physicochemical Characterization of Activated Carbons. In: Montoya, V. H. & Petriciolet, A. B. (eds.) *Lignocellulosic Precursors Used in the Synthesis of Activated Carbon Characterization Techniques and Applications in the Wastewater Treatment*. Croatia: InTech.
- Eslami, H., Hashjin, M.S., and Tahriri, M. (2008): Synthesis and Characterization of Hydroxyapatite Nanocrystals via Chemical Precipitation Technique, *Iranian Journal of Pharmaceutical Sciences*, 4(2): 127-134.
- Fan, X., Parker, D., Smith, M. (2003): Adsorption kinetics of fluoride on low-cost materials, *Water Research*, 37, 4929–4937.

- Fang, J., Qin, G., Wei, W., Zhao, X. (2011): Preparation and characterization of tubular supported ceramic microfiltration membranes from fly ash, *Separation and Purification Technology*, vol. 80: 585-590.
- Fantong, W.Y., Satake, H., Ayonghe S. N. (2010): Geochemical provenance and spatial distribution of fluoride in groundwater Mayo Tsanaga River Basin, Far North Region, Cameroon: implications for the incidence of fluorosis and optimal consumption dose,” *Environmental Geochemistry and Health*, 32(2)147–163.
- Farmer, V.C., (1974): *The Infrared Spectra of Minerals*. Monograph, Mineralogical Society, London, 4: 331-363.
- Faustine, A, and S. Obwoya, K.(2014): Effect of Grog on the performance of ceramic water filters, *Science Journal of Physics*, 1:45-57.
- FMoH, (2007): Rapid assessment of drinking water quality in the Federal Republic of Ethiopia, country report. The Federal Democratic Republic of Ethiopia, Ministry of Health, Addis Ababa, Ethiopia.
- FMoH and FEPA. (2010): *Situation Analysis and Needs Assessment on the Libreville Declaration on Health and Environment Interlinkage*. Federal Ministry of Health and Federal Environment Protection Agency. Country report. Addis Abab, Ethiopia.
- Franco, F., Pe´rez-Maqueda, L.A., & Pe´rez-Rodri´guez, J.L.(2004): The effect of ultrasound on the particle size and structural disorder of well-ordered kaolinite, *Journal of Colloid and Interface Science*, 274: 107-117.
- Franz, A. (2005): *A performance study on Ceramic Candle filters in Kenya Including Tests for Coliphage Removal*, Masters of Engineering Thesis. MIT, Department of Civil and Environmental Engineering. Cambridge, MA.
- Galdiero, S., Falanga, A., Vitiello, M., Cantisani, M., Marra, V., and Galdiero M. (2011): Silver Nanoparticles as Potential Antiviral Agents, *Molecules*, 16(10): 8894-8918.

Gates, K. (2002): Site Occupancies by Iron in Nontronites. *Clays and Clay Minerals*, 50: 223-239. <http://dx.doi.org/10.1346/000986002760832829>.

Gatseva, P., Argirova M.D. (2008b) High nitrate levels in drinking water may be a risk factor for thyroid dysfunction in children and pregnant women living in rural Bulgarian areas. *International Journal of Hygiene and Environmental Health*, 211(5–6):555–559.

Gensburger, I. (2011): Investigation of the critical parameters in the production of ceramic water filters. Technische Universiteit Delft, Delft, The Netherlands.

Gerba, C. (2000): Indicator Microorganisms. In I. P. Raina Maier, *Environmental Microbiology*. San Diego, CA: Academic Press.

Ghosh, S. K., Prakash, A., Datta, S., Roy, S. K., and Basu, D. (2010): Effect of fuel characteristics synthesis of calcium hydroxyapatite by solution combustion route, *Bulletin of Materials Science*, 33 (1):7–16.

Gitahi, C. M.(2012): Efficacy of Bone Char Defluoridation in Water. Department of Civil and Construction Engineering, UON.

Gray, C. G. (2003): *The Coliform Index and Waterborne Disease; Problems of Microbial Drinking Water Assessment*. London: Chapman & Hall.

Grimshaw, R.W. (1971): *The Chemistry and Physics of Clays and Allied Ceramic Materials*, 4th edition, Wiley Interscience, New York, pg 421,538.

Haddis J. A., Baruch,W.D.,2, Zera,K.M., and Aster F. P. (2017): Bacteriological quality of drinking water from sources and households in Ethiopia, *Global Journal of Microbiology Research*, 5(1): 183-191.

Hagan, J. M., Harley, N., Pointing, D., Sampson, M., and Smith, K. (2009): A performance evaluation and modification of the UNICEF water filter', *Waterlines*, Vol.12, No.2, IT Publications, London.

Hagan, J., Harley, N., Pointing, D., Sampson, M., and Soam, V. (2008): *Ceramic Water Filter Handbook*, Resource Development International, Cambodia.

Hillie, T., Munasinghe, M., Hlope, M., Deraniyagala, Y.(2003): Nanotechnology, Water and Development, Meridian Institute's Global Dialogue on Nanotechnology and the poor: Opportunities and Risks (GDNP).

Holtslag, H., (2010): Simple Water Filters, Green World Actions, Vol 40: 8-15. [.http://www.gaia movement.org](http://www.gaia movement.org).

Houdry, E., Burt, W.F., Pew, A.B., and Peters, W.A. (1938): Catalytic Processing by the Houdry Process. Nat. Petroleum News, 39: 570-580.

HWTFR. (2011). Household Water Treatment for Fluoride Removal Factsheet: Bone Char Filter. Calgary, Alberta, Canada: CAWST (Centre for Affordable Water and Sanitation Technology).

Huang, Y., Shih, Y., Chang, C. (2011): Adsorption of fluoride by waste iron oxide: The effects of solution pH, major coexisting anions, and adsorbent calcination temperature. Journal of hazard Mater, 186, 1355–1359.

Huisman, L., (1996): Rapid Filtration, Faculty of Civil Engineering, Sanitary Engineering Section, Delft University of Technology.

Ilker, E. S., and Rukayya, A. S.(2016): Comparison of Convenience Sampling and Purposive Sampling. Department of Biostatistics, Near East University, Nicosia-TRNC, Cyprus American Journal of Theoretical and Applied Statistics; 5(1): 1-4.

Inglezakis, V.J., Stylianou, M., Loizidou, M. (2010): Ion exchange and adsorption equilibrium studies on clinoptilolite, bentonite, and vermiculite. J. Phys. Chem. Solids, 71, 279–284.

International Union of Pure and Applied Chemistry Physical Chemistry Division Commission on Colloid and Surface Chemistry, (1994): Subcommittee on Characterization of Porous Solids: "Recommendations for the characterization of porous solids (Technical Report)", Pure Appl. Chem, 66(8):1739–1758.

Jedidi, I., Saïdi, S., Khmakem, S., Larbot, A., Elloumi-Ammar, N., Fourati, A., Charfi, A., Amar, R.B.(2009): New ceramic microfiltration membranes from mineral coal fly ash, Arabian Journal of Chemistry, 2: 31- 39.

Jianhua, W .L ., and Hui, P. Q. (2012): Study on the hydrogeochemistry and non-carcinogenic health risk induced by fluoride in Pengyang County, China, *International Journal of environmental sciences*, 2: 1127-1134.

Jinior, O.K., Gurgel, L.V., Gil, L.F.(2010): Removal of Ca(II) and Mg(II) from aqueous single metal solutions by mercerized cellulose and mercerized sugarcane bagasse grafted with EDTA dianhydride (EDTAD), *Carbohydr. Polym*, 79:184–191.

Johari, I., Said, S., Jaya R.P., Bakar, B.H.A., and Ahmad, Z.A. (2010): Chemical and Physical Properties of Fired- Clay Brick at Different Type of Rice Husk Ash. *International Conference on Environmental Science and Engineering IPCBEE*, IACSIT Press, Singapore. 8: 171- 174.

Joong, S., and Kang, L. (2005): *Sintering, Densification, Grain Growth, Microstructure*, Elsevier Butterworth-Heinemann.

Kaminska, A., and Valuikевичius, C.(2005): Influence of petroleum Refining waste product Contaminated soil on properties of porous ceramic Articles. *material science (Medziagotryra)*, 11: 159-161.

Kaneko, K.(1994): Determination of pore size and pore size distribution, *Adsorbents and catalysts, Review*”, *J. Membrane Sci.*, 96: 59–89.

Katherine, L.C., Lauren., E. F., Krause, C.F., Manto, P..J., Dara, J. P., and Brooke, L. Y.(2015): Implementation of an appropriate household water purification system in Tourou, Cameroon. www.sys.virginia.

Kato, C., Kuzuyuki, K., and Hideyuki, T. (1981): Preparation and Electrical properties of Quaternary Ammonia montmorillonite-Polystyrene Complex. *Clay and clay minerals*, 29(4): 294-298.

Kefyalew Gomoro, Feleke Zewge, Bernd and Negussie Megersa, (2012): Fluoride removal by adsorption on thermally treated laterite soils, *Bull Chem. Soc Ethiop*, Addis Ababa University, vol. 26(3): 361-371.

Kenesa Chali, (2017): Microbial and physicochemical evaluation of wastewater released from Mojo tannery wastewater treatment plant, Ethiopia. The research report, Adama Science and Technology University, Ethiopia.

Kerr, P.F. (1952): Formation and Occurrence of Clay Minerals. *Clays and Clay Minerals*, 1: 19-32. <http://dx.doi.org/10.1346/CCMN.1952.0010104>

Klarman, M., (2009): Investigation of Ceramic Pot Filter Design Variables. Atlanta, Georgia: Emory University.

Kofa, P., Gomdje, H., Telegang, C., NdiKoungou, S. (2017): Removal of Fluoride from Water by Adsorption onto Fired Clay Pots: Kinetics and Equilibrium Studies, *Journal of Applied Chemistry*, 2017, 1-7.

Lantagne, D. (2001a): Investigation of the Potters for Peace colloidal silver impregnated ceramic filter report 1: intrinsic effectiveness. Alethia Environmental, Allston, Massachusetts.

Lantagne, D., Klarman, M., Mayer, A., Preston, K., Napotnik, J. and Jellison, K. (2009): Effect of production variables on microbiological removal in locally-produced ceramic filters for household water treatment. *International Journal of Environmental Health Research*.

Lantagne, D., Meierhofer, R., Allgood, G., McGuigan, K.G. and Quick, R. (2009): Comment on "Point of Use Household Drinking Water Filtration: A Practical, Effective Solution for Providing Sustained Access to Safe Drinking Water in the Developing World". *Environ. Sci. Technol*, 43(3): 968-969.

Lantagne, D., Quick, R., Mintz, E.(2006): Household Water Treatment and Safe Storage Options in Developing Countries: A Review of Current Implementation Practices; Water Supply and Sanitation Collaborative Council: Geneva, Switzerland.

Lantagne, D., Quick, R., Mintz, E.(2006): Household Water Treatment and Safe Storage Options in Developing Countries: A Review of Current Implementation Practices; Water Supply and Sanitation Collaborative Council: Geneva, Switzerland.

Lechevallier, M.W., Evas, T.M., and Sadler, R.J. (1981): Effect of Turbidity on chlorination Efficiency and Bacterial efficiency in drinking water. *Applied Microbiology*, 1(42): 159-167.

Lee, T.L. (2001): Bio-sand Household Water Filter Project in Nepal, Master of Engineering thesis. Department of Civil and Environmental Engineering, Massachusetts Institute of Technology. Cambridge, MA – USA.

Liang, L., Li, J., Lin, H., Yang, X., Guo, G., He, M. (2006): Relation between porosity and permeability of ceramic membrane supports, *Adv. Mater. Res.* 11–12: 39–42.

Low, C.S. (2002): Appropriate Microbial Indicator Tests for Drinking Water in Developing Countries and Assessment of Ceramic Water Filters. Master of Engineering thesis.

Mahvi AH, Nouri J, Babaei AA, Nabizadeh R. (2013): Agricultural activities impact on groundwater nitrate pollution. *Int J Environ Sci Technol*, 2(1):41–7.

Martikainen, K., Kauppinen, A., Matikka, V., Veijalainen, A. M Torvinen, E., Pitkänen, Ta., Miettinen, I.T., and Tanski, H .H.,(2018): Efficiency of Private Household Sand Filters in Removing Nutrients and Microbes from Wastewater in Finland, *Journal of Water*: 10: 1-16.

Martins, O. I., and Emmanuel, N. A. (2011): Evaluation of a ceramic pot made from local materials as water purification systems, 1(6):17-32.

Marty, A., Quinones. A., Cosgrove, B., and Ackerman, L. (2007): Operating Procedure Field Turbidity Measurements. US Environmental Protection Agency, Athens Georgia.

Mattelet, C. (2006): Household Ceramic Water Filter Evaluation Using Three Simple Low-Cost Methods: Membrane Filtration, 3M Petri film and hydrogen sulfide Bacteria in Northern Region, Ghana.12-24.

Mcallister, S. (2005): Analysis and comparison of sustainable water filters. EPD397 Technical report. <http://pottersforpeace.org>

Mebratu,J. (2007): Assessment of Physicochemical and Microbiological Quality of rural Drinking water supply at the source in Menge Woreda, Benshangul Gumuz Regional state, Ethiopia. M.Sc Thesis. Addis Ababa University, Addis Ababa.

- Michael, H., Siri, M., Khanjan, M. (2013): Designing a Low-Cost Ceramic Water Filter Press, *International Journal for Service Learning in Engineering*, 8(1):62-77.
- Miller, G.A. (1977): Fluctuation Theory of the Rayleigh scattering in Absorbing Media. *Journal of Physical Chemistry* Vol.82, No.5.
- Miller, J.N., and Miller J.C.(2010): *Statistics and Chemometrics for Analytical Chemistry* 6th Edition. London, United Kingdom: Pearson Education Limited.
- Mintz, E., Reiff, F., Tauxe, R. (1995): Safe water treatment and storage in the home: A practical new strategy to prevent waterborne disease. *JAMA*, 273: 948-53.
- Mjengera, H.(2001): Optimization of bone char material for defluoridation of drinking water. Ph.D.: Thesis. The University of Dares Salaam.
- Molina Félix, L.C., Blanche Muñoz, L.A. (2005): Representing a relation between porosity and permeability based on inductive rules, *J. Pet. Sci. Eng.* 47: 23-30.
- Molly, K.,(2009): Investigation of Ceramic Pot Filter Design Variables. M Sc. thesis. Emory University.
- MOWIE (2017), *Drinking Water Quality in Ethiopia, Results from the 2016 Ethiopia Socioeconomic Survey, A Report by the Central Statistical Agency of Ethiopia Collaboration with the Ministry of Water, Irrigation and Electricity (MOWIE), LSMS, World Bank, UNICEF, WHO, and JMP, December 2017.*
- Mukwasibwe, S., (2005): Thermal Conductivity of Selected Ugandan Clays, MSc Dissertation, Makerere University.
- Naddafi, K., Mahvi, A.M., Nasser, S., Mokhtari, M., Zeraati, H. (2005): Evaluation of the Efficiency of Clay Pots in Removal of Water Impurities, *Iranian J EnvHealthSciEng*, 2(2):12-16.
- Nardo R. (2005). *Factory Start up Manual for the Production of Ceramic Filters.*(www.elfiltron.com).

Nasir Subriyer. (2013): Treatment of domestic water using the ceramic filter from natural clay and fly-ash Journal of Engineering studies and research, 19 (3): 71-75.

Ndungu, J. N., (2009): Nanoporous ceramics filters for water purification. Master of Science in Physics at the University of Nairobi.

Nguetnkam, J.P., Kamga, R., Villieras, F., Ekodeck, G.E., and Yvon, J. (2008): Assessing the Bleaching Capacity of Some Cameroonian Clays on Vegetable Oils. Applied Clay Science, 39: 113-121.

Obwoya, K. S., (2003): Effects of Microstructure on Mechanical Strength of Selected Clays from Uganda, Ph.D. Thesis at Makerere University.

Oyanedel, C., and Smith, J. (2008): A Sustainable Colloidal-Silver-Impregnated Ceramic Filter for Point-of-Use Water Treatment. Environmental Science and Technology, 42(3): 927-933.

Palacio. L., Bouzerdi, Y., Ouammou, M., Albizane, A., Bennazha, J., Hernández, A., Calvo, J.I.(2009): Ceramic membranes from Moroccan natural clay and phosphate for industrial water treatment, Desalination, 245: 501-507.

Potters Without Borders, (2012): The Difficulty of Improving Simplicity: Ceramic Water Purifier: <http://www.potterswithoutborders>.

Ragland, K.W., Aerts, D.J., and Baker, A.J. (1991): Properties of wood for Combustion analysis. Bio-resource technology journal, 37: 161-168.

Rango, T.J., Kravchenko, B., Atlas, P. G., McCornick, M., Jeuland, B., Vengosh, M. A: (2012): Groundwater quality and its health impact: An assessment of dental fluorosis in rural inhabitants of the Main Ethiopian Rift, Environment International, 43: 37-47.

Rayner, J. (2006): Potters for Peace Ceramic Filter Production Manual

Rob, D., Xanat, F., Melanie, P., Georges, T. (2003): Point-of-use water treatment technology investigations in Nepal. Clean Water for Nepal, Inc, Cambridge, MA 02139.

Robillard, P.D., Sharpe, W.E., and Swistock, B.R. (2006): Nitrates in Drinking Water. College of Agricultural Sciences, U.S. Department of Agriculture.

Pennsylvania Counties Cooperating. Rosalam, H., and Duduku, K. (2007): Free chlorine residual content within the drinking water distribution system International Journal of Physical Sciences, 2 (8):196-201.

Sagara, J., (2000): Study of Filtration for Point-of-Use Drinking Water Treatment in Nepal Masters of Engineering Thesis. MIT.

Sakka, Y., Fengqw, T., Hiroshi, F., and Tetsuo U.K. (2003): Fabrication of porous ceramics with controlled Pore size by colloidal processing, National Institute for Material sciences.

Scheutz, F., Strockbine, N.A., Brenner, D.J., Krieg, N.R., and Staley, J.T. (2005): Genus Escherichia. In Bergey's Manual of Systematic Bacteriology, 2nd ed. Eds. Springer New York, NY, USA, Vol 2, Part B: 607–623.

Schiefer, K. (2003): Water quality monitoring report 2003. Township of Georgian Bay. Water Chemistry: http://www.georgianbay.ca/pdf/water_qualit.

Schweitzer, R.W., Cunningham, A., Mihelcic, J. R. (2013): Hydraulic Modeling of Ceramic Water Filters for Point-of-Use Water Treatment, Environmental Sci. and Technol., 47, 429-435.

Shahbazi, P., Vaezi, F., Mahvi, A.H., Naddaffi, K., Rahmani, A.R. (2010): Nitrate removal from drinking water by the point of use ion exchange. J Res HealthSci, 10(2):91–7.

Shafiquzzaman, Md., Azam, M.S., Nakajima, J., Bari, Q.H. (2011): Investigation of arsenic removal performance by a simple iron removal ceramic filter in rural households of Bangladesh, Desalination, 265: 60– 66.

Shittu, O.B., Olaitan, J.O., Amusa, T.S. (2008): Physico-Chemical and Bacteriological Analyses of Water Used for Drinking and Swimming Purposes in Abeokuta, Nigeria. African Journal of Biomedical Research, 11: 285 – 290.

Simonis, J.J., Basson, A.K. (2012): Manufacturing a low-cost ceramic and filter system for the elimination of common pathogenic bacteria, Phys. Chem. Earth 50–52.

Singer, F., and Singer, S.S., (1963): Industrial Ceramics, Chemical publishing co., 1st ed. New York, 9-12.

Sing, K., Everett, D., Haul, R., Moscou, L., Pierotti, R., Rouquérol, J., Siemieniowska, T. (1985): Reporting physisorption data for gas/solid systems with special reference to the determination of surface area and porosity. International Union of Pure and Applied Chemistry. Pure and Appl. Chem. 57.

Sing, K.S.W., Everett, D.H., Haul, R.A.Q., Moscou, L., Pierotti, R.A., Rouquerol, J., et al. (1984): Reporting physisorption data for gas/solid systems with special reference to the determination of surface area and porosity, Pure Appl Chem, 57:603–19.

Sobsey, M., Brown, J., Kaida, L., Proum, S., Sampson, M. (2007): UNC Household Water Filter Treatment and Health Research in Cambodia: 2005-2007.

Sobsey, M.D., Stauber, C.E., Casanova, L.M., Brown, J.M. and Elliott, M.A. (2008): Point of use household drinking water filtration: A practical, effective solution for providing sustained access to safe drinking water in the developing world. Environmental science & technology, 42(12): 4261-4267.

Sommer, B., Marion, A., Solarte, M., Dierolf, C., Valiente, C., Mora, D., Rechsteiner, R., Setters, P. (1997): SODIS – An Emerging Water Treatment Process, J Water SRT- Aqua, 46,127-137.

Sunil, K. B., and Arti J. (2012): Equilibrium and Thermodynamic Studies for Adsorption of Crystal Violet onto Spent Tea Leaves (STL), water, 4:52-71.

Teixeira, M.R., Rosa, M.J. (2006): The impact of the water background inorganic matrix on the natural organic matter removal by nanofiltration, J. Membr. Sci. 279: 513–520.

Thole, B., (2011): Defluoridation kinetics of 200°C calcined, bauxite, gypsum, and magnetite and breakthrough characteristics of their composite filter, Journal of Fluorine Chemistry, vol. 132: 529-535.

Wakida FT, Lerner DN. (2005): Non-agricultural sources of groundwater nitrate: a review and case study. *Water Res*, 9(1):3–16.

WHO,(2017): *Guidelines for Drinking-water Quality: Fourth Edition Incorporating the first Addendum*.

WHO (2017): and the United Nations Children’s Fund (UNICEF), *Progress on drinking water, sanitation and hygiene: 2017 update and SDG baselines*.

WHO.(2016): *Protecting surface water for health, Identifying, assessing and managing drinking water quality risks in surface water catchments*, WHO Library Cataloguing-in-Publication Data, 20 Avenue Appia, 1211 Geneva 27, Switzerland, ISBN 978 92 41510554:13-163.

WHO,(2013): *Influencing factors for household water quality improvement in reducing diarrhea*, *South-East Asia Journal of Public Health*, 2: 1.

WHO /UNICEF, (2012): *Joint Monitoring Program for Water Supply and Sanitation Estimates for the use of Improved Drinking-Water Sources Ethiopia*. was info. Org

WHO, (2011): *Hardness in Drinking-water Background Document for Development of WHO: Guidelines for Drinking-water Quality*. WHO Press.

WHO, (2010): *Enterohaemorrhagic Escherichia coli (EHEC)*.

WHO, (2006): *Guidelines for Drinking-water Quality. (First Addendum to Third Edition)*, Volume 1.19-27.

WHO, (2002): *Managing water in the home: Accelerated Health Gains from Improved Water Supply*, Geneva.

WHO, (1996): *Water Quality Assessments - A Guide to use of biota, sediments, and water in environmental monitoring*. 2nd ed. Great Britain at the University Press, Cambridge.

WHO,(1985): *Health hazards from nitrates in drinkingwater. Report on a WHO meeting*. WHO Regional Office for Europe, Copenhagen.

Wongsakoonkan, W.A., Prechthai, T. A., and Tantrakarnapa, K.(2014): Suitable Types and Constituent Ratios for Clay-Pot Water Filters to Improve the Physical and Bacteriology quality of drinking water, *J. EnvironmentAsia* 7(2): 117-123.

van Halem, D., (2006): Ceramic silver-impregnated pot filters for household drinking water treatment in developing countries. Unpublished Thesis, Delft University of Technology, Delft.

Vinka, A., Oyanedel C., and James A.S.(2008): Sustainable Colloidal-Silver-Impregnated Ceramic Filter for Point-of-use water treatment. *Environmental Science and Technology*, 42,927-933.

Xiaolong, L., and Yi, M. (2005): The method to define the pore diameter and its distribution for porous membrane, TianjinMountain Company, Tianjin Polytechnic University, Tianjin.

Yakub, I., Du, J. and Soboyejo, W.O. (2012): Porosity, flow and filtration characteristics of frustum-shaped ceramic water filters.” *Journal of Environ. Eng.*139(7):86-994.

Yakub, I., Plappally, A ., Leftwich, M., Malatesta, K, K.C. Friedman, Obwoya, S. Nyongesa, F., Usoro, A., Rivera, R., Piascowy, S., Maiga, A., Logothetis, S., A. B. O. Soboyejo, A.B.O., and Soboyejo W.O. (2013):. Porosity, flow and filtration characteristics of frustum-shaped ceramic water filters.” *Journal of Environ. Eng.*139, (7):986-994.

Yakub, I. (2012): Micro- and Nano-porous Adsorptive Materials for Removal of Contaminants From Water at Point of Use (Ph.D. Thesis).

Yan, M., Wang, D., Ni, J., Qu, J., Yan, Y., Chow, C.W.K. (2008): Effect of polyaluminum chloride on enhanced softening for the typical organic-polluted high hardness North-China surface waters, *Sep. Purif. Technol.* 62: 401–406.

Yang, G.C.C., Tsai, C.M. (2008): Effects of starch addition on characteristics of porous ceramic membrane substrates, *Desalination*, vol. 233: 129–136.

Yong, R., (2001): *Geoenvironmental Engineering – Contaminated Soils, Pollution Fate, and Mitigation*, CRC Press LCC, Florida.

Yousefi, N., Fatehizedeh, A., Ghadiri, K., Mirzaei, N., Ashrafi, S.D., Mahvi, A.H. (2016): Application of nanofiller in the removal of phosphate, fluoride and- trite from groundwater. *Desalination Water Treat*, 57(25):11782–8.

Zereffa, E. A., Seghne, T. A. (2018): Sintering temperature, microstructures and electrical properties of $(\text{Na}_{1/2}\text{Bi}_{1/2})_{0.94}\text{Ba}_{0.06}\text{Ti}_{0.97}(\text{Mg}_{1/3}\text{Nb}_{2/3})_{0.03}\text{O}_3$ Ferroelectric ceramic, *Journal of Science of sintering* 47(3).

APPENDIXES

Appendix A: Flow rate results of selected filters						
Batch	Filter Code	Trial 1	Trial 2	Trial 3	Average	
A	F1	C800-50-15-35	2.96	2.5	2.73	2.73±0.23
	F2	C850-50-15-35	2.43	1.87	2.15	2.15±0.28
	F3	C900-50-15-35	2.46	1.64	2.05	2.05±0.41
	F4	C950-50-15-35	2.46	1.36	1.91	1.91±0.55
	F5	C800-60-15-25	2.48	1.84	2.16	2.16±0.32
B	F6	C850-60-15-25	2.8	2.32	2.56	2.56±0.24
	F7	C900-60-15-25	2.2	1.74	1.97	1.97±0.23
	F8	C950-60-15-25	1.81	1.31	1.56	1.56±0.25
C	F9	C800-70-15-15	2	1.56	1.78	1.78±0.22
	F10	C850-70-15-15	1.61	1.31	1.46	1.46±0.15
	F11	C900-70-15-15	1.31	1.01	1.16	1.16±0.15
	F12	C950-70-15-15	1.35	1.05	1.2	1.20±0.15
D	F13	C800-70-10-20	2.13	1.53	1.83	1.83±0.30
	F14	C850-70-10-20	1.88	1.52	1.7	1.70±0.18
	F15	C900-70-10-20	1.94	1.32	1.63	1.63±0.31
E	F16	C900-70-5-25	3.32	2.56	2.94	2.94±0.38
	F17	C950-70-5-25	2.77	2.23	2.5	2.50±0.27
	F18	C1000-70-5-25	2.52	1.88	2.2	2.20±0.32
F	F19	C900-75-5-20	2.48	1.96	2.22	2.22±0.26
	F20	C950-75-5-20	2.34	1.34	1.84	1.84±0.50
	F21	C1000-75-5-20	1.93	1.31	1.62	1.62±0.31
	F22	C900-80-5-15	2.61	1.81	2.21	2.21±0.40
G	F23	C950-80-5-15	1.76	1.18	1.47	1.47±0.29
	F24	C1000-80-5-15	1.36	1.06	1.21	1.21±0.15

Appendix B: Porosity results of the selected filter.

Batch	Filter Code	Trial 1	Trial 2	Trial 3	Mean \pm SD
A[F1-F4]	C800-50-15-35	40.39	40.25	40.32	40.32 \pm 0.07
	C850-50-15-35	37.05	36.95	37	37.00 \pm 0.05
	C900-50-15-35	35.93	35.85	35.89	35.89 \pm 0.04
	C950-50-15-35	36.38	36.28	36.33	36.33 \pm 0.05
	C800-60-15-25	31.09	31.05	31.07	31.07 \pm 0.02
B[F5-F8]	C850-60-15-25	30.39	30.35	30.37	30.37 \pm 0.02
	C900-60-15-25	32.98	32.92	32.95	32.95 \pm 0.03
	C950-60-15-25	32.68	32.66	32.67	32.67 \pm 0.01
	C800-70-15-15	27.68	27.56	27.62	27.62 \pm 0.06
C[F9-F12]	C850-70-15-15	28.55	28.47	28.51	28.51 \pm 0.04
	C900-70-15-15	29.51	29.49	29.5	29.5 \pm 0.01
	C950-70-15-15	30.69	30.61	30.65	30.65 \pm 0.04
	C800-70-10-20	24.81	24.75	24.78	24.78 \pm 0.03
D[F13-F15]	C850-70-10-20	22.35	22.29	22.32	22.32 \pm 0.03
	C900-70-10-20	20.69	20.61	20.65	20.65 \pm 0.04
	C900-70-5-25	25.49	25.37	25.43	25.43 \pm 0.06
E[F16-F18]	C950-70-5-25	23.66	23.58	23.62	23.62 \pm 0.04
	C1000-70-5-25	19.75	19.67	19.71	19.71 \pm 0.04
	C900-75-5-20	22.65	22.57	22.61	22.61 \pm 0.04
F[F19-F21]	C950-75-5-20	21.56	21.54	21.55	21.55 \pm 0.01
	C1000-75-5-20	19.25	19.17	19.21	19.21 \pm 0.04
	C900-80-5-15	17.78	17.7	17.74	17.74 \pm 0.04
G[F22-F24]	C950-80-5-15	15.44	15.42	15.43	15.43 \pm 0.01
	C1000-80-5-15	13.21	13.05	13.13	13.13 \pm 0.08

Appendix C: EDS Results of used filter for Modjo river.

eZAF Smart Quant Results

Element	Weight %	Atomic %	Net Int.	Error %	Kratio	Z	R	A	F
C K	5.23	9.93	7.93	15.48	0.0199	0.7937	0.6404	0.4799	1.0000
O K	30.89	44.02	84.93	6.79	0.1618	0.7540	0.6578	0.6945	1.0000
FeL	1.62	0.66	1.81	40.92	0.0087	0.5645	0.7596	0.9549	0.9979
CuL	0.00	0.00	0.00	87.40	0.0000	0.5467	0.7774	1.0938	0.9969
AlK	13.93	11.77	51.65	5.51	0.0928	0.6780	0.7055	0.9704	1.0132
SiK	23.25	18.87	77.10	4.92	0.1568	0.6967	0.7159	0.9607	1.0078
P K	10.13	7.45	25.35	5.67	0.0644	0.6735	0.7266	0.9371	1.0070
SnL	3.20	0.62	1.85	21.43	0.0172	0.4960	0.9005	1.0473	1.0338
CaK	11.75	6.68	12.92	15.95	0.0828	0.6971	0.7919	0.9968	1.0139

Appendix-D

ANOVA of water hardness (Mg^{2+}) ion removal efficiency of ceramic filters with different percent composition of clay to sawdust.

SUMMARY					
Groups	Count	Sum	Average	Variance	
F2 F6 F10	3	188	62.67	86.33	
F3 F7 F22	3	207	69.00	25.00	
F4 F8 F23	3	195	65.00	37.00	
One way: ANOVA					
Source of variation	Sum of Squares	df	Mean Square	F	Sig.
Between Groups	61.556	2	30.778	.622	0.568
Within Groups	296.667	6	49.444		
Total	358.222	8			

The water hardness(Mg^{2+} ions) removal efficiency of different groups of ceramic filters do not differ significantly.

Appendix-E

ANOVA of water hardness (Ca^{2+}) removal efficiency of ceramic filters with different percent composition of clay to sawdust.

SUMMARY						
Groups	Count	Sum	Average	Variance		
F2 F6 F10	3	150	50	403		
F3 F7 F22	3	218	72.66667	14.33333		
F4 F8 F23	3	197	65.66667	2247		
One way: ANOVA						
Source of variation		Sum of Squares	df	Mean Square	F	Sig.
Between Groups		808.222	2	404.111	2.379	0.174
Within Groups		1019.333	6	169.889		
Total		1827.556	8			

There is no significant difference in the efficiency of removing water hardness (Ca^{2+} ions) for groups of ceramic water filters with different percentage composition of clay to organic waste.

Appendix-F

ANOVA test for iron removal efficiency of ceramic filters with different percent composition of clay to sawdust.

SUMMARY						
Groups	Count	Sum	Average	Variance		
F2 F6 F10	3	222.75	74.25	12.2988		
F3 F7 F22	3	226.45	75.48333	0.016133		
F4 F8 F23	3	207.14	69.04667	35.22943		
One way: ANOVA						
Source of variation	Sum of Squares	df	Mean Square	F	Sig.	
Between Groups	70.026	2	35.013	2.209	.191	
Within Groups	95.089	6	15.848			
Total	165.115	8				
Post Hoc Tests						
	Mean Difference (I-J)	Std. Error	Sig.	95% Confidence Interval		
				Lower Bound	Upper Bound	
(2)F3 F7 F22 (3)F4 F8 F23	-1.23333	3.25045	.925	-11.2066		
(1)F2 F6 F10 (3) F4 F8 F23	5.20333	3.25045	.316	-4.7699	8.7399	
(1)F2 F6 F10 (2)F3 F7 F22	1.23333	3.25045	.925	-8.7399		15.1766
(1)F2 FF10 (2)F3 F7 F22	6.43667	3.25045	.198	-3.5366	11.2066	
(1)F2 FF10 (2)F3 F7 F22	-5.20333	3.25045	.316	-15.1766		16.4099
	-6.43667	3.25045	.198	-16.4099	4.7699	

Appendix G

ANOVA test of nitrite removal efficiency of ceramic filters made for different percentage composition of clay to sawdust.

SUMMARY						
Groups	Count	Sum	Average	Variance		
F2 F6 F10	3	155.47	51.82333	53.98723		
F3 F7 F22	3	202.76	67.58667	91.18793		
F4 F8 F23	3	216.19	72.06333	4.921267		
One way: ANOVA						
Source of variation	Sum of Squares	df	Mean Square	F	Sig.	
Between Groups	678.181	2	339.090	11.641	.009	
Within Groups	174.767	6	29.128			
Total	852.947	8				
Post Hoc Tests						
	Mean Difference (I-J)	Std. Error	Sig.	95% Confidence Interval		
				Lower Bound	Upper Bound	
(2)F3 F7 F22 (3)F4 F8 F23	15.76333*	4.40664	.027	-29.2841	-2.2425	
(1)F2 F6 F10 (3) F4 F8 F23	20.24000*	4.40664	.009	-33.7608	-6.7192	
(1)F2 F6 F10 (2)F3 F7 F22	15.76333*	4.40664	.027	2.2425	29.2841	
	-4.47667	4.40664	.595	-17.9975	9.0441	
(1)F2 F6 F10 (2)F3 F7 F22	20.24000*	4.40664	.009	6.7192	33.7608	
	4.47667	4.40664	.595	-9.0441	17.9975	

From the ANOVA test, there is a significant difference in removing nitrite between ceramic filters of design F3, F7, F22, F3 F7 F22 and filter design F4, F8, F23. The post Hoc result analysis also confirmed the ANOVA results.

Appendix H

Filter codes: F1F5F13 (pH)					
Source of Variation	Sum of Squares	df	Mean Square	F	Sig.
Between Groups	.420	2	.210	30.000	.001
Within Groups	.042	6	.007		
Total	.462	8			
F2,F6,F14(pH)					
Source of Variation	Sum of Squares	df	Mean Square	F	Sig.
Between Groups	9453.140	2	4726.570	4889555.172	.000
Within Groups	.006	6	.001		
Total	9453.146	8			
F3,F7,F16 (pH)					
Source of Variation	Sum of Squares	df	Mean Square	F	Sig.
Between Groups	.140	2	.070	10.048	.012
Within Groups	.042	6	.007		
Total	.182	8			

Appendix I

F1,F5,F13 (conductivity)					
Source of Variation	Sum of Squares	df	Mean Square	F	Sig.
Between Groups	2008.500	2	1004.250	9315.863	.000
Within Groups	.647	6	.108		
Total	2009.147	8			

F2,F6,F14 (conductivity)					
Source of Variation	Sum of Squares	df	Mean Square	F	Sig.
Between Groups	3003.500	2	1501.750	25744.286	.000
Within Groups	.350	6	.058		
Total	3003.850	8			

F3,F7,F16 (conductivity)					
Source of Variation	Sum of Squares	df	Mean Square	F	Sig.
Between Groups	2162.580	2	1081.290	12433.384	.000
Within Groups	.522	6	.087		
Total	2163.102	8			

Appendix J: Zero point charge data.

pH initial	1	2	3	4	5	6	7	8	9	10	11	12
pH final	7.19	6.99	6.79	6.66	7.5	8.0	7.66	7.8	7.4	7.3	6.9	6.7
ΔpH	6.19	4.99	3.79	2.66	2.5	2.0	0.66	0.2	-1.6	-2.7	-4.1	-5.3

Appendix K: Water-quality criteria, standards, or recommended limits for selected properties and constituents.

[All standards are from the U.S. Environmental Protection Agency (1994a) unless noted. MCL, Maximum Contaminant Level; SMCL, Secondary Maximum Contaminant Level; USEPA, U.S. Environmental Protection Agency; mg/L, milligrams per liter; μ S/cm, micro-siemens per centimeter at 25 degrees Celsius; μ g/L, micrograms per liter; pCi/L, picocuries per liter; --, no limit established].

Constituent or property	Standard	Significance
Specific Conductance		A measure of the ability of water to conduct electrical current; varies with temperature. Magnitude depends on concentration, kind, and degree of ionization of dissolved constituents; can be used to determine the approximate concentration of dissolved solids. Values are reported in micro-siemens per centimeter at 25°Celsius.
pH	6.5-8.5 units SMCL	A measure of the hydrogen ion concentration; pH of 7.0 indicates a neutral solution, pH values smaller than 7.0 indicate acidity, pH values larger than 7.0 indicate alkalinity. Water generally becomes more corrosive with decreasing pH; however, excessively alkaline water also may be corrosive.
Hardness and noncarbonate		Related to the soap-consuming characteristics of water; results in the formation of scum when soap is added. May cause deposition of scale in boilers, water heaters, and pipes. Hardness contributed by calcium

hardness (as mg/L CaCO ₃)		and magnesium, bicarbonate and carbonate mineral species in water is called carbonate hardness; hardness in excess of this concentration is called noncarbonate hardness. Water that has a hardness less than 61 mg/L is considered soft; 61-120 mg/L, moderately hard; 121-180 mg/L, hard; and more than 180 mg/L, very hard (Heath, 1983).
Fluoride	1.5 mg/l MCL	Reduces the incidence of tooth decay when optimum fluoride concentrations present in water consumed by children during the period of tooth calcification. Potential health effects of long-term exposure to elevated fluoride concentrations include dental and skeletal fluorosis (U.S. Environmental Protection Agency, 1994b).
Nitrite (mg/L as N)	1.0 mg/L MCL	Commonly formed as an intermediate product in bacterially mediated nitrification and denitrification of ammonia and other organic nitrogen compounds. An acute health concern at certain levels of exposure. Nitrite typically occurs in water from fertilizers and is found in sewage and wastes from humans and farm animals. Concentrations greater than 1.0 mg/L, like nitrogen, may be injurious to pregnant women, children, and the elderly.
Iron	200 µg/l SMCL	Forms rust-colored sediment; stains laundry, utensils, and fixtures reddish brown. Objectionable for food and beverage processing. Can promote the growth of certain kinds of bacteria that clog pipes and well openings.
Conductivity	2500 µS/cm at 20°C	This is a measurement of the mineral salts dissolved in the water
<i>E. coli</i>	0 per 100 ml	These bacteria are found in the gut of humans and warm-blooded animals and their presence in water supplies indicate possible fecal contamination. Immediate action is taken if these organisms are detected in drinking water.
turbidity	4 NTU at	This is due to fine particles suspended in the water, causing cloudiness.

	customer taps 1 NTU at water treatment works	Turbidity can sometimes arise following burst mains. Sometimes minute air bubbles give the supply a milky appearance but on standing for a few minutes these will clear from the bottom of the glass upwards
--	---	--



Figure 38. Preparation of the standard solution of nitrite before UV-detections.

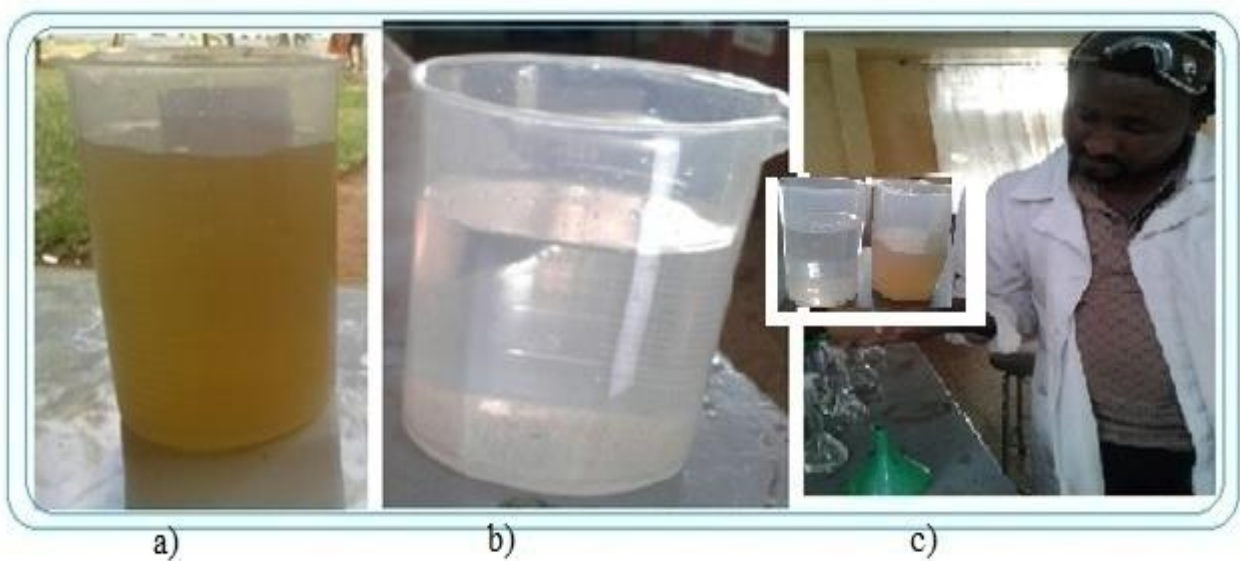


Figure 39. The color difference of the raw and filtered water sample with ceramic filters.

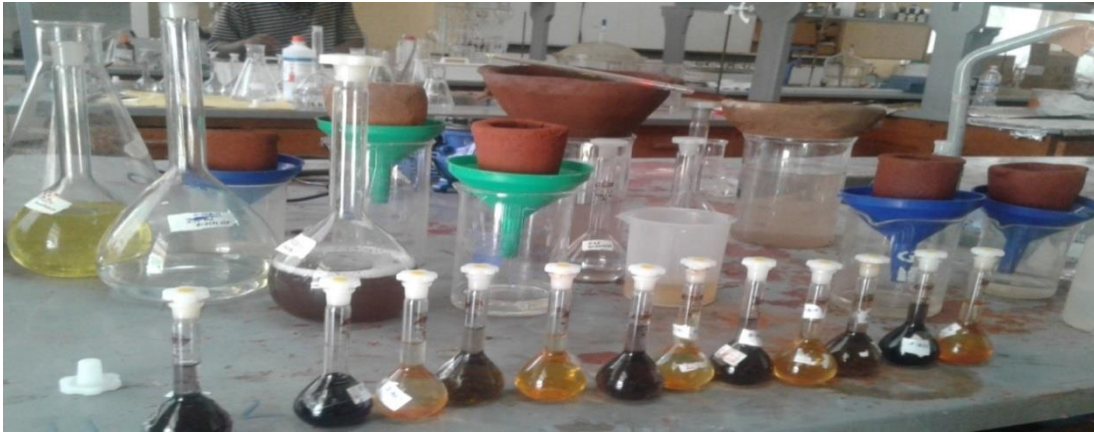


Figure 40. Prepared standard solution of iron.



Figure 41. Kechene women's pottery cooperation, where raw materials were prepared, stored, and molded.



Figure 42. Photograph had captured during testing the filters developed.



Figure 43. Photograph of sample filter developed by the research team.